HYDROGEOLOGIC INVESTIGATION OF THE BOULDER VALLEY, JEFFERSON COUNTY, MONTANA: INTERPRETIVE REPORT

Andrew Bobst, Julie Butler,[1] and Luke Carlson[2]

Montana Bureau of Mines and Geology

Ground Water Investigations Program

[1]Currently employed by Massachusetts Department of Environmental Protection, Boston, MA

[2]Currently employed by Morrison-Maierle, Inc., Helena, MT

Montana Bureau of Mines and Geology

Cover photo by Andrew Bobst, MBMG.

HYDROGEOLOGIC INVESTIGATION OF THE BOULDER VALLEY, JEFFERSON COUNTY, MONTANA: INTERPRETIVE REPORT

Andrew Bobst, Julie Butler,[1] and Luke Carlson[2]

Montana Bureau of Mines and Geology

Ground Water Investigations Program

[1]Currently employed by Massachusetts Department of Environmental Protection, Boston, MA

[2]Currently employed by Morrison-Maierle, Inc., Helena, MT

Montana Bureau of Mines and Geology Open-File Report 682

2016

Montana Bureau of Mines and Geology

TABLE OF CONTENTS

FIGURES

TABLES

PREFACE

The Ground Water Investigations Program (GWIP) at the Montana Bureau of Mines and Geology (MBMG) investigates areas prioritized by the Ground-Water Assessment Steering Committee (2-15-1523 MCA) based on current and anticipated growth of industry, housing and commercial activity, or changing irrigation practices. Additional program information and project-ranking details are available at: http://www.mbmg.mtech.edu/gwip/.

The final products of the Boulder Valley study are:

An **Interpretive Report** that presents data, addresses questions, offers interpretations, and summarizes project results. For the Boulder Valley Groundwater Investigation, questions included: what are the potential impacts to surface-water availability from increased groundwater development, and what is the feasibility of using managed recharge to enhance late-summer flows?

A **Groundwater Modeling Report** that describes the construction, the assumptions used, and the results from groundwater models. Groundwater modelers should be able to evaluate and use the models as a starting point for testing additional scenarios and for site-specific analyses. The GWIP website (http://www.mbmg.mtech.edu/gwip/) provides access to the files needed to run the models.

MBMG's Groundwater Information Center (GWIC) online database (http://mbmggwic.mtech.edu/) provides a permanent archive for the data from this study.

ABSTRACT

Portions of the Lower Boulder River often dry up in the late summer; the Montana Department of Fish Wildlife and Parks has identified the reach from the town of Boulder to Cold Spring as "chronically dewatered." The Boulder Valley groundwater investigation evaluated 377 mi^2 of the drainage basin between the towns of Boulder and Cardwell, but focused on: (1) impacts to surface-water availability from potential increased groundwater development; and (2) the feasibility of using managed recharge to enhance late-summer flows.

The MBMG used groundwater monitoring data and a groundwater budget to develop an area-wide groundwater flow model and evaluate four subdivision scenarios of 58 to 128 new domestic wells on 10- or 20-acre lots. Results showed that the most intense development of 128 residences on 10-acre lots would cause a depletion of 0.06 cfs from the Boulder River after 20 years of pumping. However, the stream depletion rate would slowly increase during succeeding decades until it provided all of the water consumptively used by the wells.

A second groundwater flow model helped the MBMG assess the potential of managed recharge to supplement late-summer flows in the Boulder River. This model simulated diversion of early spring Boulder River flow into infiltration basins. The water would become groundwater and then flow back to the Boulder River. The potential benefits of storing water in the infiltration basins were evaluated by varying the location and size of infiltration basins. One scenario included a 35-acre basin on the lower bench that would enhance late-summer flows in the Boulder River by about 2 cfs. Although managed recharge appears to be physically feasible, water quality, water rights, and economics still need to be addressed.

The amount of water potentially depleted from stream flows by new domestic wells or newly available because of managed recharge are slight relative to the effects of irrigation practices. Irrigators divert a significant amount of water, in some cases until the river is dry. Irrigation practices also provide important unintentional recharge to the groundwater system. For example, irrigation recharge and canal leakage add approximately 23,000 acre-ft of water to the groundwater system each year. Maximizing the use of canals and flood irrigation during peak runoff would increase early season recharge to the groundwater system, and likely supplement late-summer stream flow. During low-flow periods, water conservation measures are needed to reduce water shortages. Proven cost-effective conservation measures include diversion structures that can be easily monitored and modified, and coordination between irrigators.

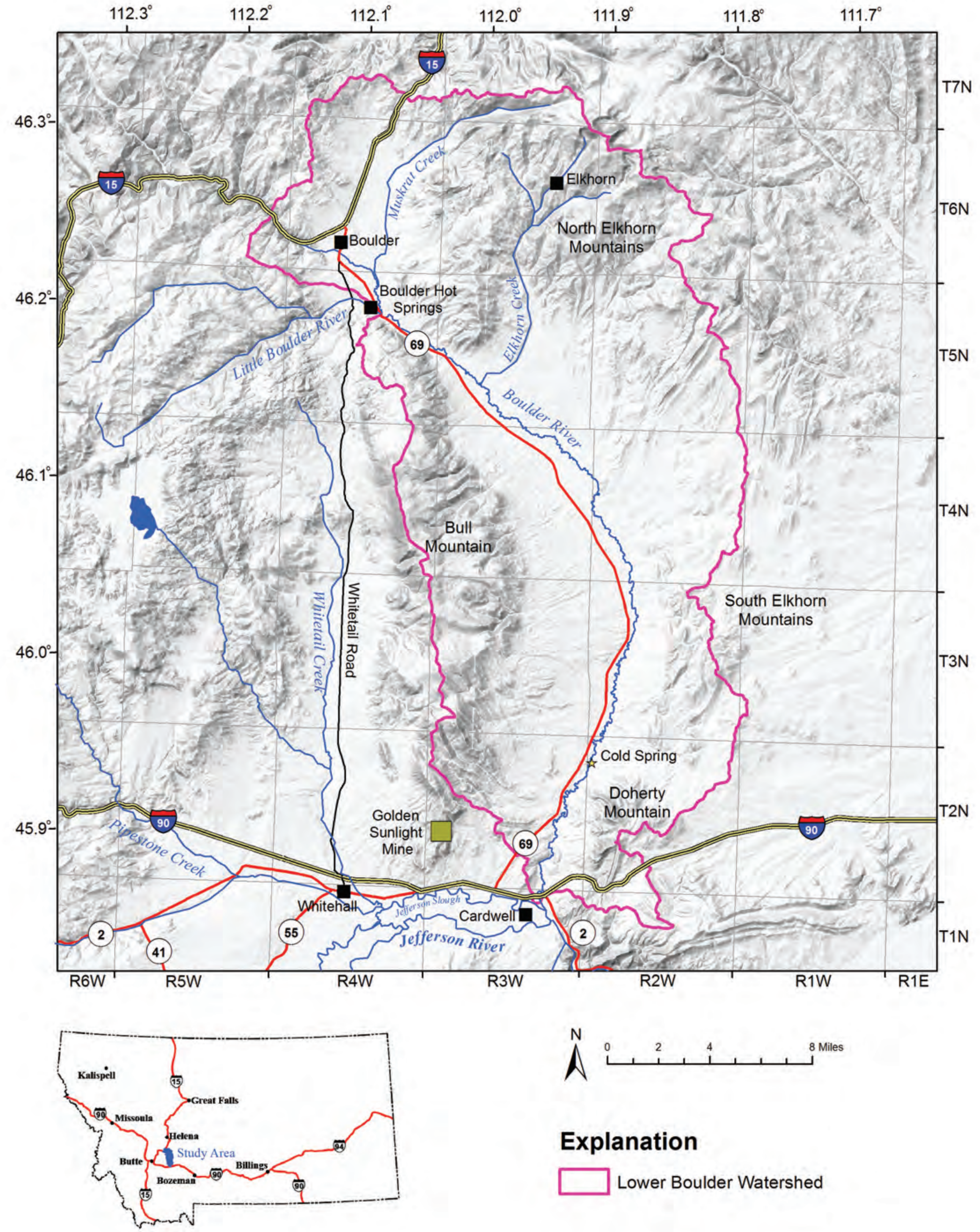

Figure 1. The Boulder Valley groundwater investigation evaluated the Lower Boulder River Watershed (USGS HUC 1002000605) between Boulder and Cardwell. The study area covers 377 mi^2.

INTRODUCTION

The Boulder Valley study area (USGS hydrologic unit code 1002000605) covers 377 mi^2, generally between the towns of Boulder and Cardwell, Montana (fig. 1). About 60 percent of the watershed is privately owned, and the rest is managed by the US Forest Service, the US Bureau of Land Management, and the State of Montana (Montana State Library, 2010). Perennial tributaries to the Boulder River in the study area are the Little Boulder River and Muskrat Creek.

Dewatering of the Boulder River is a longstanding problem (Buck and Bille, 1956; BLM, 1975). By late summer in most years, flow ceases in several reaches because all available water is diverted. There is typically some flow in the Boulder River below Cold Spring (fig. 1). The Montana Department of Fish Wildlife and Parks (FWP, 2012) has identified the reach of the Boulder River from the town of Boulder to Cold Spring as “chronically dewatered.” Some area residents are concerned that increased groundwater withdrawals for residential development will further diminish stream flows, and prolong the period over which the river is dry.

Ideas to supplement late-summer stream flows have included: (1) a surface reservoir on the Boulder River just upstream of its confluence with Basin Creek (Montana Water Resources Board, 1968); (2) supplementing the irrigation system with groundwater from the alluvial aquifer near Boulder (Botz, 1968); and (3) a surface reservoir near the mouth of the Little Boulder River (SCS, 1975; Darr, 1975; Jolly, 1982). However, none of these projects have been constructed. Recently some local residents have suggested that early spring stream flows could be diverted into strategically located infiltration basins. Water in the basins would enter the groundwater flow system and return to the Boulder River to supplement late-summer flows.

Purpose and Scope

The Boulder Valley groundwater investigation focused on: (1) addressing the potential impacts to surface-water flows from increased groundwater withdrawals; and (2) evaluating the potential of using managed recharge to supplement late-summer flows in the Boulder River. Both questions required that the MBMG evaluate the hydrogeologic properties of the unconsolidated valley-fill deposits (fig. 2). Less detailed evaluation of fractured bedrock aquifers surrounding the valley provided information about upland recharge mechanisms that support groundwater recharge to the valley-fill deposits (i.e., mountain front recharge). These results provide a basis for future groundwater management and a hydrogeologic framework within which site-specific issues can be considered.

Previous Investigations

Nobel and others (1982, p. 73) and Kendy and Tresch (1996, p. 56) provided reviews of previous work in the Boulder Valley. The MBMG’s Groundwater Assessment Program (GWAP) monitors quarterly water levels in 11 wells as part of the statewide long-term groundwater monitoring network (MBMG-GWAP, 2016), and the United States Geological Survey (USGS) measured groundwater levels in 35 wells in 1991 (Dutton and others, 1995, p. 24–27). These data showed that groundwater is typically flowing towards the center of the valley, and to the south (Briar and others, 1996; Kendy and Tresch, 1996).

The USGS also collected 14 groundwater-quality samples and GWAP collected 17 groundwater-quality samples in the area. These samples show that groundwater in the area contained <500 mg/L total dissolved solids (TDS). Thick basin-fill aquifers contain water with TDS typically <250 mg/L, but water from shallow aquifers overlying bedrock contains TDS between 250 and 500 mg/L. Groundwater in the northern and central basin is a calcium-bicarbonate type and in the southern basin is a mixed cation-sulfate type. In the southern basin, groundwater can contain calcium, magnesium, and sodium in any combination (Clark and Dutton, 1996; Kendy and Tresch, 1996).

Nobel and others (1982, p. 74) state that the Boulder Valley is also known as the Cold Spring Valley “…because of the cold springs (approximately 12^{o}C) that issue from the alluvium, probably discharging from the Madison near the center of the valley.” GWAP inventoried and sampled the Cold Spring complex in 2010 and estimated discharge to be 5–10 cfs of calcium-bicarbonate type water. The Montana FWP (2012) identified Cold Spring as the lower boundary of the chronically dewatered reach of the Boulder River, and noted that stream water quality improves significantly below the spring.

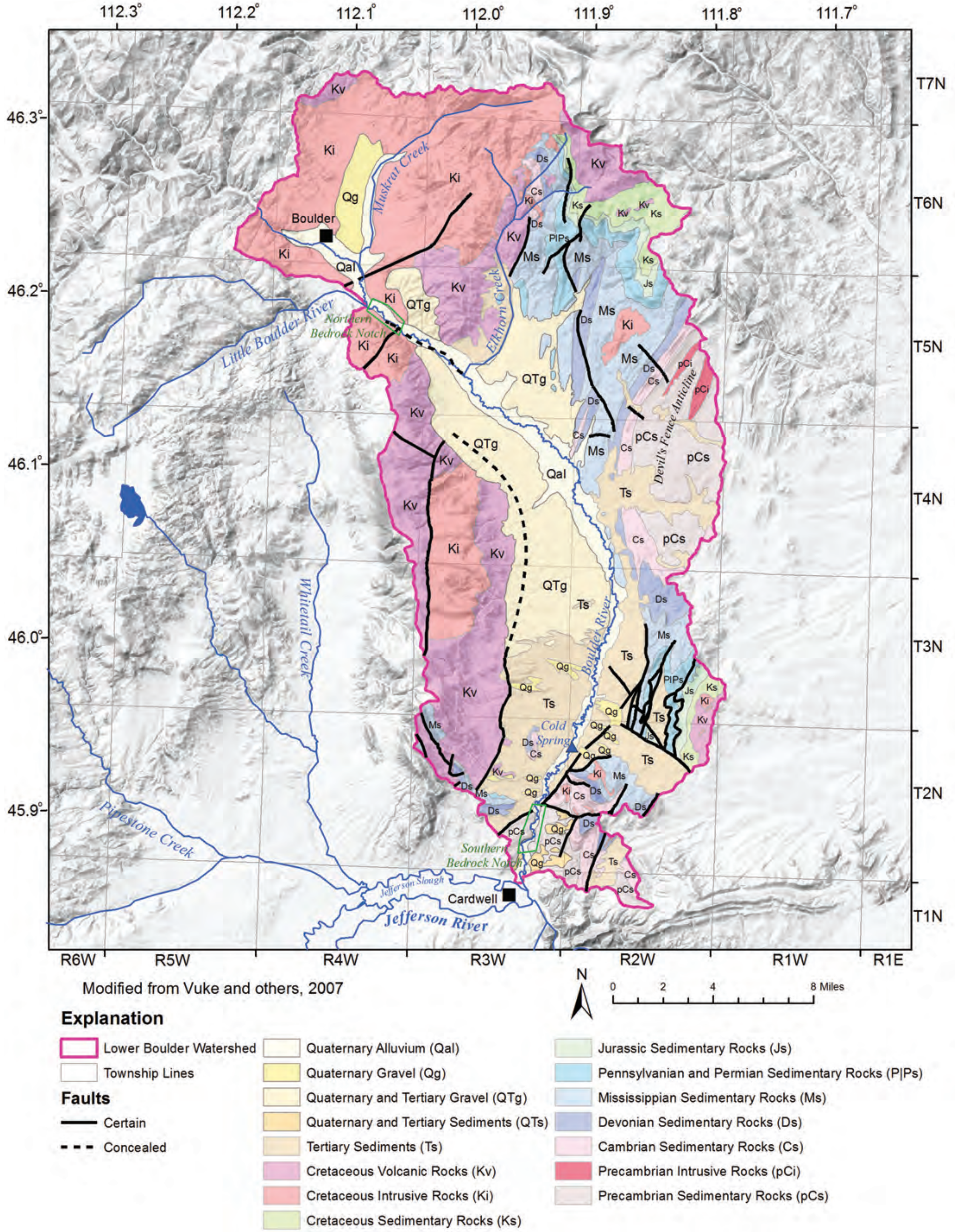

Figure 2. The northern and western parts of the study area are underlain by intrusive and extrusive igneous rocks of the Boulder Batholith and Elkhorn Mountain volcanics. The eastern and southeastern parts of the study area are underlain by fractured, faulted, and folded sedimentary rocks. The central fault-bounded valley is filled with unconsolidated Tertiary and Quaternary deposits.

The Boulder Hot Springs are just outside of the study area (fig. 1). These springs were inventoried by the MBMG during an evaluation of the geothermal resources of Montana (Sonderegger and others, 1981). The springs discharge from the Boulder Batholith have an average temperature of 76°C, and an estimated reservoir temperature of 136°C. The total discharge is approximately 1.1 cfs. The water has a major-ion chemistry dominated by sodium and bicarbonate, contains 110 mg/L silica, and has a TDS of 420 mg/L (Sonderegger and others, 1981).

Another warm spring exists in the southwestern part of the study area (T. 2 N., R. 3 W., sec. 22; Buck and Bille, 1956). A sample showed that it produces a calcium-sulfate water containing 839 mg/L TDS (K. Gallagher, oral comm., 2013).

The one USGS surface-water gauge (06033000; Boulder River near Boulder, Montana) has operated intermittently: 1929–1932, 1934–1972, and 1982–present. The USGS measured field specific conductance (SC) and temperature at this site 265 times from 1984 to 2012. Overall, the SC varied from 51 to 327 microSiemens per centimeter at 25°C (µS/cm), with the lowest SC values occurring during high flows. The river at gauge 06033000 has been sampled twice by the USGS, once on November 1,1996 and again on May 24, 1997, at stream discharges of 38 and 1,420 cfs, respectively. These samples reasonably represent river water quality at low and high stream flow. Analytical results include pH, hardness, calcium (Ca), magnesium (Mg), sodium (Na), potassium (K), chlorine (Cl), sulfate (SO_4), fluoride (F), silica (SiO_2), total arsenic (As-unfiltered), and dissolved arsenic (As-filtered). Major ion concentrations were lower in the high-flow sample than in the low-flow sample. Dissolved As was also lower in the high-flow sample (5 micrograms per liter (µg/L) vs. 7 µg/L); however, total As was higher (97 µg/L vs. 11 µg/L) in the high-flow sample. The elevated As concentration likely results from adsorbed As on sediment being carried by the high flows.

Physiography

The Boulder Valley is a north–northwest-trending intermontane basin within the Northern Rocky Mountains physiographic province. Bull Mountain is on the west side of the valley, and the Elkhorn Mountains on the east (fig. 1). The Boulder River meanders within a well-defined floodplain that ranges from about 0.5 to 1 mi wide. Between the mountains and the floodplain there are pediments and alluvial fans. Where the alluvial fans meet the mountains the slope changes abruptly. Elevations within the study area range from 4,270 ft above sea level, where the Boulder River flows into the Jefferson Slough, to 9,414 ft above sea level, at the top of Crow Peak in the Elkhorn Mountains. Below the confluence of the Boulder and Little Boulder Rivers, a bedrock notch splits the study area into two basins (fig. 2). A second bedrock notch occurs at the southern end of the study area near Cardwell, Montana.

Climate

The Boulder Valley has cold winters and mild summers. Climate data for Boulder (NOAA, 2011) shows that December is the coldest month, with a mean monthly temperature of -5.7°C. July is the warmest month, with a mean monthly temperature of 18.4°C. Average annual precipitation within the study area ranges from about 11 in. in the valley to about 38 in. in the upper elevations of the Elkhorn Mountains [fig. 3; Parameter-Elevation Regressions on Independent Slopes Model (PRISM), 2012; Farnes and others, 2011]. Precipitation is greatest in June, based on a monthly average of 2.16 in at Boulder; February is the driest month based on an average of 0.65 in (NOAA, 2011). The average annual precipitation at Boulder is 11.37 in; however, year to year variability is significant (fig. 4).

Monthly PRISM data were used to calculate monthly study-area-wide average precipitation values from January 2010 to June 2013 (fig. 5). These values show significant variation, with monthly totals ranging from 0.19 to 3.70 in. In 2010 and 2011 total precipitation was near normal (106% and 99% of normal, respectively). The year 2012 and the first half of 2013 were dry (78% and 86% of normal, respectively). Although total precipitation in 2011 was near normal, peak flow in the Boulder River was the second highest on record. This resulted from high precipitation in the spring (138% of normal from April to June), and high snow pack at high elevations, which melted late (NRCS, 2014).

Vegetation

Within the study area, vegetation varies with elevation, precipitation, and depth to groundwater.

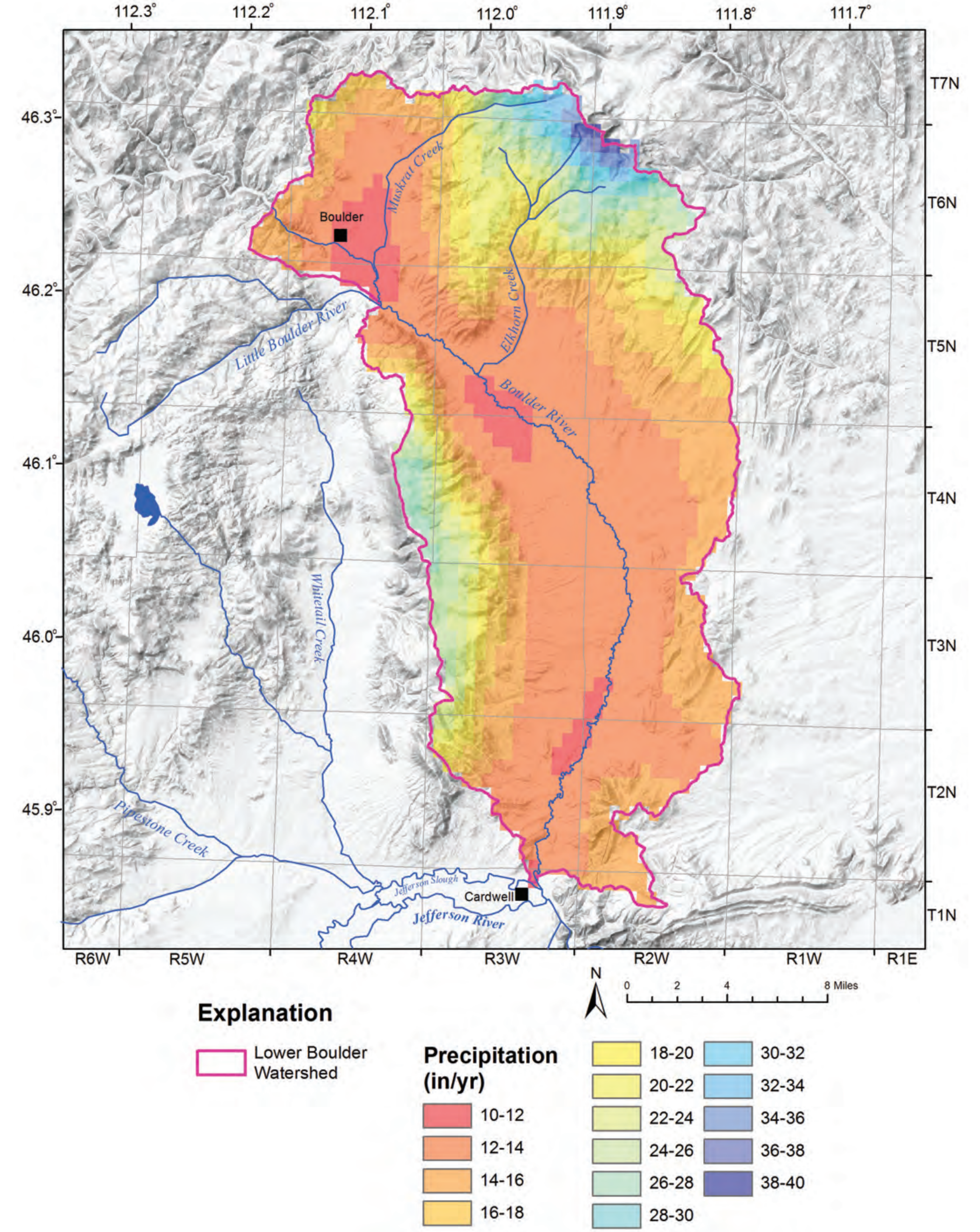

Figure 3. Precipitation within the study area varies with elevation. Central areas in the valley may receive less than 12 in/yr, but the highest peaks receive more than 38 in/yr (data from PRISM, 2012; 800 m resolution; 1981–2010 normal).

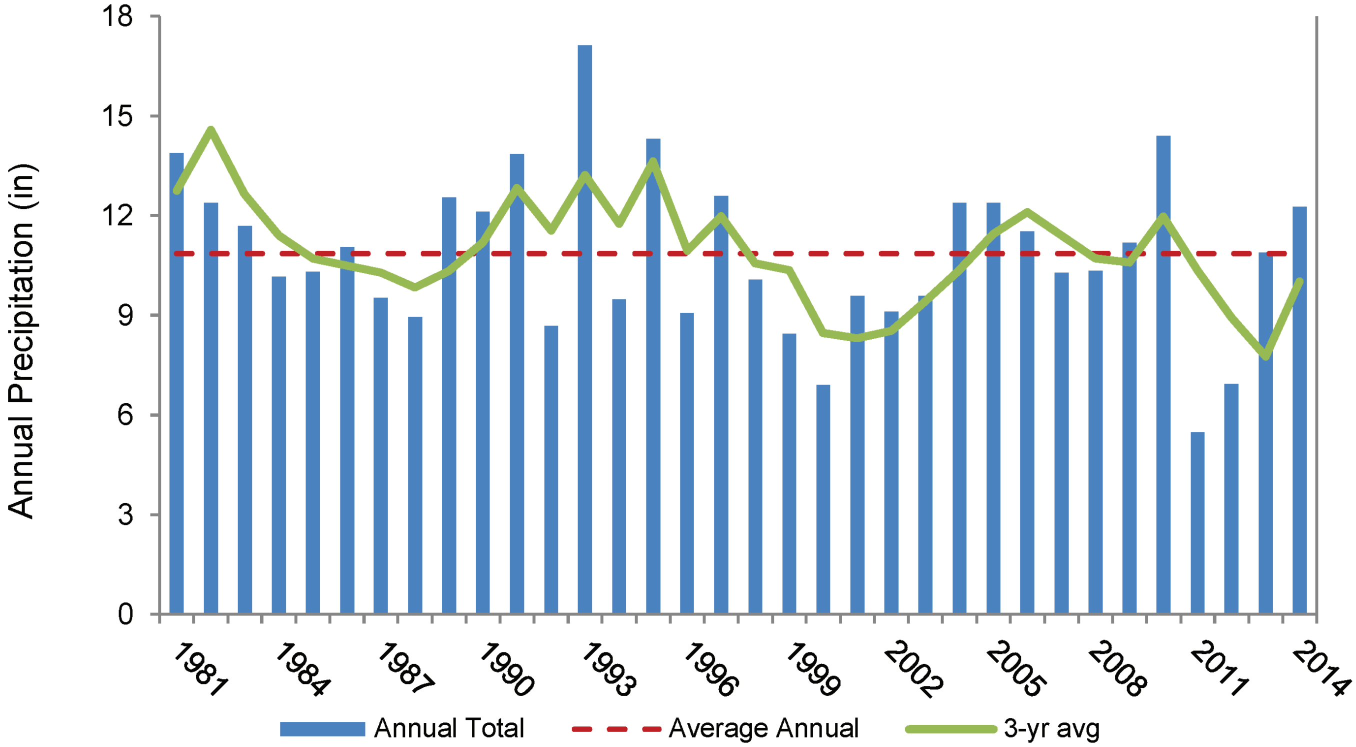

Figure 4. Precipitation at Boulder from 1981 to 2014 averaged 10.86 in/yr (NOAA, 2016); however, it varies significantly from year to year, with values from 50% to 158% of average over this period.

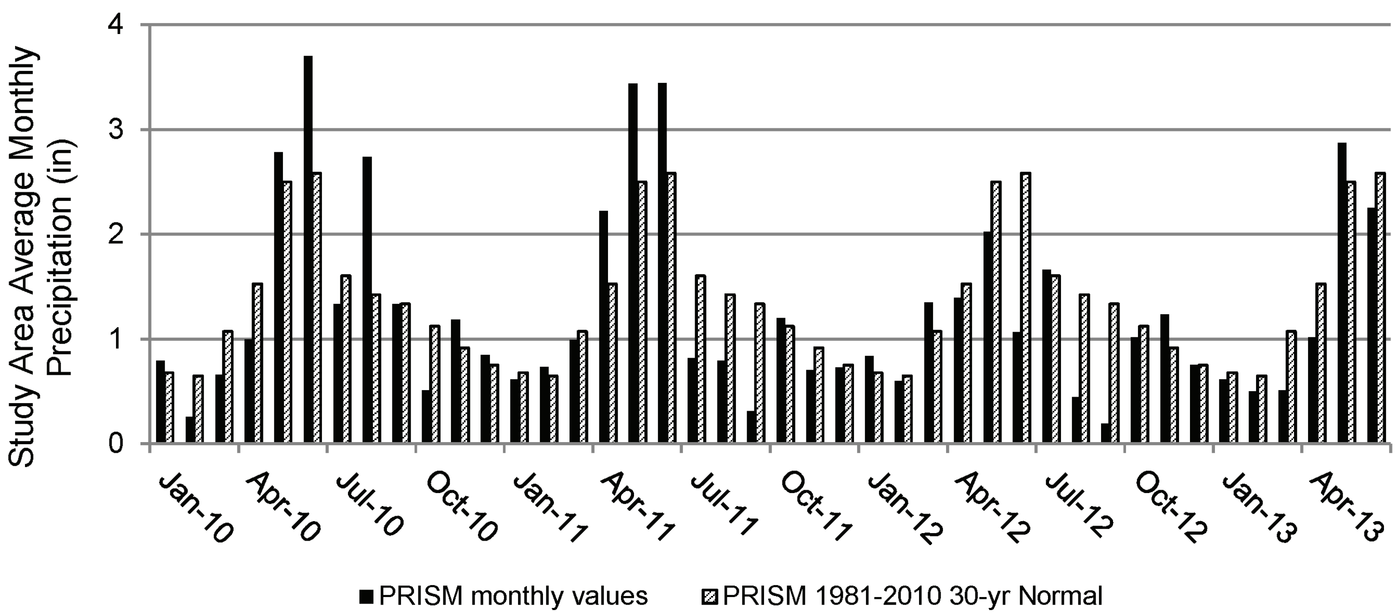

Figure 5. Study-area-wide average monthly precipitation values based on PRISM varied from 0.19 to 3.70 in from 2010 to mid-2013. 2010 and the first half of 2011 were wetter than average. The second half of 2011 and 2012 were relatively dry. The first half of 2013 was near normal. The wet spring in 2011 combined with high late season snowpack resulted in substantial flooding.

Along the Boulder River and some tributaries, willow, cottonwood, aspen, and wetland grasses are common. These phreatophytes occur where groundwater is shallow and accessible by plant roots. Upland vegetation includes grasses, sagebrush, Ponderosa pine, Douglas-fir, lodgepole pine, Engelmann spruce, and whitebark pine. Alfalfa and grass hay are the dominant agricultural crops. The type of vegetation determines the potential evapotranspiration, which aids in developing a reasonable water budget for the area.

A simplified vegetation map for the study area was developed using information from the LANDFIRE Existing Vegetation Type database (USGS, 2010a), the National Land Cover database (USGS, 2011), the GAP land cover database (USGS, 2010b), aerial photo-

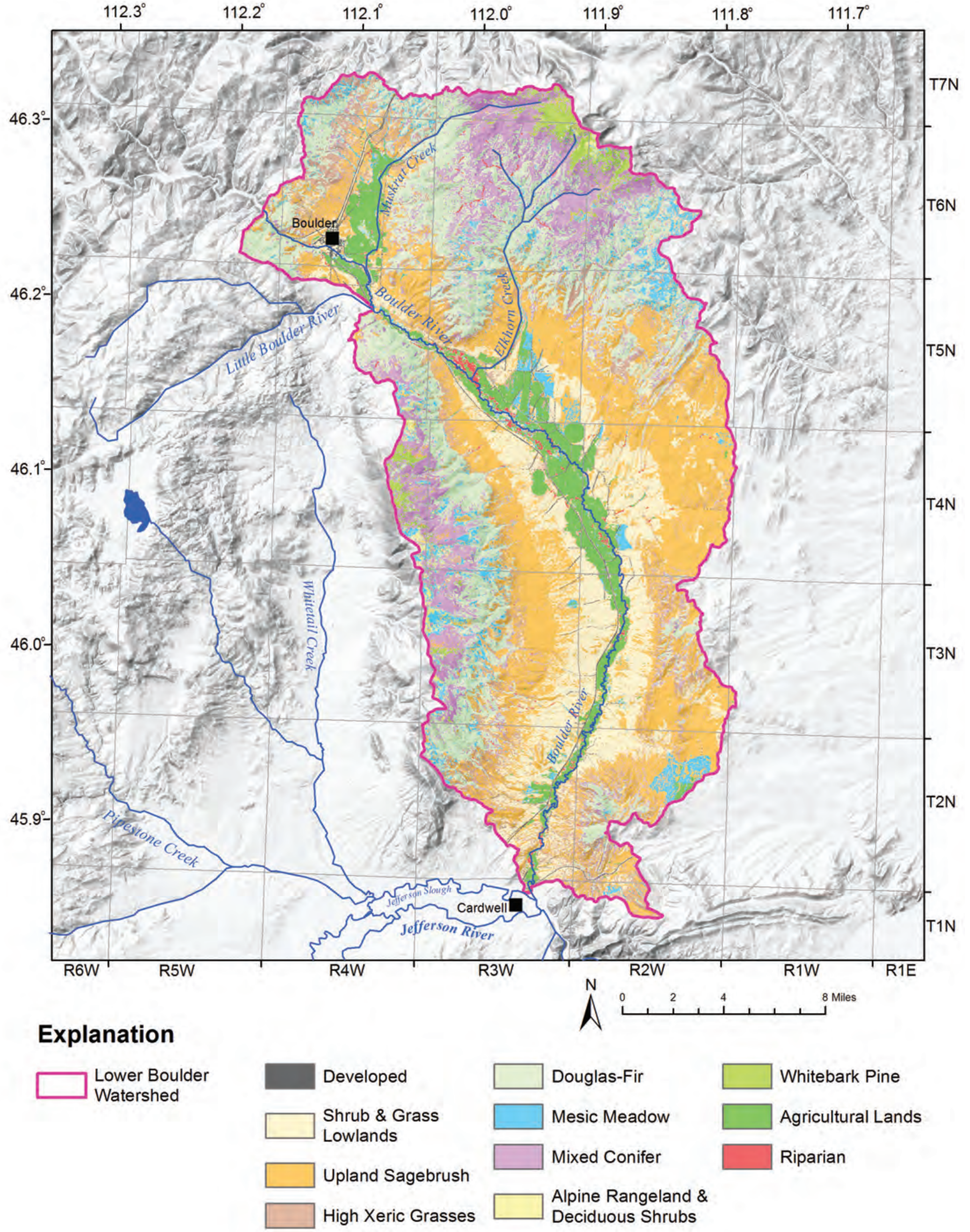

Figure 6. Vegetation within the study area varies with elevation and precipitation. Shrubs and grasses dominate at lower elevations; conifers dominate at higher elevations.

Table 1. Simplified Vegetation Groups from LANDFIRE (USGS, 2010)

Vegetation Group	Acres	% of Area
Upland Sagebrush	64,734	26.8
Douglas-Fir	49,790	20.6
Shrub/Grass Lowlands	40,393	16.7
Mixed Evergreen	27,186	11.3
High Xeric Grasses	20,988	8.7
Ag Lands	15,161	6.3
Mesic Meadow	12,926	5.4
Whitebark Pine	4,179	1.7
Alpine Rangeland, Deciduous Shrubs	2,818	1.2
Developed	1,971	0.8
Riparian	1,468	0.6
TOTAL	**241,616**	**100.0**

graphs, and field visits (fig. 6, table 1).

Water-Development Infrastructure

Within the study area, significant water-development infrastructure includes 177 mi of irrigation canals, 8,700 acres of irrigation, and 445 wells [with associated septic systems; fig. 7; MT-DNRC, 2007; Montana Department of Revenue (MT-DOR), 2012; Montana Ground Water Information Center, 2011]. Most irrigation water is obtained from the Boulder River, Elkhorn Creek, and Muskrat Creek. Irrigation occurs along the floodplains of these streams, and to a lesser degree on the adjacent benches. Canals affect groundwater by recharging aquifers through leakage. Irrigated fields provide recharge when water is applied in excess of crop demand. Wells supply domestic, stock, and irrigation water. Septic systems return water to the groundwater system.

Geologic Setting

Early geologic mapping focused on areas near ongoing mining operations (Peale, 1896; Weed, 1901; Stone, 1911; Weed, 1912; Knopf, 1913; Billingsley, 1915; Pardee and Schrader, 1933). More aerially extensive geologic mapping occurred in the 1940s and 1950s (Berry, 1943; Alexander, 1955; Klepper and others, 1957). In the 1960s graduate students from Indiana University provided geologic mapping and geophysical interpretations (Parker, 1961; Nelson, 1962; Wilson, 1962; Richard, 1966; Burfiend, 1967). Geological and geophysical work was also conducted in the 1960s by Becraft and Pinckney (1961), Becraft and others (1963), Johnson and others (1965), and Kinoshita and others (1965). In the 1970s Weeks (1974) conducted detailed mapping of Bull Mountain. More recently, area-wide geologic maps have been developed using previous geologic information and additional field mapping (Wallace and others, 1986; Lewis, 1998; Dixon and Wolfgram, 1998; Vuke and others, 2004; Reynolds and Brandt, 2006; Vuke and others, 2014).

Faults along the mountain fronts have down-dropped the Boulder Valley relative to the adjacent mountains. The valley has been filled with unconsolidated to poorly consolidated Tertiary and Quaternary deposits that range in size from clay to gravel (fig. 2; Ts, QTs, QTg, Qg, Qal). Depth to bedrock is greatest in the central valley, west of the Boulder River, where gravity data suggest that the basin-fill is more than 4,000 ft thick (Parker, 1961; Nelson, 1962; Wilson, 1962; Burfiend, 1967).

The northern part of the Elkhorn Mountains, and Bull Mountain, are composed of intrusive and extrusive igneous rocks of the Boulder Batholith and the Elkhorn Mountains volcanics. The southern Elkhorn Mountains are composed of fractured, faulted, and folded sedimentary and metasedimentary rocks that range in age from Precambrian to Cretaceous. In the southern Elkhorn Mountains, the most prominent structural feature is the Devil's Fence Anticline. Doherty Mountain at the south end of the Elkhorn Mountains is composed of highly deformed sedimentary and igneous rocks (fig. 2; Vuke and others, 2004, 2014; Reynolds and Brandt, 2006).

The entire Boulder River watershed has been affected by historical mining operations (Nimick and others, 2004). There are 97 abandoned mines within the Boulder Valley study area (Marvin and others, 1997, 1998; Metesh and others, 1998; MBMG, 2016a). The greatest concentration of abandoned

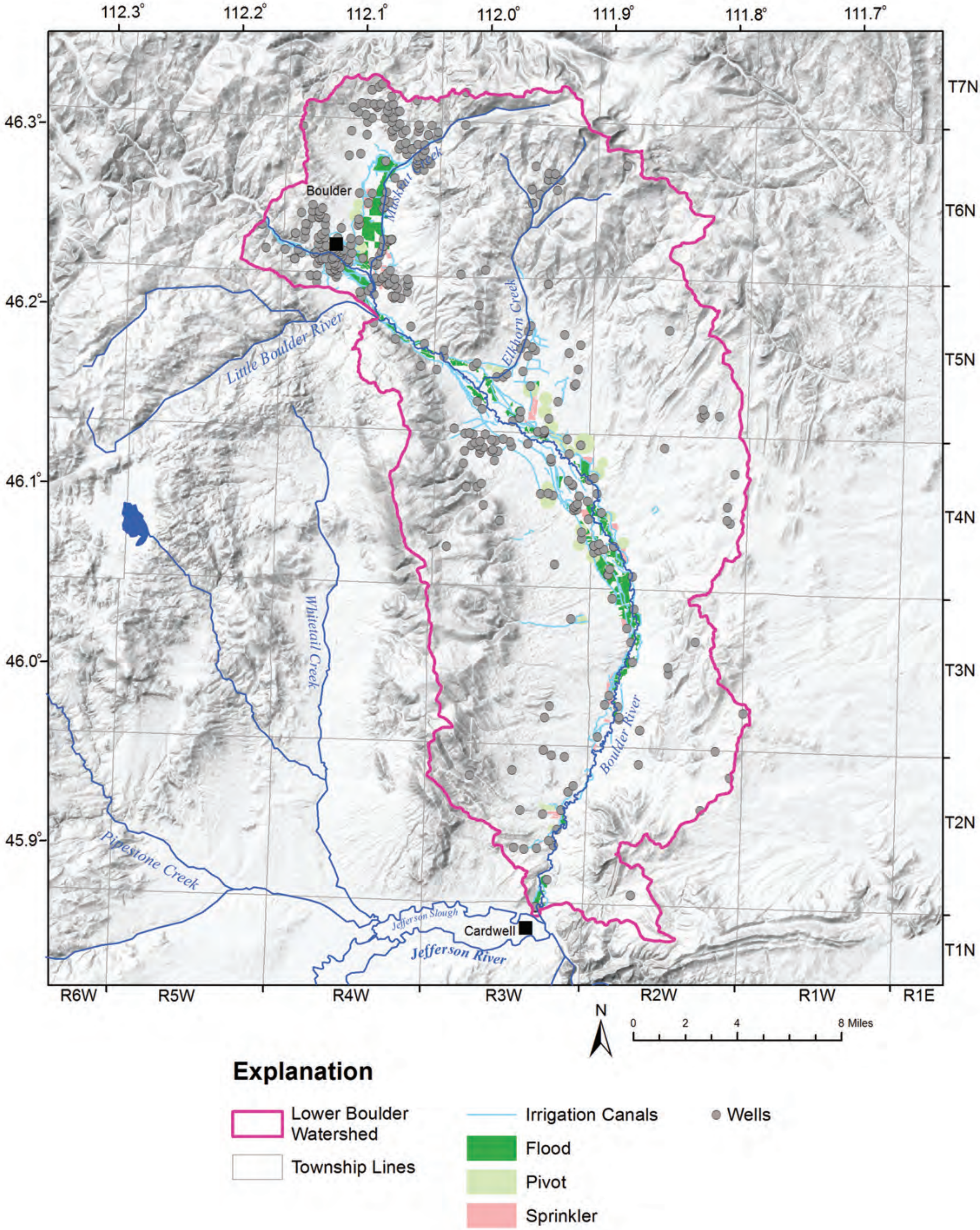

Figure 7. Irrigation infrastructure includes canals and fields. Wells are used to supply domestic, stock, and irrigation water.

mines is near Elkhorn, where prospecting began before 1870. The Elkhorn mine produced silver ore from 1875 to 1900. Several companies attempted to reopen the Elkhorn mine, and the tailings were reworked several times through 1951 (Byrne and Hunter, 1901; Weed, 1901; Stone, 1911; Buck and Bille, 1956; Roby and others, 1960; Tucker, 2008; MDEQ, 2013). Elkhorn Goldfields Inc. has recently pursued mining at Elkhorn (MDEQ, 2008); however, no new development has occurred. The MDEQ (2012) has identified historical mining and milling as the probable source of elevated arsenic levels in the Boulder River.

METHODS

Monitoring and Sampling

Groundwater

The MBMG established a monitoring network of 78 wells to obtain water-level and water-quality information (figs. 8, 9; appendices A and B). The MBMG also drilled 23 dedicated monitoring wells that became part of the network. Monitoring sites were selected based on hydrogeologic setting, geographic location, historical groundwater information, and well owner permission. Static water levels were measured monthly from February 2012 until June 2013. Thirty-one wells were equipped with pressure transducers that recorded water levels hourly.

Forty-eight water-quality samples were collected from 36 wells (fig. 9; appendix B). Most sampling occurred in late July and early August 2012 to better define the distribution of different water types. Some wells installed to monitor canal leakage were sampled in March (pre-irrigation season), June (early irrigation season), and late August (late irrigation season) 2012 to evaluate water-quality changes caused by canal leakage. (fig. 9; appendix B).

Surface Water

Surface-water data were collected by the MBMG at 16 locations (figs. 9, 10; appendices A and B) and from USGS Station 06033000 (Boulder River near Boulder). Stilling wells and staff gauges were installed at 15 of the MBMG stations. A transducer was installed in each stilling well to collect hourly stage readings. Staff gauges were surveyed by a registered surveyor. Discharge and stage were measured approximately every 2 weeks during the ice-free period of 2012, and through June 2013. Flow measurements were made with a Marsh-McBirney flow meter in wadeable streams or a SonTek RiverSurveyor acoustic Doppler profiler for large streams. The flow measurements were used to develop rating curves. At the Murphy Ditch/Hadley Park site [Ground Water Information Center (GWIC) ID 267934], only periodic discharge measurements were collected. Each station's period of operation is shown in table 2.

Twelve surface-water quality samples were collected at 10 of the surface-water stations (figs. 9, 10). Most of these samples were collected in late July or early August 2012 (appendix B).

Springs

Discharge and stage measurements were made on Cold Spring (fig. 9). However, because of the changing configuration of the outlet structure, a reliable rating curve could not be developed. Several other springs were inventoried, but they did not produce measurable flows.

Because Cold Spring is an important source of water for the lower Boulder River, the MBMG collected water-quality samples from it in July of 2012 and April 2013. During April 2013, the MBMG also collected samples from three wells and two surface-water sites to aid in identifying the spring's source. In addition to the standard suite of analytes, the April 2013 samples were analyzed for the stable isotopes of water (δD and $\delta^{18}O$), tritium (^{3}H), radon (Rn), dissolved inorganic carbon (DIC), stable carbon isotopes ($\delta^{13}C$), and strontium isotopes ($^{87}Sr/^{86}Sr$; fig. 9; appendix B).

Canal Leakage

The MBMG measured leakage from the Carey and Murphy canals. The Carey canal diverts up to 85 cfs; flow in the Murphy canal is about 8 cfs.

Leakage from the Carey canal was measured twice in September 2011. On September 13 measurements were made at eight sites, along 4.5 mi of canal. On September 14, measurements were made at five sites along a different 1.5-mi reach.

In the spring of 2012, before water was diverted into the Carey canal, two surface-water stations with automatic recording devices were installed 2.5 mi apart on the Carey Canal (fig. 10; sites 262899 and 265346). Stage data were recorded hourly at each site

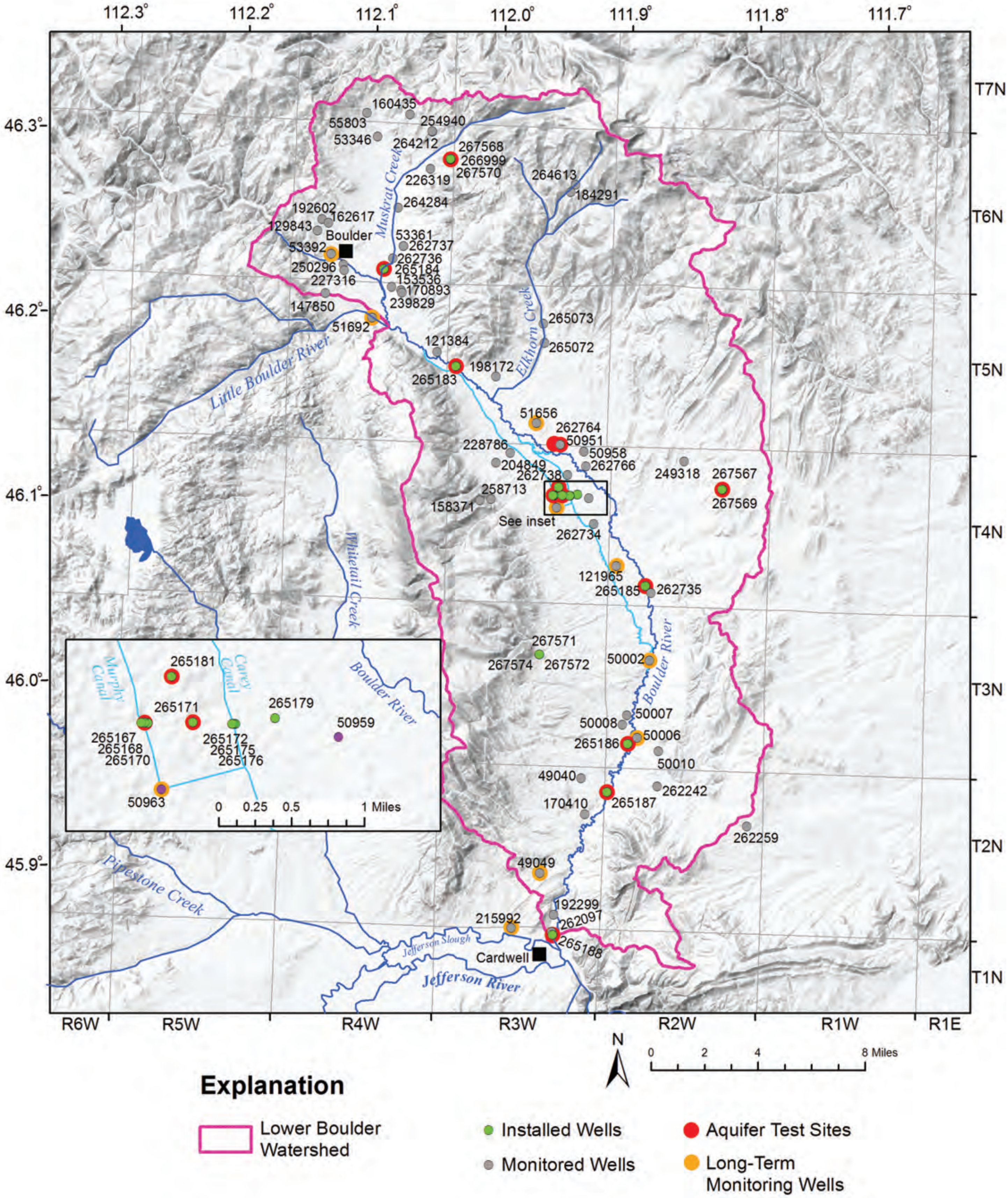

Figure 8. Twenty-three wells were installed at ten sites at which 13 aquifer tests were conducted. Seventy-eight wells were monitored monthly. There are 9 long-term monitoring wells from the Ground Water Assessment Act Monitoring (GWAAMON) network in or near the project area. See appendix A and GWIC for site details.

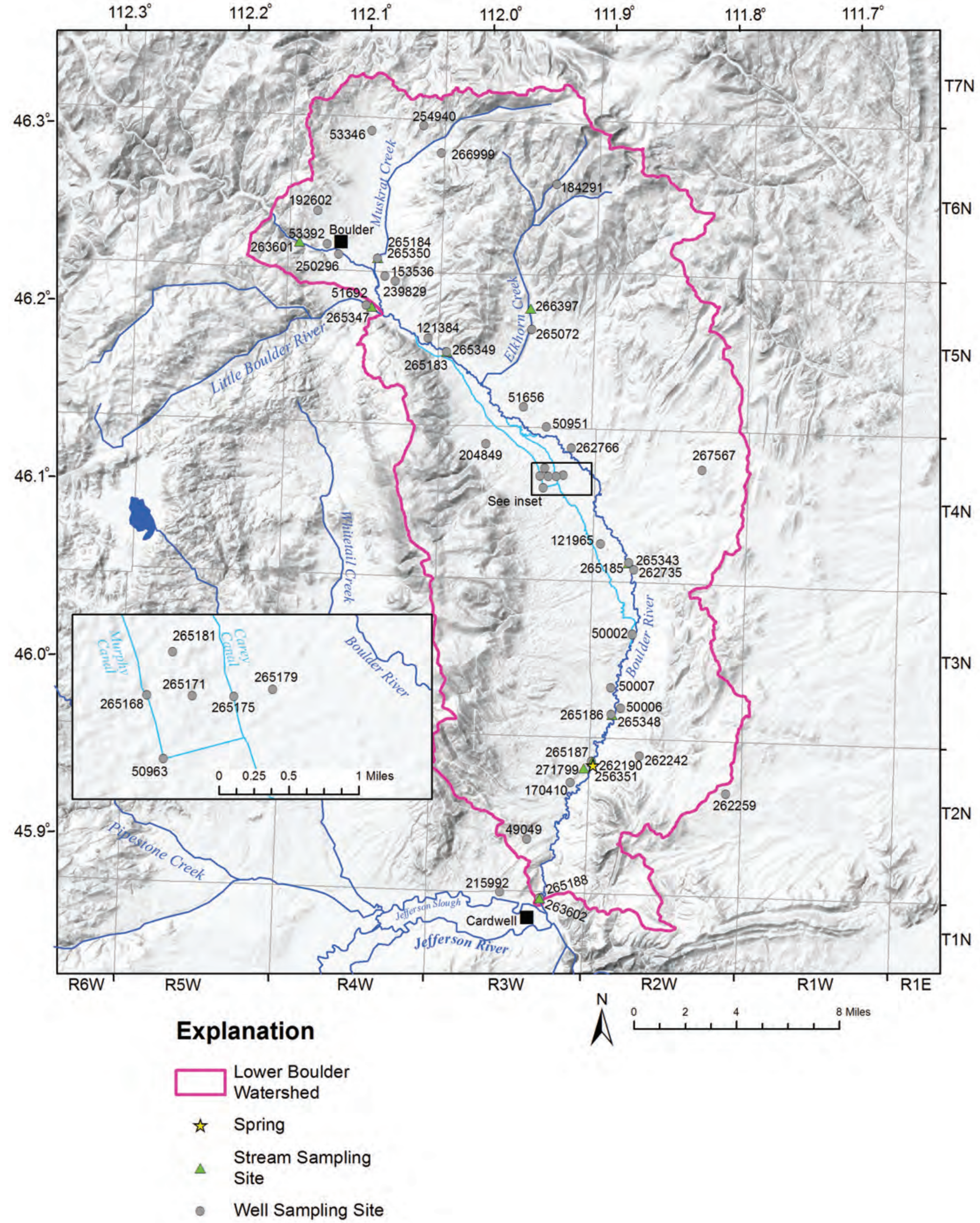

Figure 9. Water-quality samples were collected from 34 wells, 14 surface-water sites, and one spring.

Table 2. Recorded Mean Monthly Flows (cfs).

GWIC ID		263601	265943	265349	265344	265343	265348	262190	263602	265350	265347	266397	262899	265346	265345
Station Name		Boulder at I-15	USGS Boulder nr Boulder	Boulder at White Bridge	Boulder at Quantance	Boulder at Dunn Lane	Boulder at Boulder Cutoff	Boulder above Cold Springs	Boulder at Cardwell	Muskrat Creek	Little Boulder	Elkhorn Creek	Carey Canal at Flume*	Carey Canal at CT*	Murphy Canal at CT**
2011	July	NM	287.7	NM	NM	NM	NM	NM	NM	NM	NM	NM	NM	NM	NM
	Aug	NM	70.2	NM	NM	NM	NM	NM	NM	NM	NM	NM	NM	NM	NM
	Sept	61.6	33.7	NM	NM	NM	NM	49.5	79.3	NM	NM	NM	NM	NM	NM
	Oct	79.7	54.9	NM	NM	NM	NM	98.9	135.9	NM	NM	NM	NM	NM	NM
	Nov	NM	46.4	NM	NM	NM	NM	NM	NM	NM	NM	NM	NM	NM	NM
	Dec	NM	41.2	NM	NM	NM	NM	NM	NM	NM	NM	NM	NM	NM	NM
2012	Jan	NM	40.5	NM	NM	NM	NM	NM	NM	NM	NM	NM	off	off	off
	Feb	NM	39.8	NM	NM	NM	NM	NM	NM	NM	NM	NM	off	off	off
	March	162.8	83.3	247.4	NM	NM	115.5	124.1	148.7	8.9	25.9	NM	off	off	off
	April	358.9	222.2	487.8	365.7	317.0	379.6	349.2	382.0	7.0	46.0	NM	off	off	off
	May	429.9	420.5	450.6	322.3	252.0	330.4	313.2	349.1	5.4	32.9	NM	62.8	54.4	2.5
	June	319.7	303.5	308.1	256.0	172.7	237.7	229.8	261.7	5.4	31.8	7.9	60.1	51.2	6.0
	July	80.8	67.6	90.9	27.9	16.9	39.1	35.2	69.4	4.0	9.4	2.6	31.6	29.7	2.0
	Aug	28.1	24.0	35.9	0.0	1.1	10.0	5.9	25.1	3.1	2.8	1.7	25.1	22.2	0.2
	Sept	19.5	14.8	22.5	0.0	0.5	2.0	1.1	23.9	3.3	2.3	1.6	16.9	15.2	off
	Oct	27.0	29.8	39.9	1.3	6.7	7.8	7.9	50.1	4.6	4.9	2.0	22.9	19.7	off
	Nov	NM	37.7	NM	NM	NM	NM	NM	NM	NM	NM	NM	off	off	off
	Dec	NM	31.2	NM	NM	NM	NM	NM	NM	NM	NM	NM	off	off	off
2013	Jan	NM	28.3	NM	NM	NM	NM	NM	NM	NM	NM	NM	off	off	off
	Feb	NM	33.3	NM	NM	NM	NM	NM	NM	NM	NM	NM	off	off	off
	March	NM	40.8	NM	NM	NM	NM	NM	NM	NM	NM	NM	off	off	off
	April	102.8	96.0	195.3	NM	7.1	34.9	46.2	87.6	2.2	11.3	1.4	38.9	27.5	off
	May	365.2	370.0	420.0	NM	147.1	208.6	216.7	241.2	4.9	30.5	7.4	72.3	49.1	4.5
	June	216.8	231.9	275.2	NM	65.8	153.3	168.3	169.2	6.2	16.1	10.5	57.6	45.6	5.2
	July	55.5	46.2	NM	NM	NM	NM	NM	37.2	NM	NM	NM	35.8	26.8	off
	Aug	32.4	23.7	NM	NM	NM	NM	NM	19.5	NM	NM	NM	27.8	19.7	off
	Sept	36.1	27.2	NM	NM	NM	NM	NM	27.2	NM	NM	NM	17.5	12.6	off
	Oct	55.9	52.9	NM	NM	NM	NM	NM	91.9	NM	NM	NM	off	off	off

Note. NM, not monitored. Off, canal was off.

*Carey ditch was on from 5/3 to 10/3 in 2012; from 4/24 to 10/1 in 2013. Reported means for partial months are for the time the ditch was on (minimum 3 days on).
**Murphy ditch had flow at this location from 5/10 to 8/17 in 2012, and from 5/18 to 7/2 in 2013. Reported means for partial months are for the time the ditch was on (minimum 3 days on).

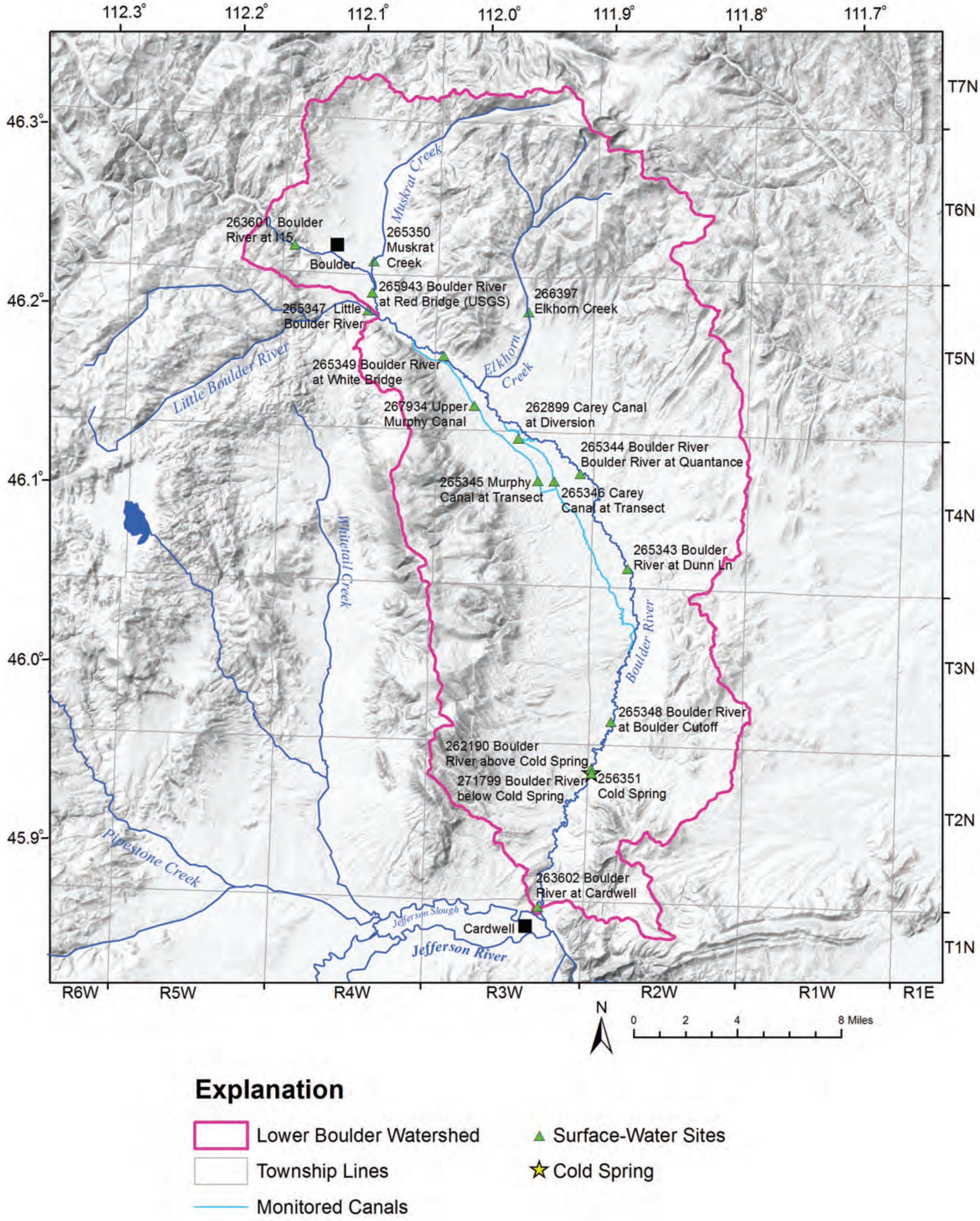

Figure 10. Surface water was monitored at 16 sites. One spring was also monitored.

during 2012 and 2013; rating curves, developed from bi-weekly discharge/stage measurements made in 2012, were used to calculate hourly discharge. Discharge could not be calculated from stage data collected in 2013 because the rating curves at both sites shifted and there were too few discharge measurements to develop new rating curves. There were no diversions between the stations. The net difference in hourly discharge was used to calculate hourly leakage rates. No time lag was used because flow rates were relatively stable.

The MBMG also monitored two sites on the Murphy canal (fig. 10). A surface-water station with a recorder was installed at site 265345 to measure hourly canal stages; discharge was measured at site 265345 in 2012 on the same schedule, as was discharge in the Carey canal. At site 267934, 4.0 mi upstream, the MBMG measured discharge approximately every 2 weeks. The net difference in flow between the stations was used to calculate leakage rates. There are no diversions between stations 265345 and 267934.

Monitoring wells were installed near the Carey and Murphy canals to document effects of canal leakage on groundwater levels (see inset box in fig. 8). Three sets of water samples were collected from a subset of these wells (see inset box in fig. 9; appendix B) in March (pre-irrigation season), June (early irrigation season), and August (late irrigation season) to document potential changes in groundwater chemistry. The results from canal leakage monitoring were used to develop the groundwater budget and the groundwater flow models.

Aquifer Tests

Thirteen aquifer tests were conducted in accordance with ASTM standards (ASTM, 2010) to determine a reasonable range of values for hydraulic conductivity and storativity (fig. 8). Six aquifer tests were conducted in the alluvium, five were in the fan sediments, one was in argillite bedrock, and one was in granitic bedrock (table 3). Nine aquifer tests, about 4 h long each, were done in wells with open bottom completions, providing rough estimates of aquifer properties. The other four tests were 2 to 3 days long in screened monitoring wells. Aquifer test details are available on GWIC (http://mbmggwic.mtech.edu/) by accessing the aquifer test data (DNRC form 633) and hydrologic assessment from the sites page for the pumping wells.

Data Management

Data collected for the Boulder Valley investigation are permanently stored in the MBMG's GWIC database. This database stores data for more than 242,000 water wells statewide, including information on well completions, groundwater levels, water chemistry, and aquifer tests. A list of monitoring sites with GWIC ID numbers is included in appendix A. GWIC is accessible online at http://mbmggwic.mtech.edu/

Table 3. Summary of Aquifer Tests

Name	Aquifer Type	Pumping Well GWIC ID*	Observation Wells?	Test Duration (h)
BLM Granite	Granite Bedrock	267570	Yes	47
Muskrat Creek	Alluvium	265184	No	4
White Bridge	Alluvium	265183	No	4
Hand Dug	Fan	262764	Yes	72
Pond Site	Fan	50951	Yes	72
Dunn Lane	Alluvium	265185	No	4
Boulder Cutoff	Alluvium	265186	No	4
Cold Spring	Alluvium	265187	No	4
Cardwell	Alluvium	265188	No	4
BRV Argillite	Argillite Bedrock	267569	Yes	72
CT2	Fan	265168	Yes	4
CT4	Fan	265171	No	4
CT9	Fan	265181	No	4

*Aquifer test details are available on GWIC by accessing the aquifer test data (DNRC form 633) and hydrologic assessment from the pumping well's site page.

Numerical Modeling

Purposes

The MBMG developed two numerical groundwater models:

• The Area-Wide model evaluates impacts from increased groundwater development caused by new housing developments (Butler and Bobst, in prep.).

• The Managed-Recharge model tests the potential for using managed recharge through infiltration basins fed by the Murphy canal to enhance late-summer Boulder River stream flows (Carlson, 2013).

Data Used

The numerical models were developed based on observed groundwater and surface-water elevations, surface-water flows, aquifer test results, and the groundwater budgets. The calibration data set for the Area-Wide model was collected from July 2011 to June 2013. The Managed-Recharge model was calibrated to data collected from March to December of 2012.

Software Used

MODFLOW-NWT (NWT) was used for the Area-Wide model and is a Newton–Raphson formulation for MODFLOW-2005 that provides stability under nonlinear unconfined flow conditions (Niswonger and others, 2011). NWT uses the Upstream-Weighting Package (UPW) as a solver. Groundwater Vistas (Vistas) was used as the graphical user interface (Environmental Simulations Incorporated, 2011; v. 6.59 Build 1), and PEST was used for automated parameter estimation (v. 13.0; Doherty, 2010, 2013).

The Managed-Recharge model used MODFLOW-2000 (Harbaugh and others, 2000) with the Preconditioned Conjugate-Gradient 2 (PCG2) solver (Hill, 2003). Groundwater Modeling System (GMS; Aquaveo, 2010, v. 8.3) was used as the graphical user interface and PEST was used for automated parameter estimation (v. 13.0; Doherty, 2010, 2013).

Model Designs

Area-Wide Model. The Area-Wide model's active grid covered an area of approximately 377 mi^2 (fig. 11). Grid cells measured 400 ft by 400 ft horizontally (3.7 acres each). The top of the model was based on the National Elevation Dataset model (NED; USGS, 1999), with a resolution of 1/3 arc second (~10 m). The top of the model was adjusted where surveyed elevations significantly deviated from the NED.

The bottom of the model was set at 200 ft below the valley bottom, resulting in a sloping plain from north to south. This thickness included the active alluvial aquifer, and it maintained a reasonable thickness to aid parameter estimation.

The model used a single layer that ranged from 193 to 4,713 ft (188 to 3,332 ft of saturated thickness). The single layer optimized solution stability, parameter estimation, and model run times. A single layer was also appropriate as there are no known regional aquitards. Although multiple layers in the floodplain alluvium could have allowed more detailed representation of flux to and from the riverbed, thin shallow layers would have caused a high rate of cell drying and rewetting at the interface between the alluvium and the fan deposits, thus increasing numerical instability. Furthermore, a separate deep layer would have no observation points, because wells are typically completed in the shallow alluvium.

The steady-state numerical model simulated average annual conditions for all elements of recharge and discharge. The simulation was calibrated to mean annual water-level altitudes calculated for 63 wells, based on observations from January 2012 to January 2013. Observed stream flows at 8 stations during 2012 were also used. The steady-state model represents the system in equilibrium under a specified set of stresses and is the baseline against which changes caused by new stresses can be compared.

The transient numerical model used the calibrated steady-state model as its first stress period. Subsequent stress periods were monthly, with five time steps each. The transient model was calibrated from April 2010 to April 2013 (37 stress periods). The transient simulation started prior to the study period to allow the aquifer system to respond to recharge conditions that occurred immediately before and early in the study period. During the pre-study period, water-level measurements from MBMG long-term monitoring wells (http://www.mbmg.mtech.edu/gwap/grw-assessment.asp), and flow/stage measurements from the USGS station at Red Bridge (USGS station 06033000; fig. 10) were used for calibration.

The calibrated transient model was modified to

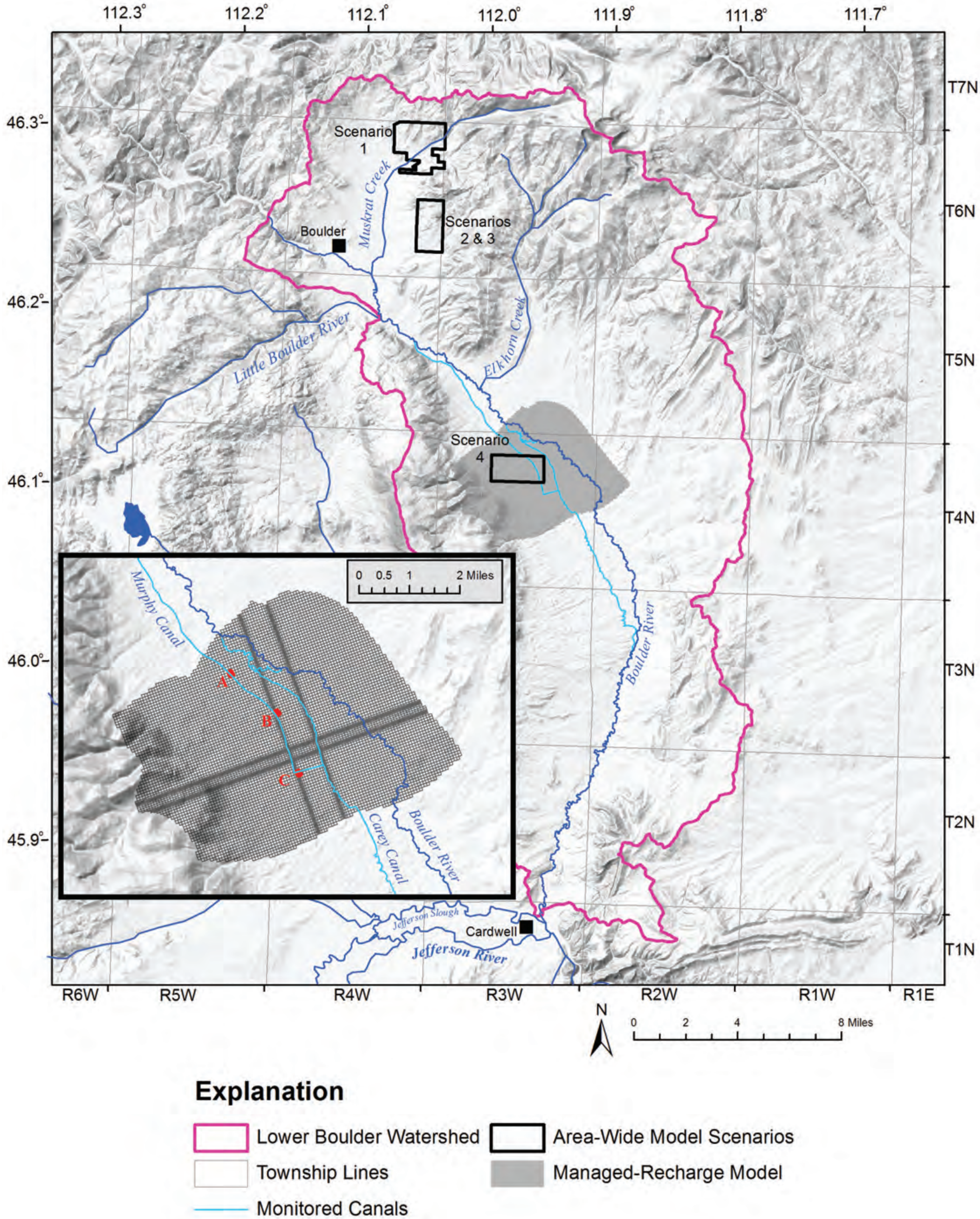

Figure 11. The Area-Wide model covered the entire study area. Four groundwater development scenarios at the locations shown were simulated with the Area-Wide model. The Managed-Recharge model covered a limited area (see inset box) and was used to simulate seven managed-recharge scenarios.

increase the monthly stress periods to 240 (20 yrs) and boundary conditions were assigned based on average rates from 1981 to 2010. The baseline 20-yr model was used to simulate four hypothetical future housing development scenarios (fig. 11).

Managed-Recharge Model. The Managed-Recharge model's active grid covered an area of approximately 17 mi^2 (fig. 11). The base grid cell size was 150 by 150 ft horizontally, but was adjusted to 25 by 25 ft near densely located monitoring wells. Grid cell size was adjusted away from the dense areas using a 1.5 multiplier until reaching the base grid size. The top of the model was based on the NED (USGS, 1999), but was adjusted where surveyed elevations significantly deviated from the NED. The model bottom was set 200 ft below the potentiometric surface to give a consistent saturated thickness, incorporate the most active part of the flow system, and limit the model extent to where head observations were available. The model was built using one layer to optimize solution stability, parameter estimation, and model run times. A single layer is also appropriate because there are no known aquitards.

The steady-state numerical model simulated average annual conditions for all elements of recharge and discharge. The simulation was calibrated to observed groundwater levels from 19 wells in April 2012. To aid in calibration, two control points based on the potentiometric surface map were included. The steady-state model represents the system in equilibrium under a specified set of stresses and is the baseline against which changes caused by new stresses can be compared.

The transient simulation was derived from the steady-state model and used 26 2-week stress periods, with two time steps each. The transient model simulated the period from April 2, 2012 to April 1, 2013 and was calibrated using data collected between April and December 2012.

The calibrated transient simulation was modified to use 240 1-mo stress periods (20 yr), with 2 time steps each. The baseline scenario and scenario 1 (see below) were also run using 10 time steps per stress period. The results did not differ significantly, so the more efficient 2-time-step version was used for all runs. The MBMG then used the baseline 20-yr model to test seven managed recharge scenarios that included a variety of infiltration basin sizes and locations, and termination of canal leakage (fig. 11).

RESULTS

Hydrogeologic Setting

The geologic formations of the Boulder River study area can be assigned to eight hydrogeologic units (fig. 12): Precambrian sedimentary rocks of the Belt Supergroup; carbonate rocks (Cambrian to Permian); siliciclastic rocks (Jurassic and Cretaceous); intrusive rocks (Cretaceous "granite"); volcanic rocks (Cretaceous); fine unconsolidated deposits (Tertiary Renova Formation); unconsolidated gravel (Tertiary and Quaternary alluvial fans, including the Tertiary Sixmile Creek Formation); and alluvium (Quaternary) (fig. 12). The eight units can be grouped into: Precambrian to Cretaceous bedrock; Tertiary to Pliocene sediments (Renova and Sixmile Creek Formations as well as thin Late Pliocene to Pleistocene gravels), and Quaternary alluvium.

Although the hydrogeologic units have different aquifer properties, they readily exchange water and there are no known regional aquitards. Fractures and solution voids in the bedrock units are extensive, and when viewed at the study area scale, can be treated as equivalent porous media. At the scale of the study area the hydrogeologic units function as one aquifer system.

Bedrock

The consolidated bedrock units have little primary permeability, and water moves through, and is extracted from, fractures and solution voids. At local scales, bedrock fracture and void geometries strongly affect groundwater flow patterns, and the amount of water produced by a well is determined by the number of saturated fractures and voids encountered, the width of those openings, and how well the openings are interconnected.

The carbonate rocks differ from other bedrock units in that they are more susceptible to dissolution and re-precipitation of carbonate minerals (e.g., calcite). Where dissolution occurs, fractures widen to improve permeability. Permeability decreases where minerals are re-precipitated.

An aquifer test in the granite (table 3) showed that hydraulic conductivity (K) was about 1.2 ft/d and stor-

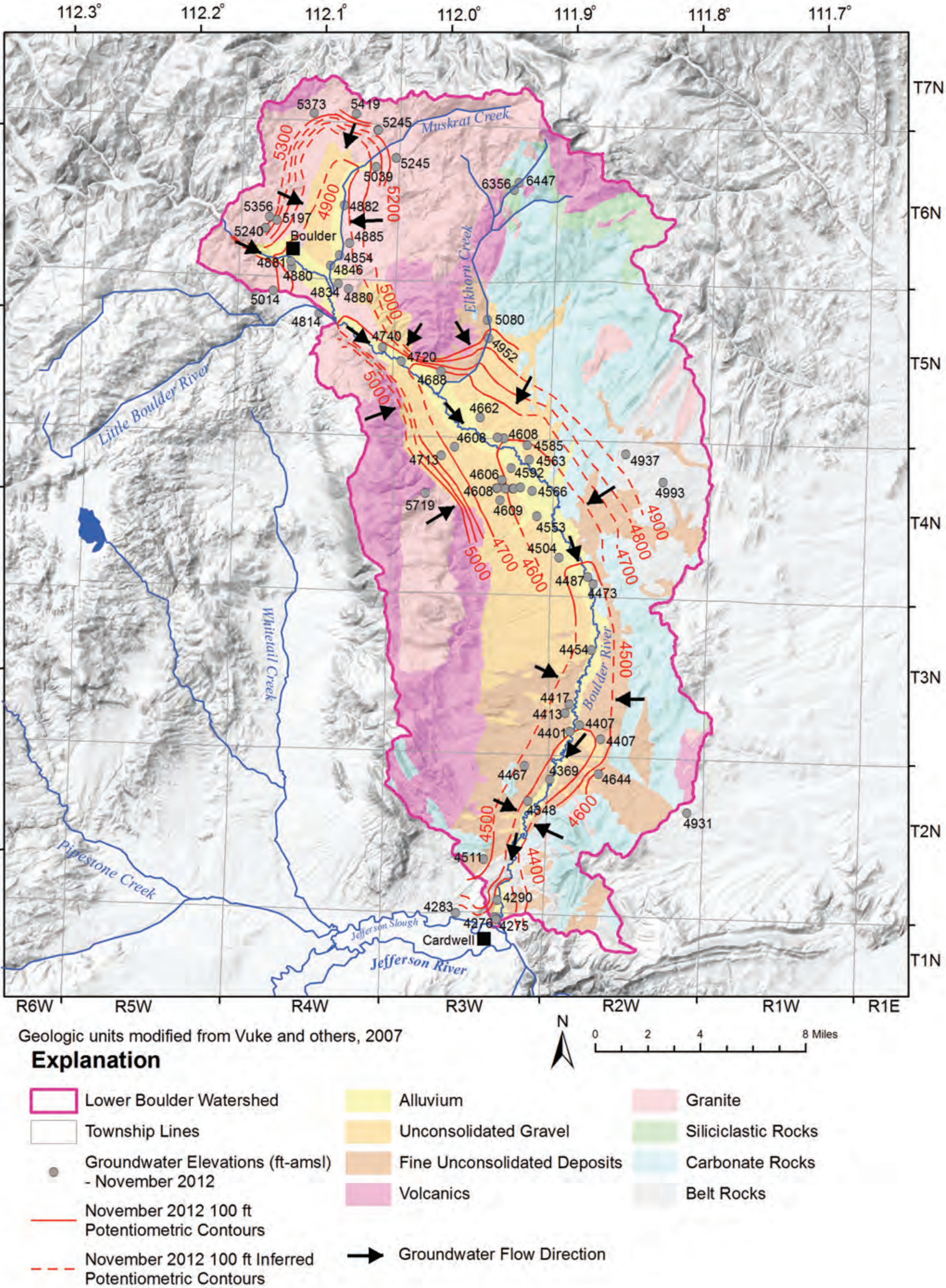

Figure 12. The geologic units within the Boulder River study area can be grouped into eight hydrogeologic units. The eight units fall into three general groups for numerical modeling purposes: Quaternary alluvium; Tertiary to Pliocene sediments; and upland bedrock. Groundwater-level monitoring from November 2012 shows that the potentiometric surface is generally a subdued representation of the land surface.

ativity (S) was about 0.0001. This hydraulic conductivity value is similar to conductivities obtained from aquifer tests in granite aquifers near Helena, Montana, which ranged from 0.001 to 14 ft/d. The geometric mean of the Helena conductivities was 0.18 ft/d (Bobst and others, 2014).

An aquifer test in the highly fractured Greyson Formation (Precambrian Belt Supergroup; table 3) produced a K of about 75 ft/day. Tests in Helena-area wells completed in argillite of the Belt Supergroup produced a range of K from 0.1 to 163 ft/d—the geometric mean was 3.7 ft/d (Bobst and others, 2014). The hydraulic conductivity obtained in the Boulder Valley was near the upper end of the range of conductivities measured near Helena, consistent with expectations based on the highly fractured rock in which the wells were completed.

Tertiary to Pliocene Sediments

Tertiary to Pliocene sediments make up most of the basin-fill in the Boulder Valley. Basin-fill is reported to be more than 4,000 ft thick in the central Boulder Valley, and the Quaternary alluvium is seldom more than 100 ft thick (Nobel and others, 1982). Erosional and angular unconformities separate the Tertiary sediments from the underlying and adjacent bedrock formations. The Tertiary basin-fill deposits crop out between the alluvium of the modern floodplain and bedrock along the mountain front. Landforms on the basin-fill include alluvial fans built to create a slope of transportation where streams enter the valley and pediments. The basin fill includes the Renova and Sixmile Creek Formations of the Bozeman Group, and a thin cap of Late Pliocene to early Pleistocene gravel (Lofgren, 1985). The Renova Formation is generally composed of >70 percent very fine sand and finer materials (Kuenzi and Fields, 1971; Vuke and others, 2004) and is mainly motmorillonitic mudstone and siltstone. Within this fine-grained matrix, the Renova contains lenses of conglomerate and sandstone. The Renova is interpreted to have been deposited in low-energy floodplain and pond environments (Kuenzi and Fields, 1971). The Sixmile Creek Formation unconformably overlies the Renova, and may be up to 600 ft thick. The Sixmile Creek Formation is typically fine sand and coarser materials (Kuenzi and Fields, 1971; Vuke and others, 2004), and is interpreted to have been deposited in fluvial environments (Kuenzi and Fields, 1971).

These poorly consolidated deposits have some intergranular primary permeability, so are generally more productive than bedrock aquifers. The five aquifer tests at wells completed in the Sixmile Creek Formation (table 3) produced hydraulic conductivities ranging from 22 to 750 ft/d; the geometric mean was 159 ft/d. Storativity in the Sixmile Creek ranged from 0.00032 to 0.03, indicating semi-confined to unconfined conditions (Freeze and Cherry, 1979, p. 60–61).

Quaternary Alluvium

Unconsolidated Quaternary gravel, sand, and some silt underlies the modern floodplain and is less than 100 ft thick (Nobel and others, 1982; Kendy and Tresch, 1996). Two aquifer tests at wells completed in alluvium near Boulder, Montana (Botz, 1968), resulted in hydraulic conductivities of 740 and 770 ft/d. Six aquifer tests conducted for this study at wells completed in alluvium (table 3) produced hydraulic conductivities from 6 to 850 ft/d; the geometric mean was 85 ft/d.

Cold Spring

Cold Spring is the most productive spring in the study area, with an average measured flow of 31 cubic feet per second (cfs). This flow is comparable to the winter flow in the Boulder River at the USGS gauge near Boulder (Red Bridge; 06033000). Montana FWP has identified Cold Spring as the lower boundary of the chronically dewatered reach of the Boulder River. The temperature of Cold Spring is relatively constant, varying from 10.1°C to 13.6°C, and averaging 11.5°C between March 16 and October 22, 2012. There are daily variations in temperature at the outflow that peak at about 2 pm and are coldest at about 3 am.

Groundwater Levels

Potentiometric Surface

The MBMG generated a potentiometric surface map for the Boulder Valley study area based on data collected in November 2012 (fig. 12). The study area scale, lack of regional confining layers, and relatively uniform primary/secondary permeability cause the different hydrogeologic units to act as one flow system. Therefore, use of groundwater elevations from different hydrogeologic units to evaluate the hydrogeology is appropriate. The lack of wells in areas outside of the floodplain aquifer limits potentiometric surface detail in the uplands (fig. 7). At this map scale local deviations of groundwater flow caused by fractures, faults, bedding planes, and differences in permeability are not visible. Potentiometric contours also shift seasonally, but changes are not noticeable at this map scale and contour interval.

The potentiometric surface shows that groundwater flows from the topographic highs towards the center of the valley (fig. 12). In the valley bottom, groundwater either flows into the Boulder River, if that reach is gaining water, or flows parallel to the river within the alluvium. Alluvial groundwater is eventually forced into the river at locations where the alluvium thins at bedrock notches (fig. 2) and transmissivity decreases. A small amount of groundwater flows out of the study area through the alluvium.

Hydrograph Trends

Groundwater-level trends during the study period (2011–2013) vary depending on the hydrogeologic setting. For wells completed in and near the irrigated floodplain, groundwater levels generally showed little net change, but water levels rise each spring in response to high river stages and irrigation (fig. 13). Water levels in wells completed in the Tertiary to Pliocene sediments had a net drop during the study period, although wells completed near irrigation canals responded when the canals were turned on (fig. 14). The water-level decline appears to follow the transition from wet to dry conditions beginning in 2010 (fig. 5). Wells completed in bedrock also show a consistent water-level drop during the study period; the magnitude of the drop in the bedrock wells is typically greater than that for wells in the Tertiary to Pliocene sediments (fig. 15).

Long-term data (19–22 yrs) were available from nine wells in or near the study area (fig. 8). Seven of these sites (wells 49049, 50002, 50006, 51656, 51692, 121965, and 215992) show slight downward groundwater-level trends over the period of record (fig. 16). Water levels in the other two wells (wells 50963 and 53392; fig. 17) declined more steeply. During the 10-yr period from 2004 to 2013, eight of these sites showed a slight rise in groundwater levels, and the other well (53392) dropped at a much reduced rate. The long-term declines are most likely due to the generally drier period that began in 1997 (fig. 4). The slight rises since 2004 likely result from the somewhat wetter climate since 2004 (fig. 4).

Groundwater/Surface-Water Interactions

At sites where groundwater elevations are lower than stream-surface elevations, water will flow from the stream to groundwater (losing stream). Where groundwater levels are higher than stream-surface elevations, water will flow from groundwater to the stream (gaining stream; Winter and others, 1999; Brunner and others, 2009). Understanding where streams are gaining or losing, and knowing the magnitudes of the gains and losses, is important for understanding groundwater flow paths and the groundwater budget.

Groundwater and surface-water temperatures can aid in understanding groundwater/surface-water exchange. Surface-water temperatures in the Boulder Valley typically range from 0 to about 25°C annually, with daily fluctuations of several degrees due to changing air temperatures. Groundwater not directly affected by surface-water inflow is typically isolated from daily temperature variations and only shows slight seasonal temperature changes. Therefore, this groundwater is typically cooler than surface water when air temperatures are warm, and warmer than surface water when air temperatures are cold.

At sites where streams are losing, infiltrating surface water will transport heat downward by conduction and advection, causing a thermal signal to be transmitted to groundwater. At locations where streams are gaining, groundwater flow into the stream will dampen diurnal and seasonal temperature variation in the stream, and the stream's thermal signal will not be conducted deeply into the ground. The amount of stream temperature dampening depends on the temperature difference between the surface water and groundwater, and the amount of each that is mixed. It is often difficult to measure this buffering because the magnitude of groundwater inflow is typically much less than the stream flow (Constantz and Stonestrom, 2003; Constantz, 2008; Eddy-Miller and others, 2009; Caldwell and Eddy-Miller, 2013).

Dampening Surface-Water Temperature Variation

Seasonal surface-water temperatures generally follow air temperatures, but diel (24-h) changes are more subdued. In 2012 and 2013 seasonal air temperatures in the Boulder Valley varied from -32°C to 33°C, and averaged 6°C (MesoWest, 2014; fig. 18). Seasonal surface-water temperatures in the Boulder

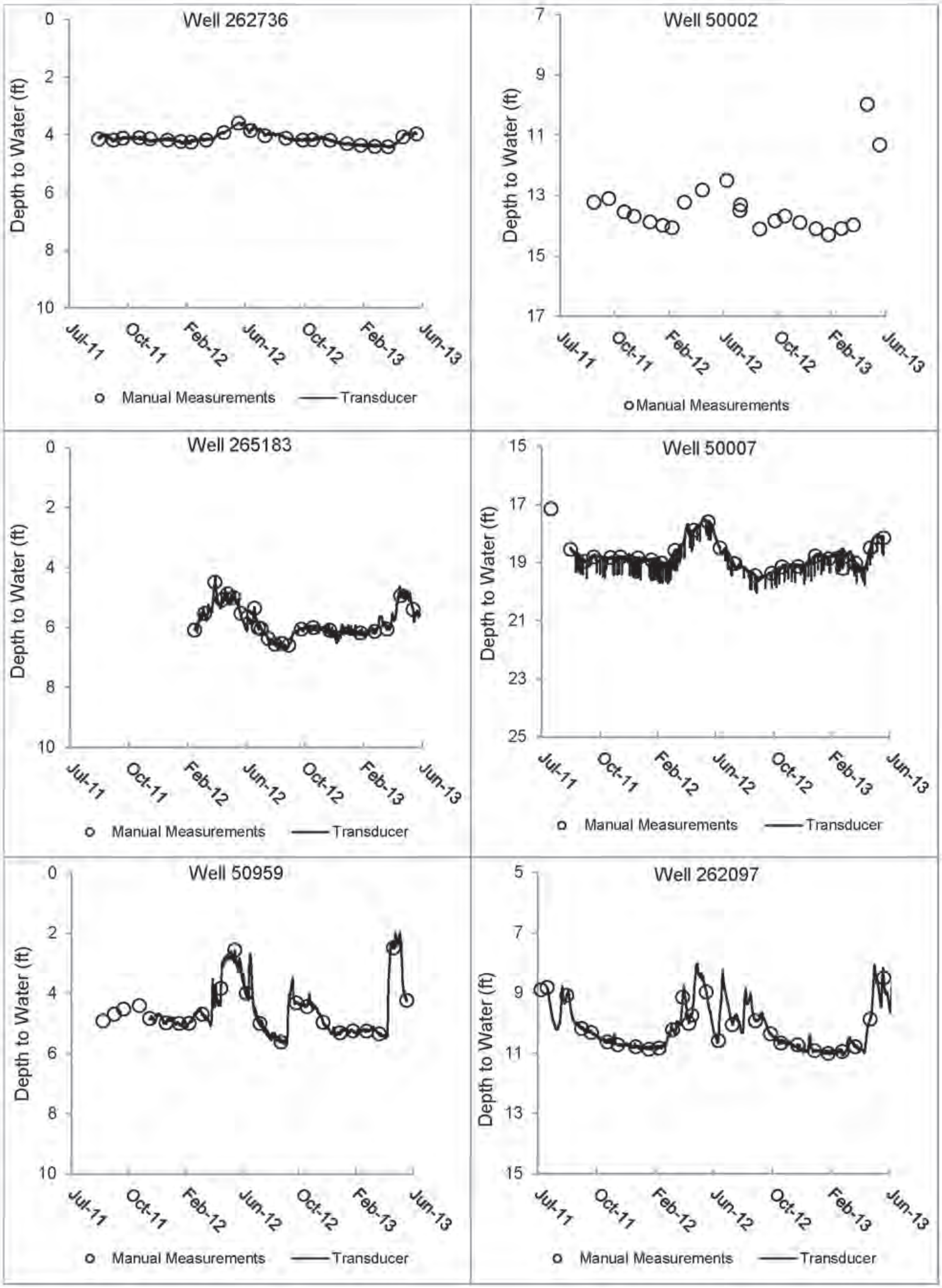

Figure 13. Hydrographs from wells completed in the irrigated floodplain showed that there was little net change in water levels during the study; however, water levels rose noticeably each spring.

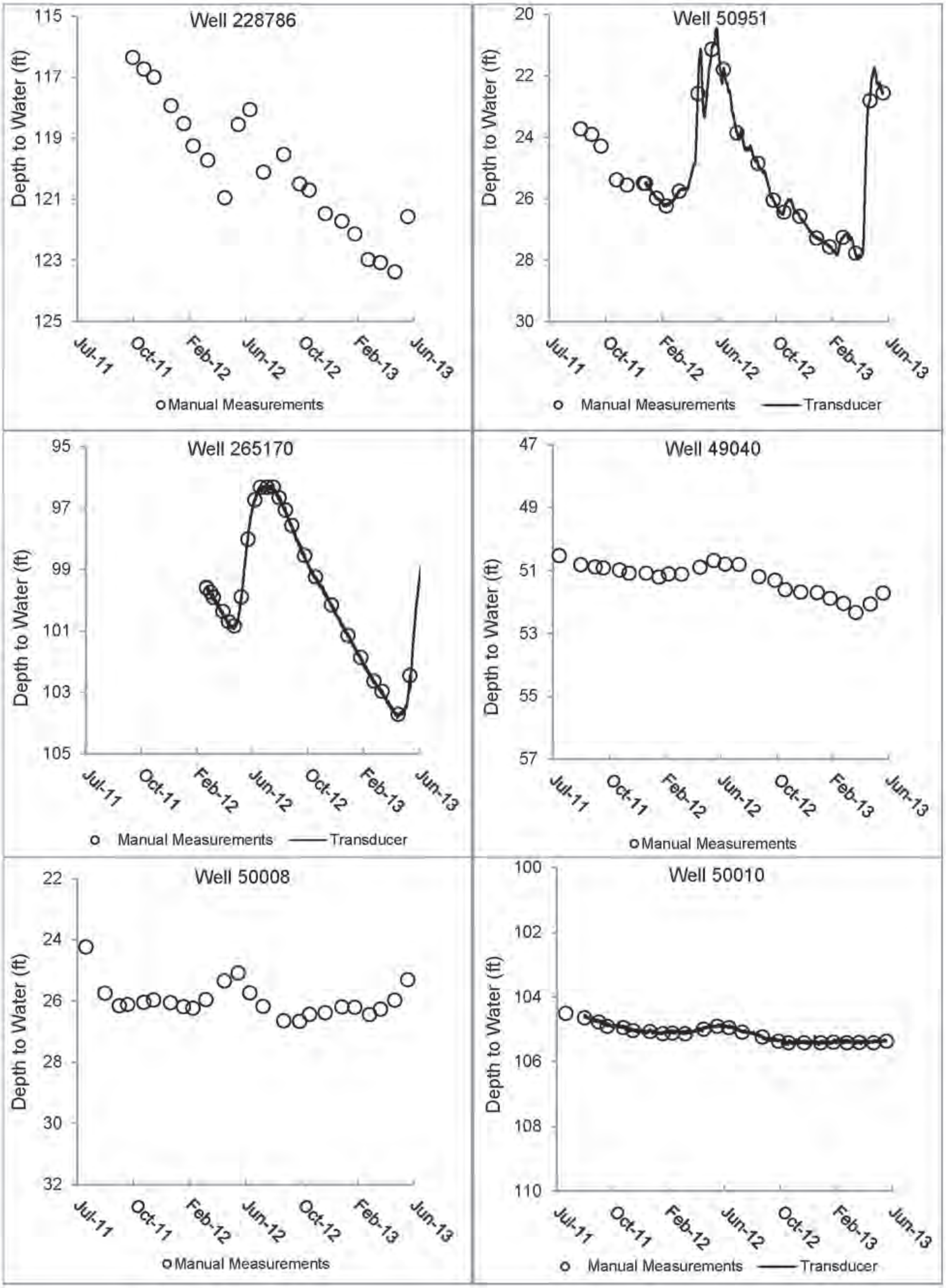

Figure 14. Hydrographs from wells completed in Tertiary basin-fill showed that water levels generally declined during the study. Water levels in wells located near and below irrigation canals rose markedly each spring, but rose slightly in wells distant from irrigation.

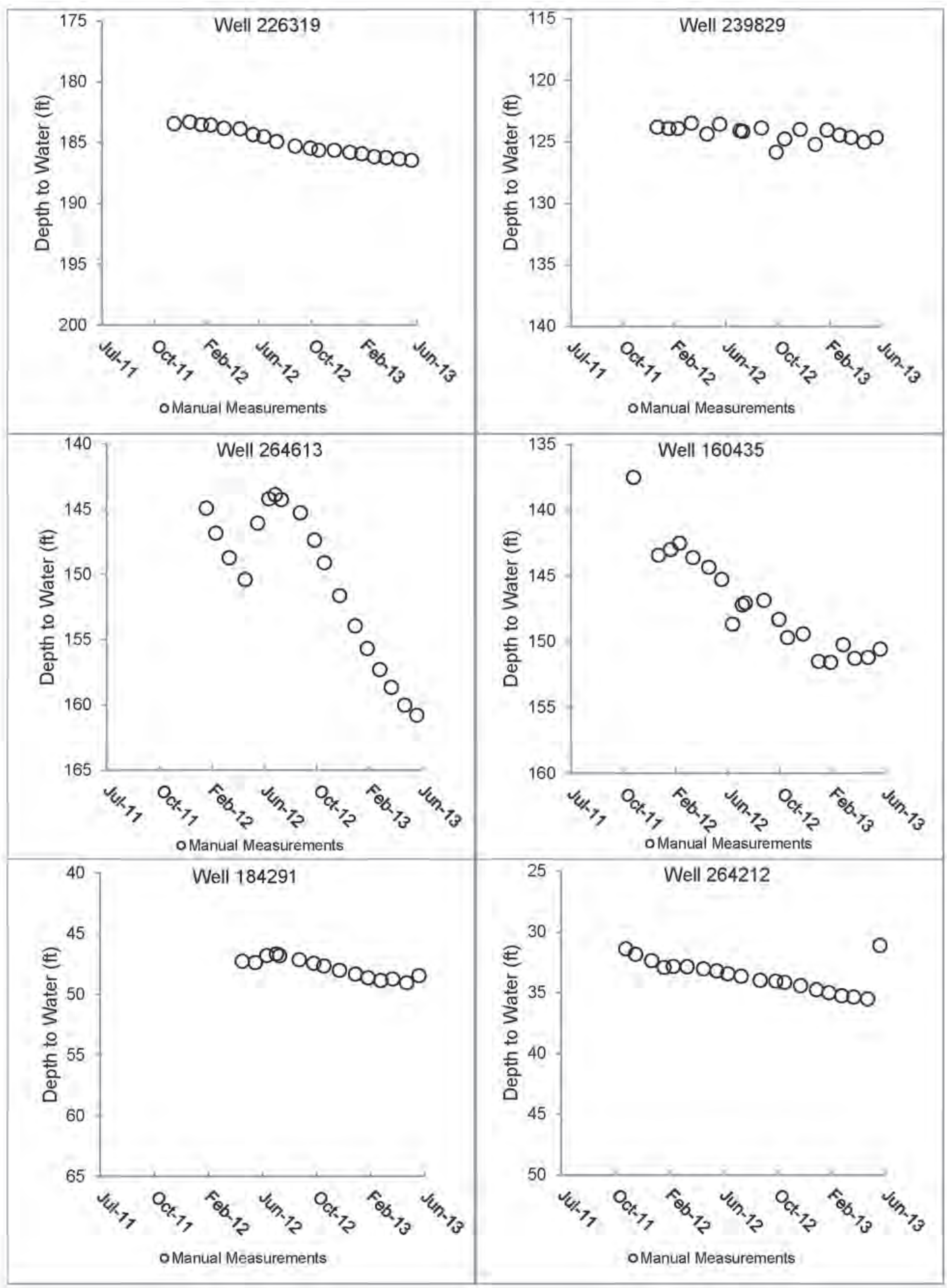

Figure 15. Hydrographs from wells completed in bedrock show that water levels generally declined during the study period.

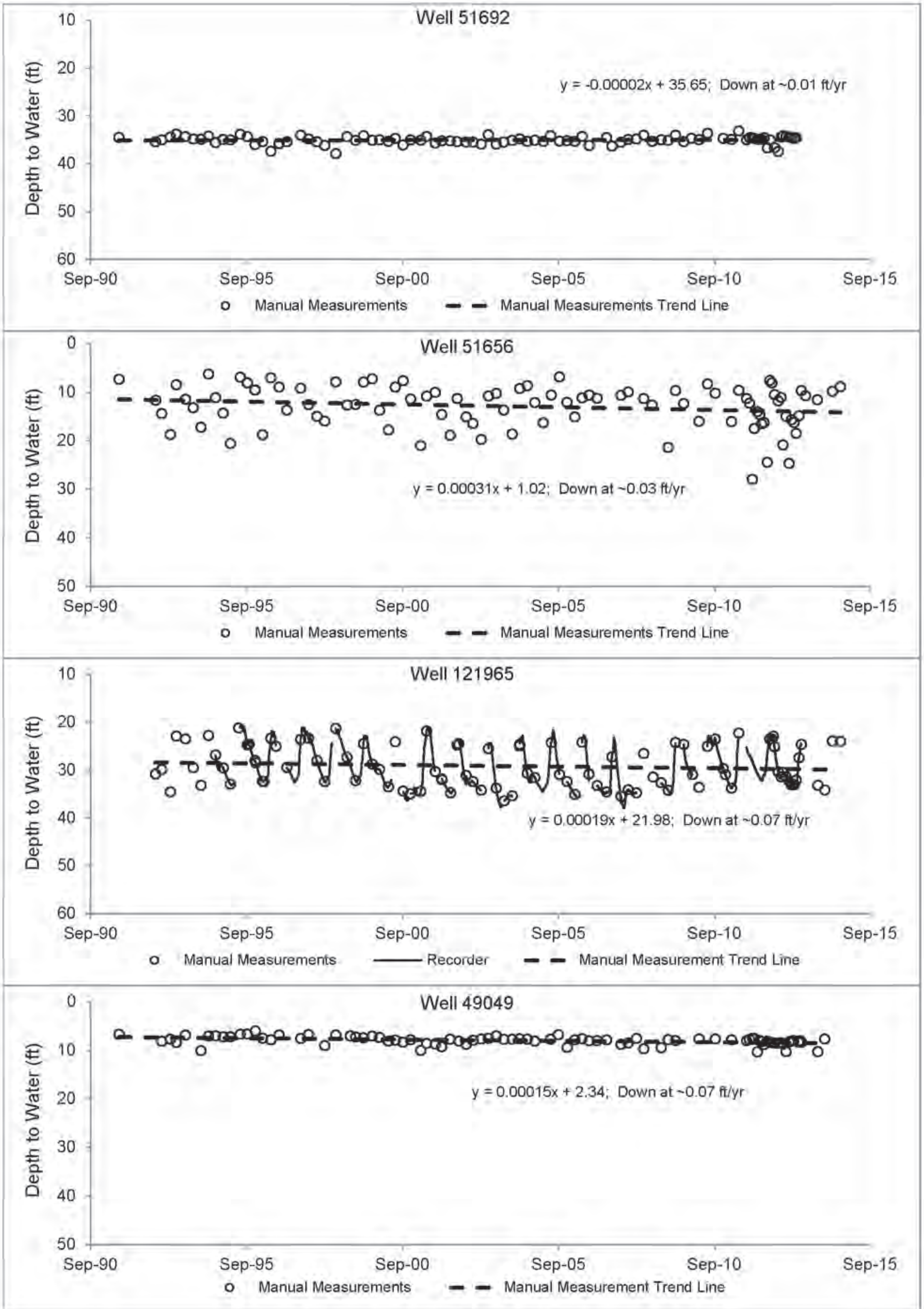

Figure 16. Most long-term hydrographs in the study area show slight downward trends.

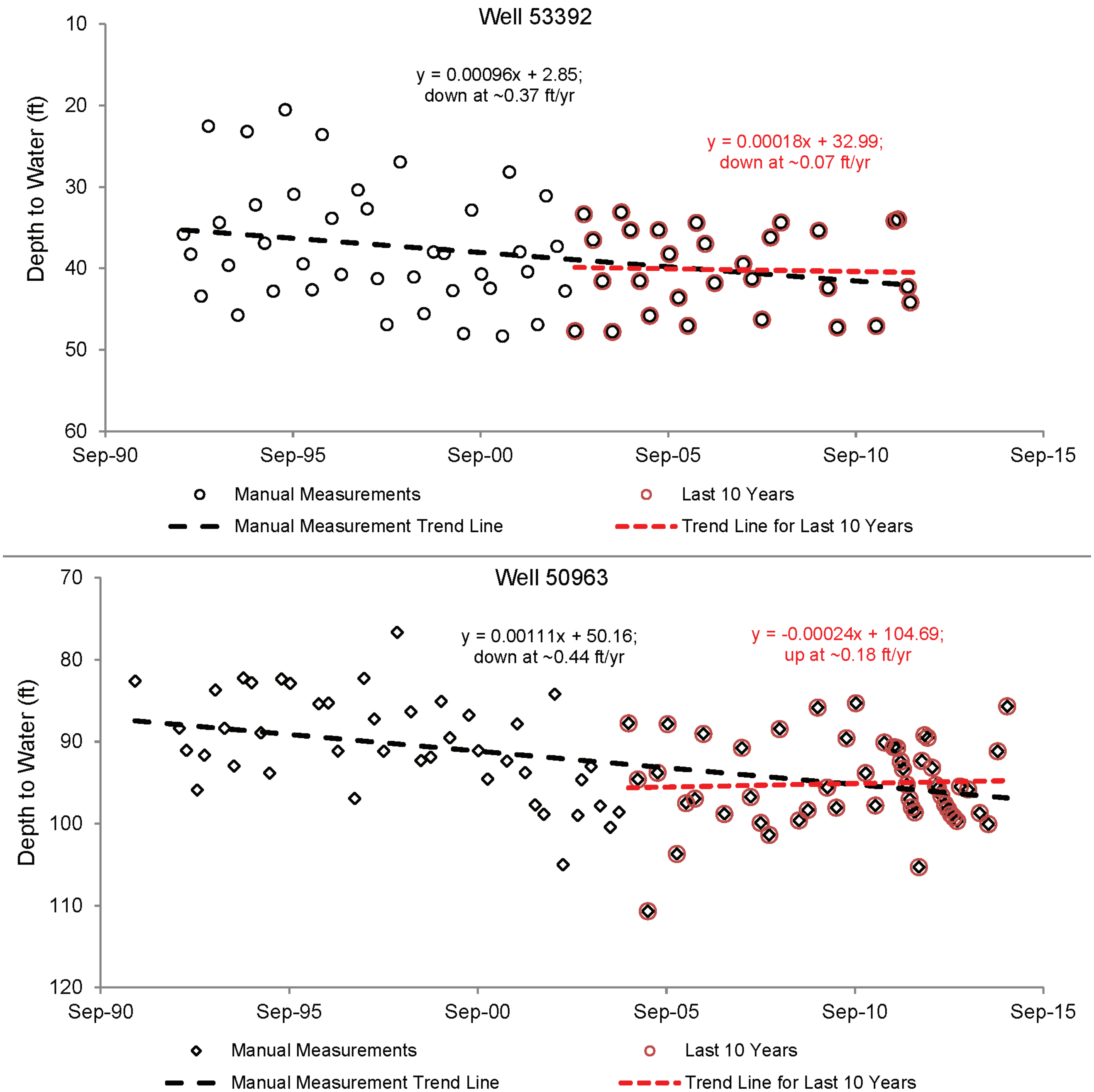

Figure 17. The two hydrographs with the most pronounced decline over the period of record have both been stable for the past 10 years. It appears that the observed groundwater-level declines result from the drier period that began in about 1998 (fig. 4).

River ranged from 0°C to 25°C. Daily temperature changes in surface water were as large as 21°C and were greatest when flows were low. The magnitude of diel variations was similar at all surface-water stations, so any groundwater inflow that might dampen the diel temperature signal appears insignificant. Detection of a measurable signal would require high groundwater inflows at or immediately upstream of the monitoring station (Caldwell and Eddy-Miller, 2013).

Temperature and Water-Level Data

The MBMG installed five wells at sites along the Boulder River and one well at a site on Muskrat Creek just above its confluence with the Boulder River (fig. 8), and instrumented them to measure groundwater levels and temperature (wells 265183, 265184, 265185, 265186, 265187, and 265188). Surface-water stages and temperatures were collected from April to October 2012 at all six sites (surface-water stations 265350, 265349, 265343, 265348, 262190, and 263602; fig. 10). In 2013, surface-water data were again collected from April to June at the same stations, but at station 236602 the data were collected from April to October.

Only the Boulder River at Boulder Cutoff Station

Table 4. Interpretation of Stream and Groundwater Elevation and Temperature Data

Site Name	Well	Surface-Water Station(s)	Gaining or Losing
Muskrat Creek	265184	265350	Gaining
Boulder at White Bridge	265183	265349	Losing
Boulder at Dunn Lane	265185	265343	Losing
Boulder at Cutoff	265186	265348	Gaining
Boulder at Cold Spring	265187	262190 256351	Gaining
Boulder at Cardwell	265188	263602	Gaining

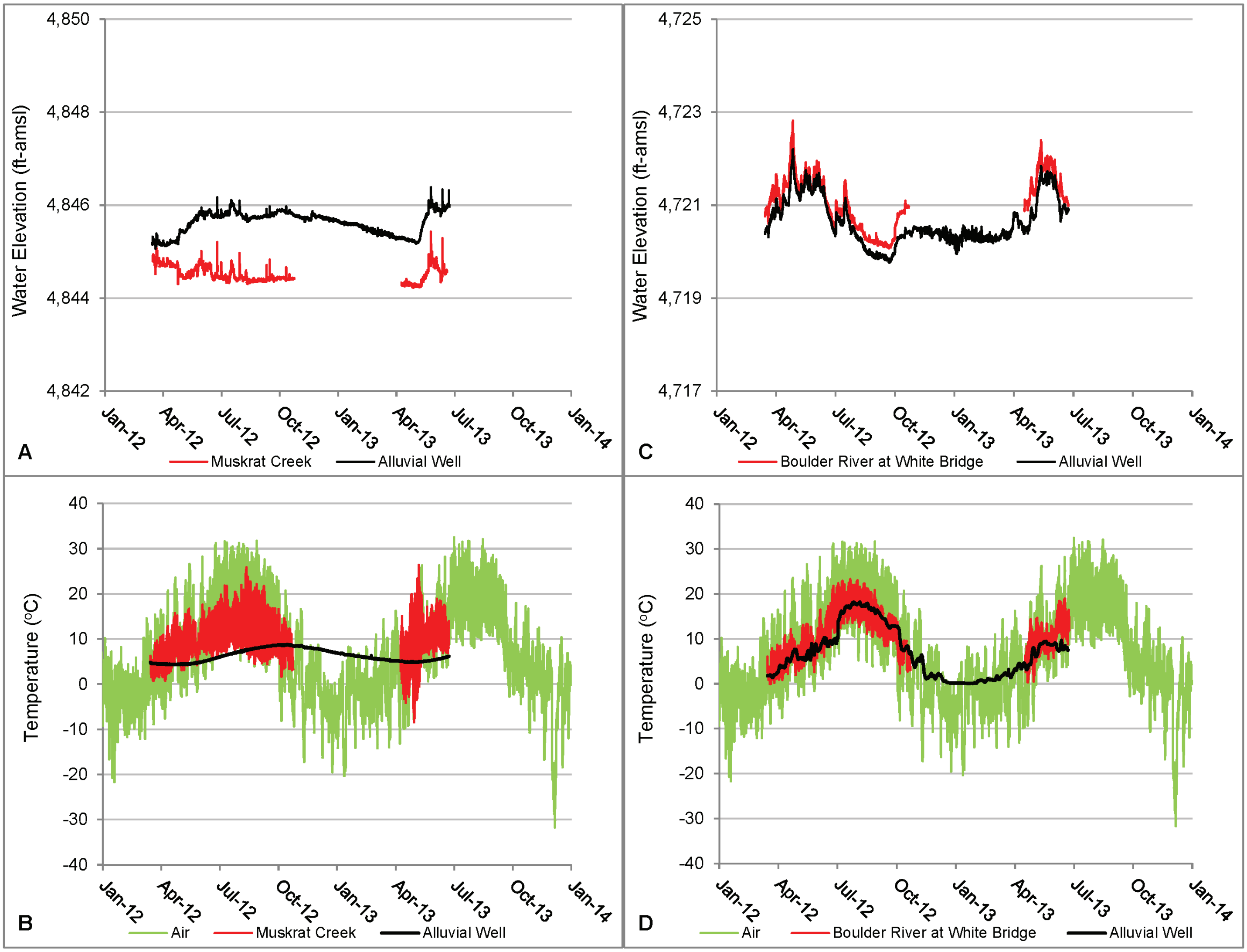

Figure 18. At the Muskrat Creek sites (265350 and 265184), groundwater elevations were always higher than stream elevations (A) and groundwater temperatures showed slight seasonal variations (B). At the White Bridge sites (265349 and 265183), groundwater elevations were always lower than stream elevations (C) and groundwater temperatures closely followed surface water temperatures (D).

(265348; fig.10) showed a change in the direction of flow by season, and the short-term change was not reflected in the temperature data. Data from the other stations showed that at each location the river was either gaining or losing water during the entire period of record (table 4 and figs. 18–20). Streams often change from gaining to losing over short distances, so each site's results are specific to that particular location (Winter and others, 1999).

Synoptic Flow Comparisons

Because ephemeral tributaries, many irrigation diversions, and tail water returns were not monitored, synoptic flow comparisons only showed net gains or losses. Early in the irrigation season, measurements showed that net losses to stream flow were largest,

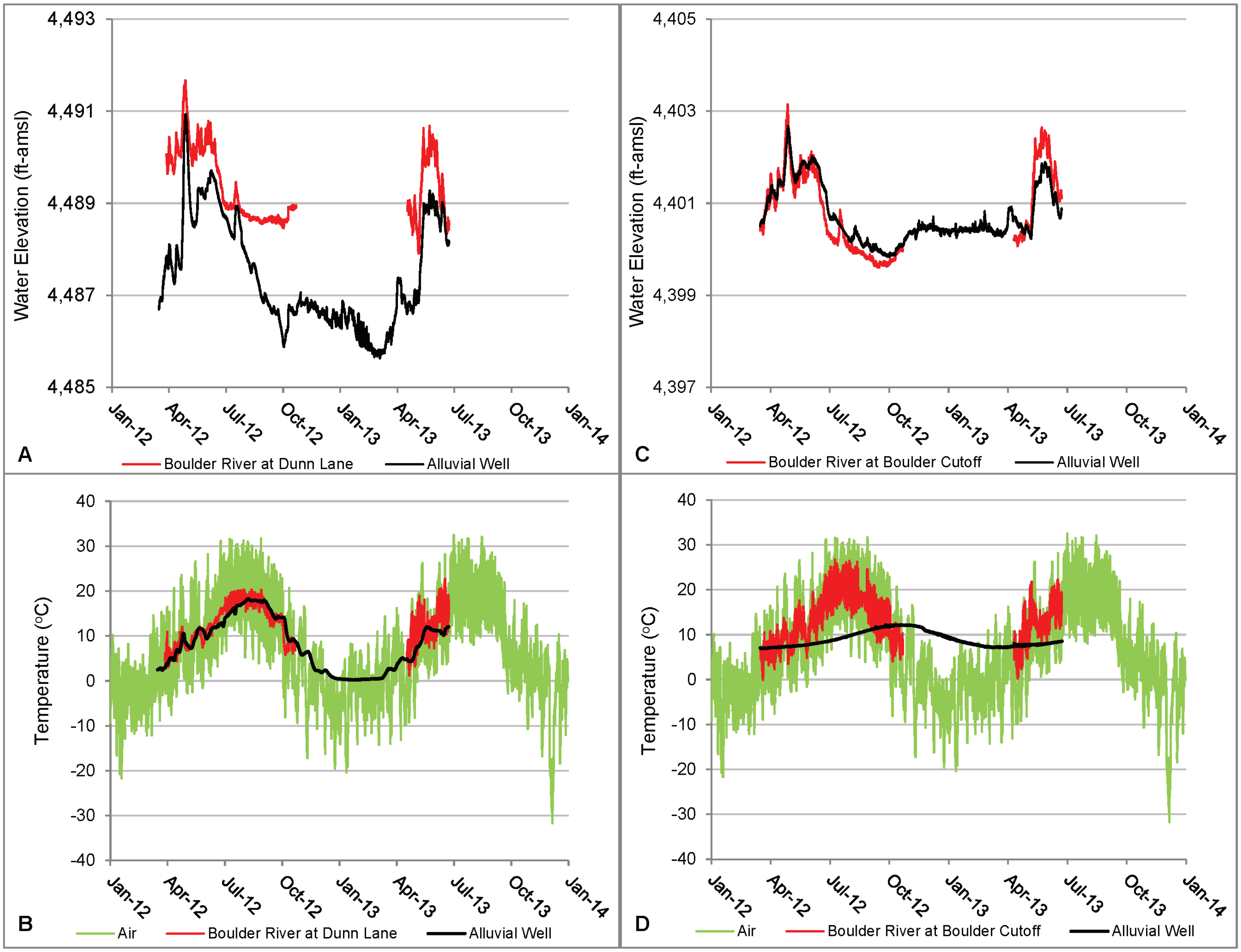

Figure 19. At the Dunn Lane sites (265343 and 265185) groundwater elevations were always lower than stream elevations (A) and groundwater temperatures closely followed surface-water temperatures (B). At the Boulder Cutoff sites (265348 and 265186) groundwater elevations were higher than stream elevations for much of the year, but were lower during high flows in the spring (C). Groundwater temperatures at the Boulder Cutoff site showed only slight seasonal variation, so they did not reflect the short-term flow reversal in the spring (D).

but that as surface-water flows decreased the volume lost also decreased. After accounting for inflows from Muskrat Creek and the Little Boulder River (265350 and 265347; fig.10), the Boulder River's net losses between Interstate 15 (263601) and Cardwell (263602), were: 225 cfs (May 9, 2012), 19 cfs (July 6, 2012), and 7 cfs (September 9, 2012). These measurements also show that there is a slight loss between Interstate 15 and Red Bridge (265943), a slight gain between Red Bridge and White Bridge (265349), a strong loss below White Bridge, a gain beginning near Boulder Cutoff (265348; fig. 21), and a strong gain occurring at and below Cold Spring (262190). In October 2012, after the irrigation season and when ephemeral streams were dry, synoptic measurements showed the same gain/loss pattern as seen earlier, but the net change between I-15 and Cardwell was a gain of 30 cfs (fig. 21).

Net Change in Flow Over Time

Time-series flow data at upstream/downstream station pairs were subtracted from each other to create a time series of net gains or losses for the monitored stream reach. As with the synoptic flow comparisons, the net differences are not necessarily the flux between surface water and groundwater. The late fall values best represent groundwater/surface-water interaction since there were minimal irrigation diversions, and ephemeral drainages were not flowing (fig. 22; table 5). There is typically a slight loss between Interstate 15 and Red Bridge, a slight gain between Red Bridge and White Bridge, a strong loss below White Bridge, a gain beginning near the Boulder Cutoff, and a strong

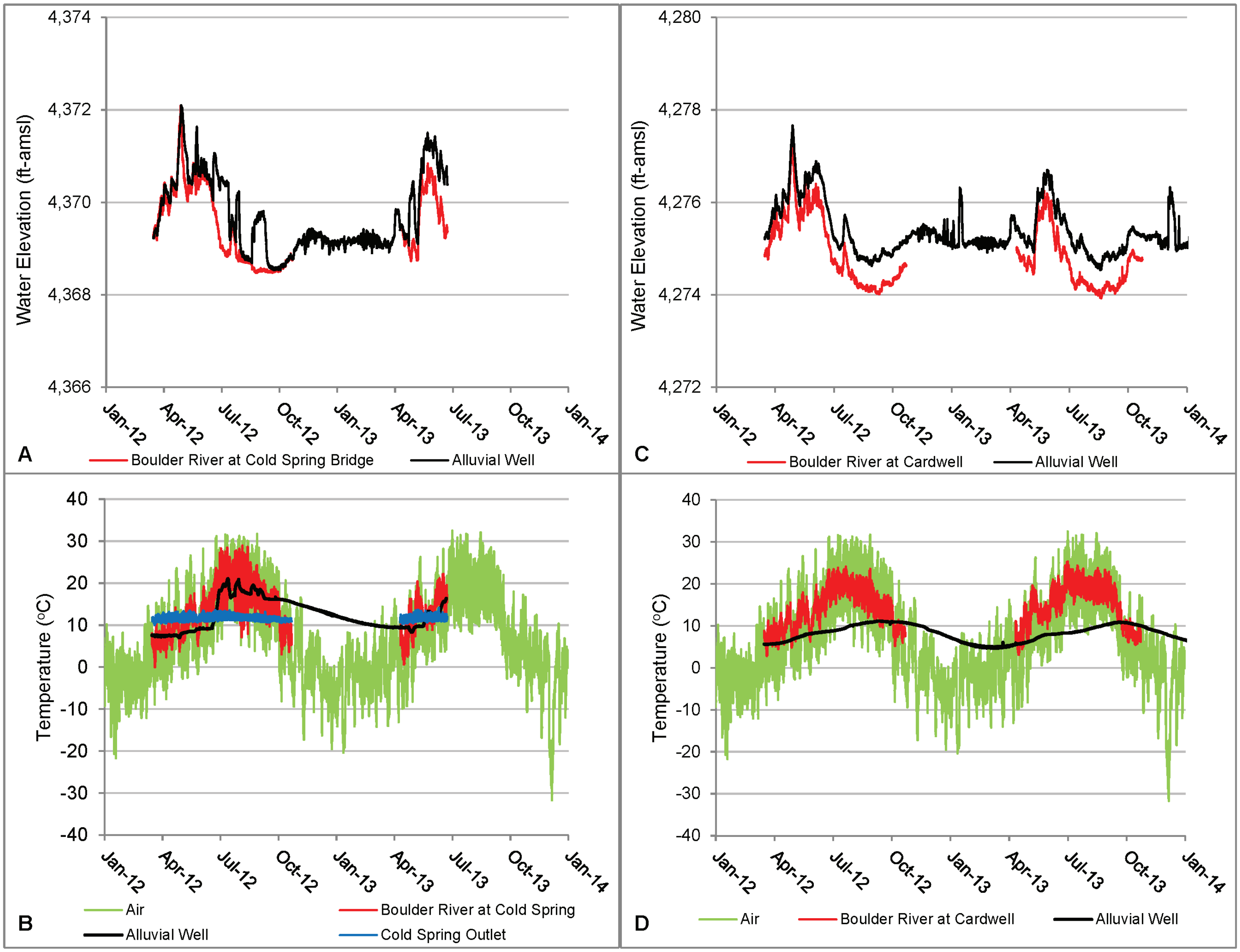

Figure 20. At the Cold Spring sites (262190, 265187, and 256351) groundwater elevations were affected by nearby flood irrigation; however, they were always higher than stream elevations (A). At the Cold Spring sites groundwater temperatures followed surface-water temperatures during the irrigation season, but otherwise showed only slight seasonal changes and did not approach zero in the winter (B). This temperature pattern was likely related to nearby flood irrigation. The temperature of the water flowing out the Cold Spring outlet (256351) was stable with only slight diel variation from solar pond warming (B). At the Cardwell sites (263602 and 265188) groundwater elevations were always higher than stream elevations (C), and groundwater temperatures showed slight seasonal variation (D).

gain at and below Cold Spring. The post-irrigation season differences between Interstate 15 and Cardwell showed an average net gain of 24 cfs. The synoptic and time-series data together with the site specific temperature and water elevation data help identify the reaches of the Boulder River that typically gain or lose (fig. 23, tables 4 and 5).

Groundwater Budget

The average annual groundwater budget is an important element in understanding the components of groundwater recharge and discharge within an area, and aids in evaluating the relative importance of each component. A well-developed budget is also needed to properly design the numerical models, which can be used to assess predictive scenarios. The budget components are summarized below, but detailed information, including monthly estimated values for each, are in the Boulder Valley Modeling Report (Butler and Bobst, in prep.).

The general form of the groundwater budget equation is:

Water in = water out ± changes in groundwater storage.

For the Boulder Valley, the general equation can be expanded to:

$$UR + IR + CL + GW_{in} = GW_{out} + ET_r + WL + \Delta S + RG,$$

where:

UR, upland recharge (acre-ft/yr);

IR, irrigation recharge (acre-ft/yr);

CL, canal leakage (acre-ft/yr);

GW_{in}, groundwater inflow (acre-ft/yr);

GW_{out}, groundwater outflow (acre-ft/yr);

ET_r, evapotranspiration by riparian vegetation (acre-ft/yr);

WL, withdrawals from wells (acre-ft/yr);

ΔS, changes in storage (acre-ft/yr); and

RG, river gain (acre-ft/yr).

Upland Recharge (UR)

Upland recharge is the net amount of water that enters the groundwater flow system through the unsaturated zone from precipitation, infiltration, and drainage (Healy, 2012). For our analysis this includes only non-irrigated areas. An upper bound estimate of upland recharge can be calculated by subtracting actual evapotranspiration from precipitation. This upper bound estimate does not account for runoff, sublimation, soil moisture retention, or any other processes that use water.

ET was calculated using the simplified vegetation dataset (based on LANDFIRE; fig. 6 and table 1) and literature values to estimate actual ET rates for different vegetation types (Hackett and others, 1960;

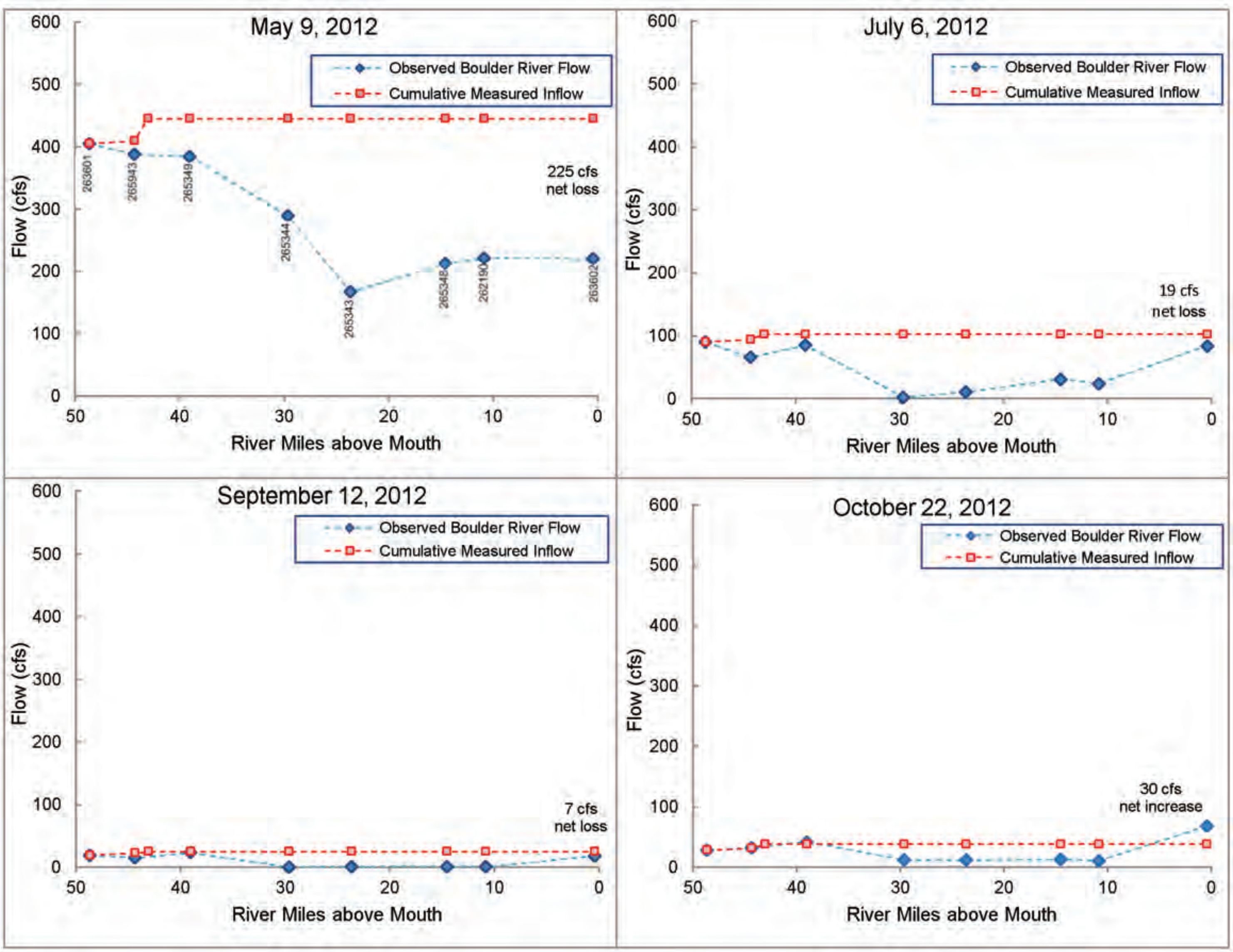

Figure 21. Synoptic stream flow measurements showed that the greatest net losses between Boulder and Cardwell occurred during high flows early in the season (May 9, 2012). As flows diminished during the summer, the net loss decreased. After the irrigation season (October 22, 2012), there was still a net loss between White Bridge and Cold Spring, but overall the river gained 30 cfs. The difference between inflow and observed flow was always greatest between White Bridge (265349) and Cold Spring (262190).

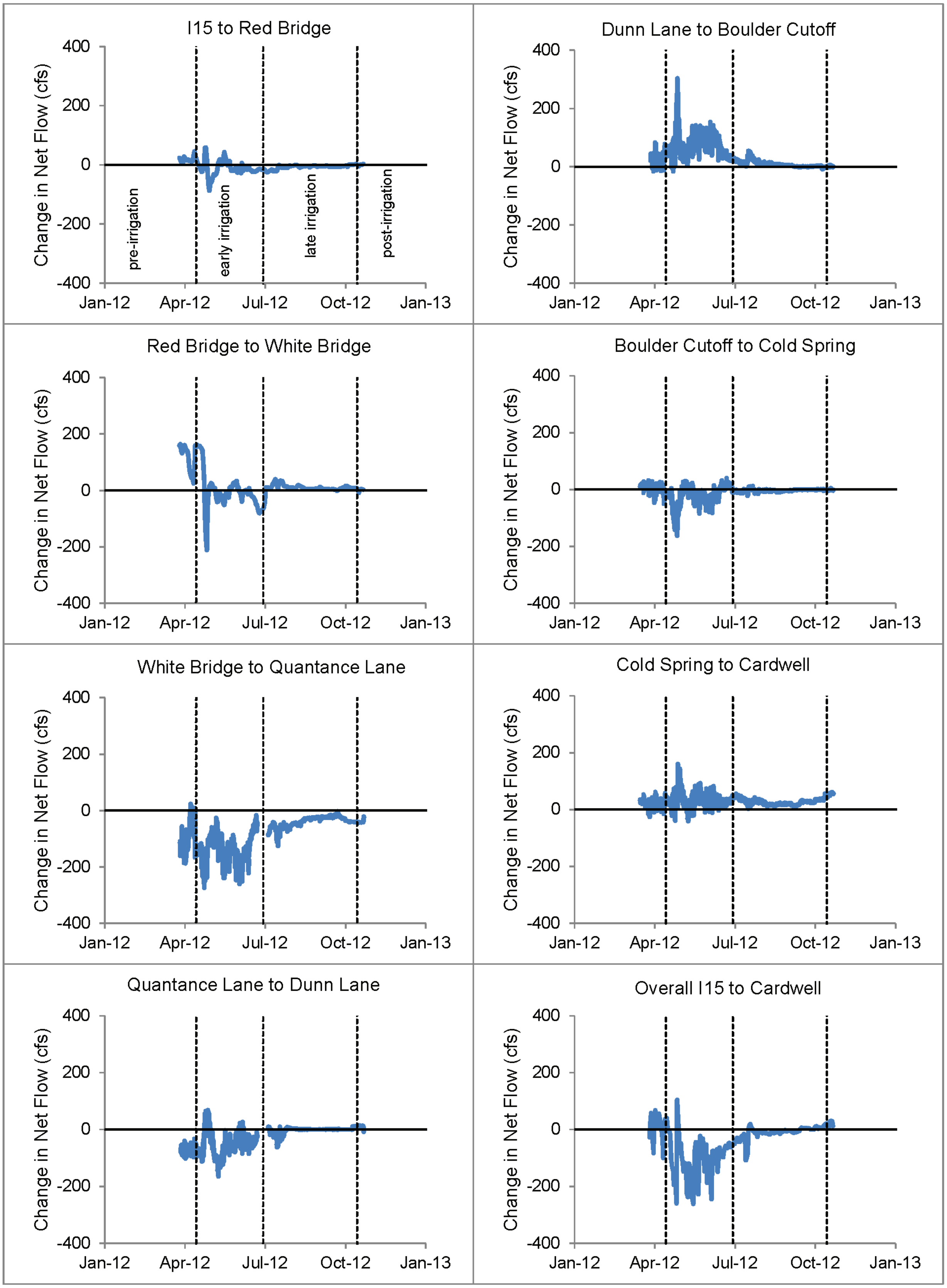

Figure 22. Because of irrigation diversions, irrigation return flows, tail water returns, and river stage the net gain or loss between stations varies with time of year.

Table 5. Average Net Change in Flow in the Boulder River (cfs)—2012

River Reach	Upstream Station GWIC ID	Downstream Station GWIC ID	Major Tributaries	Pre-Irrigation Season before 4/15	Early-Irrigation Season 4/16 to 6/30	Late-Irrigation Season 7/1 to 10/15	Post-Irrigation Season after 10/15
I 15 to Red Bridge	263601	265943	Muskrat Creek	11	-17	-10	-4
Red Bridge to White Bridge	265943	265349	Little Boulder	116	-3	10	2
White Bridge to Quantance Ln	265349	265344	---	-95	-135	-46	-41
Quantance Ln to Dunn Ln	265344	265343	---	-68	-51	-4	10
Dunn Ln to Boulder Cutoff	265343	265348	---	31	76	10	2
Boulder Cutoff to Cold Spring	265348	262190	---	4	-21	-3	-1
Cold Spring to Cardwell	262190	263602	---	22	36	27	55
Overall I 15 to Cardwell	263601	263602	Muskrat Creek & Little Boulder	12	-100	-9	24

Petersen and Hill, 1985; Johns, 1989; Persson, 1995; Rosenberry and Winter, 1997; Scott and others, 2004; Leenhouts and others, 2006; Lautz, 2008; Woodhouse, 2008; Chauvin and others, 2011; Sanford and Selnick, 2012; table 6).

The distributed ET values were subtracted from the 30-yr normal precipitation data reviewed earlier (fig. 3; PRISM, 2012). These distributed values were calculated on a 30-m pixel-by-pixel basis. The resulting values were averaged over 1-in precipitation intervals to provide information on the spatial distribution of recharge (fig. 24). The highest upland recharge rates occur in the Elkhorn Mountains (maximum of 14 in/yr), and on Bull Mountain (maximum of 4.5 in/yr). Upland recharge only occurs in the forested uplands, because precipitation across most of the valley is 10–12 ins per year and the native grasses and sagebrush will use at least that much water. This approach indicates that total upland recharge should be less than 30,000 acre-ft/yr.

Upland recharge estimates were refined during calibration of the steady-state numerical model (Butler and Bobst, in prep.). The upper-bound estimates were used as starting values. The final values were 42 percent of the upper-bound estimate, which provided for minimal cell flooding while keeping transmissivity values reasonable. This value is also similar to the deep percolation coefficient (DP_{ex}) value of 0.5 used to calculate irrigation recharge below. The final modeled upland recharge was about 12,600 acre-ft/yr, which is the value used in the water budget.

Irrigation Recharge (IR)

Irrigation recharge occurs when excess irrigation water infiltrates through the root zone and recharges aquifers (Healy, 2012, p. 10). Irrigation recharge was estimated using the Natural Resources Conservation Service (NRCS) Irrigation Water Requirements (IWR) program (NRCS, 2012). The IWR program requires information on climate, soil types, irrigation type, and crop types, and then uses the Blaney–Criddle method to estimate the crop's Net Irrigation Requirement (NIR; crop ET minus effective precipitation) (Blaney and Criddle, 1962; Dalton, 2003; L. Ovitz and R. Pierce, oral communication, 2012). Climate data were obtained from NOAA stations at Boulder and Trident. Soil type was assigned as silty loam based on SSURGO data and discussions with NRCS personnel (NRCS, 2012; L. Ovitz and R. Pierce, oral communication, 2012). The distribution of irrigation types was based on land-use data published by the Montana Department of Revenue (DOR, 2012). "Irrigated Land" is one land use in the dataset and is divided into three subclasses based on irrigation method (pivot, sprinkler, and flood). Crop type was assigned based on the irrigation type, with flood-irrigated areas assigned as grass hay and sprinkler and pivot areas growing an even mix of alfalfa and grass.

Results from the IWR program were used to calculate irrigation recharge (IR) using the following equation:

$$IR = [(NIR/IME + P_{eff} – ET) \text{ x } DP_{ex}],$$

where:

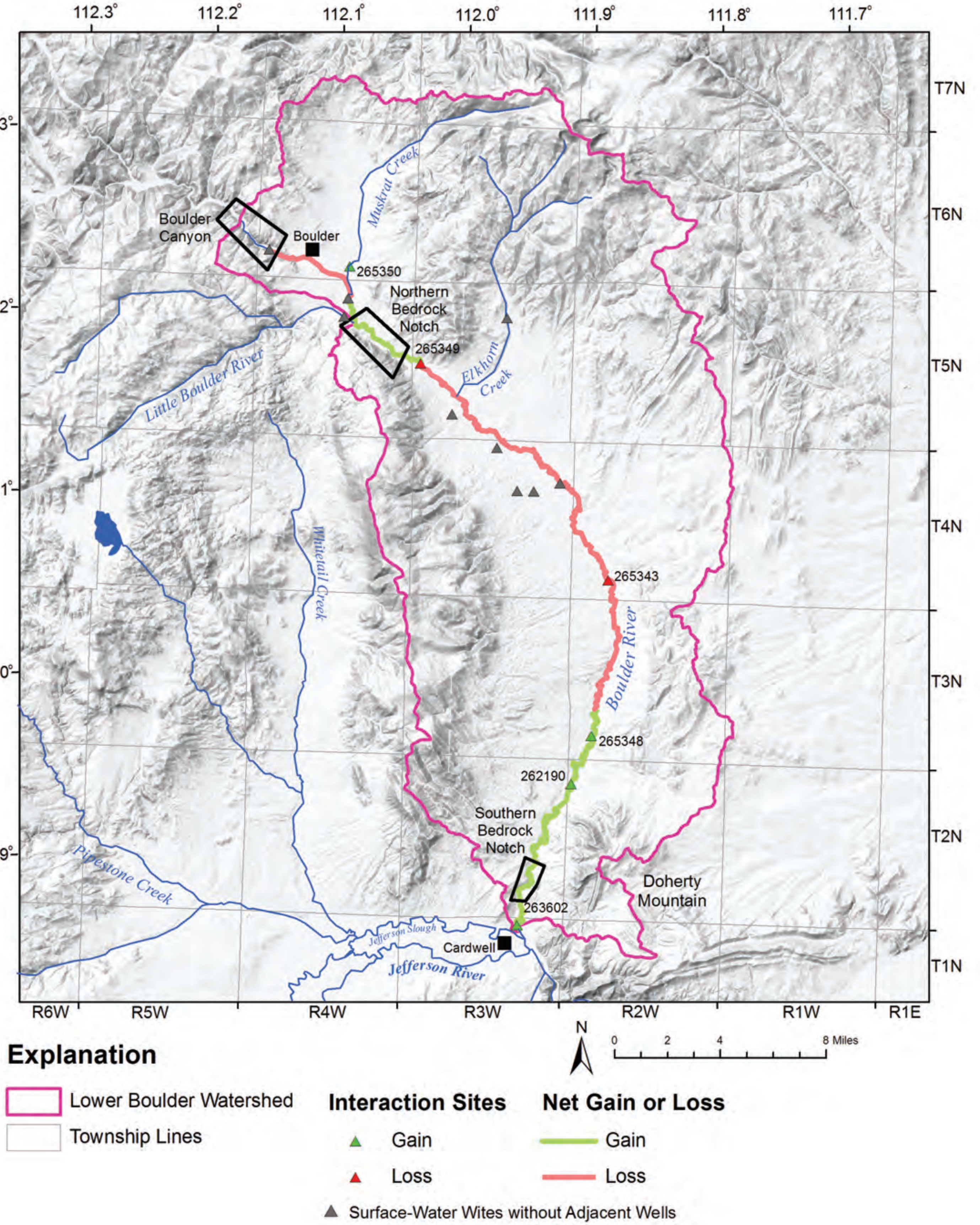

Figure 23. The surface-water/groundwater interaction sites (labeled based on surface-water site GWIC ID), and analysis of surface-water hydrographs identified reaches where the Boulder River gained or lost flow. Bedrock is exposed in the areas indicated as Boulder Canyon, Northern Bedrock Notch, and Southern Bedrock Notch.

Table 6. Evapotranspiration Values for Different Vegetation Types.

Vegetation Group	Acres	Evapotranspiration Rate (ft/yr)	Acre-ft/yr
Upland Sagebrush	64,734	1.1	70,124
Douglas Fir	49,790	1.4	68,457
Shrub/Grass Lowlands	40,393	1.0	40,391
Mixed Evergreen	27,186	1.8	49,839
High Xeric Grasses	20,988	1.2	24,484
Agricultural Lands	15,161	2.1	31,078
Mesic Meadow	12,926	1.7	21,543
Whitebark Pine	4,179	2.2	9,054
Alpine Rangeland, Deciduous Shrubs	2,818	2.0	5,635
Developed	1,971	1.0	1,971
Riparian	1,468	2.3	3,426
TOTAL	241,616		326,002

NIR, net irrigation requirement (ins, an IWR output);

IME, irrigation method application efficiency (percent);

P_{eff}, effective precipitation (in, an IWR output);

ET, evapotranspiration (in, an IWR output); and

DP_{ex}, portion of applied water in excess of ET that results in deep percolation (i.e., groundwater recharge) rather than runoff (percent).

Calculating irrigation recharge required estimates of the efficiency of different irrigation methods. The NRCS Soil Survey Manual (1993) provides a range of efficiencies for most irrigation methods. The following values were selected for each method: (1) flood, 35%; (2) sprinkler, 65%; and (3) pivot, 80%.

DP_{ex} values also needed to be assigned, and these were based on irrigation type, where DP_{ex} was set to 0.5 for flood-irrigated parcels and 1.0 for pivot and sprinkler parcels. This approach assumes that 50 percent of excess flood irrigation water becomes runoff, whereas little runoff results from pivot and sprinkler applications.

Irrigators in the Boulder Valley primarily obtain water from streams (L. Ovitz, oral communication, 2012). Because of availability in the early season, irrigation water is often applied in excess of crop demand. In the late season, water supplies fall short of crop demand. The IWR program does not take this seasonal availability into account, so irrigation recharge estimates for each field were compensated by assigning one of three recharge durations: April–October (full season); April–September (partial season); or April–July (partial season), based on field observations, water-level and discharge hydrographs, land owner interviews, and the canal that delivers its water to each irrigated field (P. Carey, oral communication, 2013; Butler and Bobst, in prep.). Multipliers were applied to the irrigation recharge values to redistribute them to the modified time periods, and to decrease the total volume infiltrated for fields that were not irrigated for the full season. These total volume multipliers were April–September, 0.93 and April–July, 0.74 (Butler and Bobst, in prep). Groundwater-irrigated parcels were assigned to the full-season period (April–October). The final irrigation recharge values are in table 7. The calculated average annual irrigation recharge is 6,800 acre-ft/yr.

Canal Leakage (CL)

Leakage measurements on the Carey canal made September 13, 2011, showed that the net change in flow was 6.0 cfs along a 4.5-mi length of canal (1.3 cfs/mi). If a ±5 percent error is assumed, the range is from 0.6 to 2.1 cfs/mi. Measurements on September 14 showed a net loss of 4.7 cfs over a different 1.5-mi reach (3.1 cfs/mi). Using ±5 percent error, the range is from 1.7 to 4.4 cfs/mi.

The 2.5-mi section of the Carey canal between the two surface-water stations (fig. 10) generally leaked between 0 and 10 cfs/mi during 2012, and leakage increased as flow increased (fig. 25). The relationship was not linear as the slope steepened when flow at the point of diversion (upstream site) was greater than about 55 cfs. During the 2012 irrigation season, this portion of the Carey canal had a median leakage rate

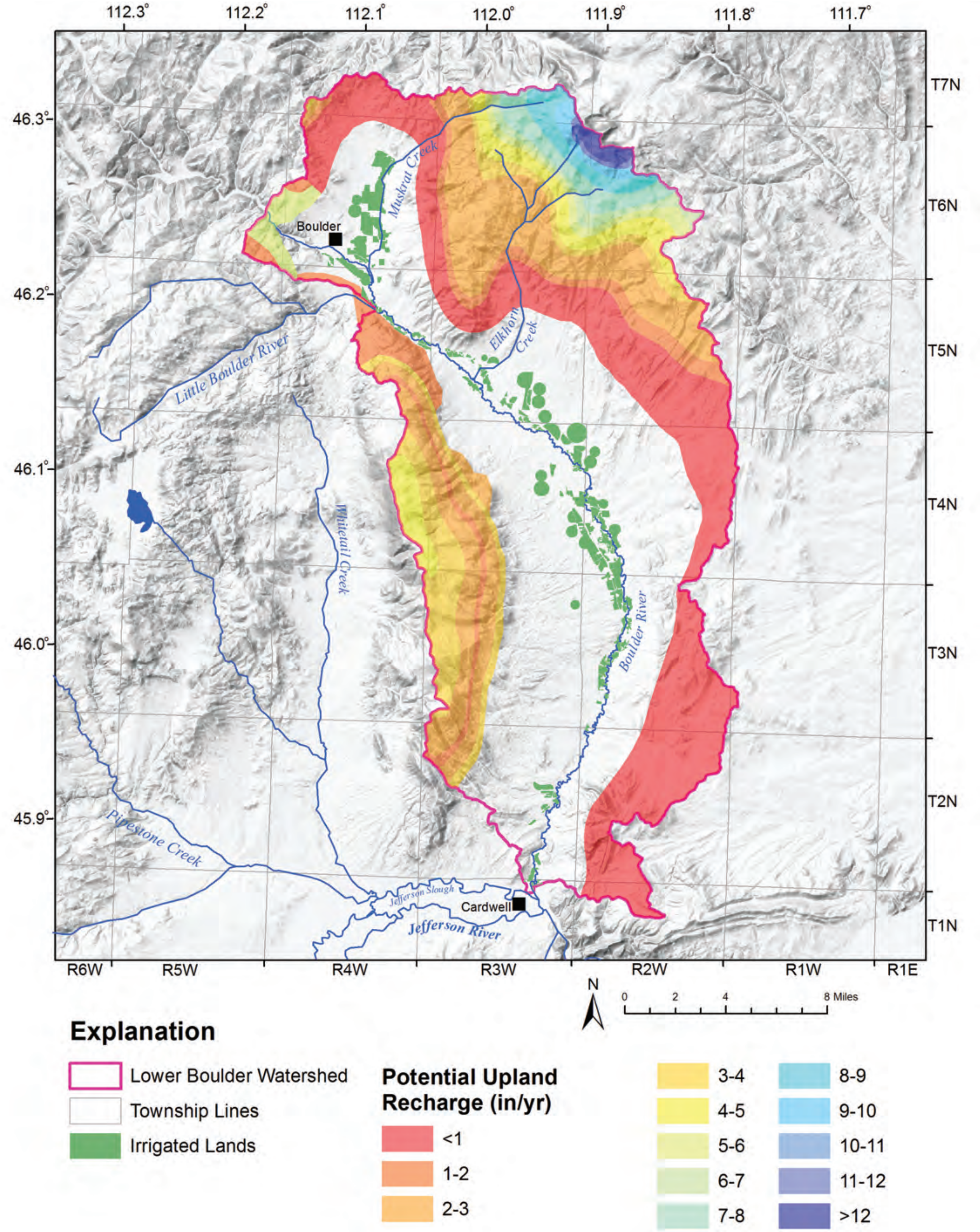

Figure 24. An upper bound estimate of the potential upland recharge was calculated by subtracting ET from precipitation on a 30-m pixel by pixel basis. Upland recharge is highest at the highest elevations and declines with elevation. In non-colored areas potential ET exceeds precipitation. Recharge in irrigated areas is calculated separately as irrigation recharge. Because processes other than infiltration and ET are not accounted for by this approach, actual upland recharge is less.

Table 7. Irrigation Recharge Estimates (in)

	April–October			April–September			April–July		
	Flood	Sprinkler	Pivot	Flood	Sprinkler	Pivot	Flood	Sprinkler	Pivot
Efficiency	**25%**	**65%**	**80%**	**25%**	**65%**	**80%**	**25%**	**65%**	**80%**
January	0	0	0	0	0	0	0	0	0
February	0	0	0	0	0	0	0	0	0
March	0	0	0	0	0	0	0	0	0
April	1.32	0.50	0.24	1.36	0.51	0.24	1.35	0.51	0.24
May	5.72	2.16	1.03	5.99	2.27	1.07	6.20	2.35	1.11
June	5.63	2.13	1.01	5.89	2.23	1.06	6.10	2.31	1.09
July	3.84	1.45	0.69	4.01	1.52	0.72	4.16	1.57	0.75
August	2.51	0.95	0.45	2.63	1.00	0.47	0	0	0
September	2.36	0.89	0.42	2.47	0.93	0.44	0	0	0
October	2.65	1.00	0.48	0	0	0	0	0	0
November	0	0	0	0	0	0	0	0	0
December	0	0	0	0	0	0	0	0	0
ANNUAL	24.04	9.09	4.31	22.36	8.45	4.01	17.82	6.74	3.2

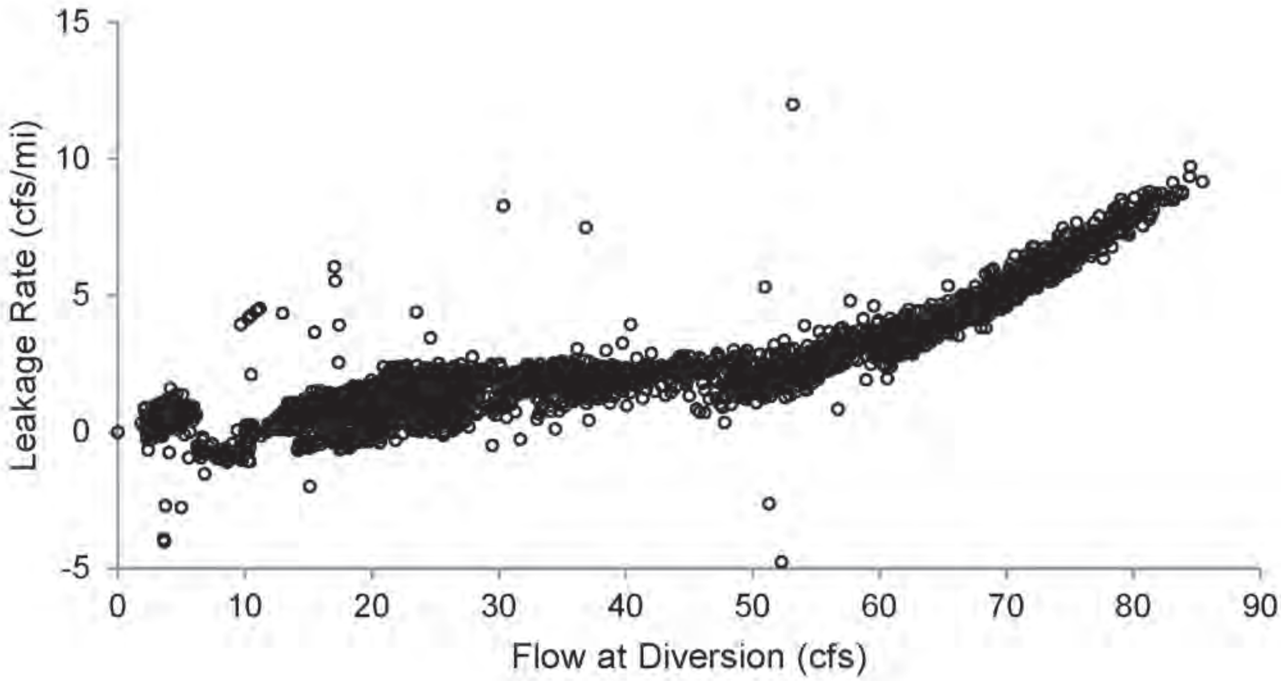

Figure 25. During 2012, leakage from the Carey canal was calculated hourly based on the discharges from two stations 2.5 mi apart. Leakage increased with increased flow, so was highest in the spring when the most water was diverted into the canal. The median leakage rate was 1.6 cfs/mi, and the average rate was 2.1 cfs/mi.

of 1.6 cfs/mi, and an average rate of 2.1 cfs/mi. These leakage rates for the Carey canal are comparable to reported canal leakage rates for other canals in Montana (Briar and Madison, 1992; Waren and others, 2012; Abdo and others, 2013; Bobst and others, 2013).

Synoptic measurements made on the smaller Murphy canal in 2012 show leakage of about 0.26 cfs/mi. This is about one order of magnitude less than that of the Carey canal, which is not unexpected given its smaller size.

During 2012 groundwater near the Carey canal was about 18 ft below ground surface before the canal turned on. Groundwater levels began rising as soon as the Carey canal turned on; short-term changes in canal stage were reflected in groundwater levels. Groundwater levels peaked about 5 ft below ground surface in early June, and generally declined through summer. By the time the canal turned off in October, groundwater levels had declined to about 16 ft below ground surface. From October 2012 to April 2013, groundwater levels declined another 4 ft and were about 20 ft below ground surface when the canal turned on again (fig. 26).

In 2012, water levels approximately 100 ft below ground surface in monitoring wells near the Murphy canal gradually rose, starting about 2 weeks after the canal was turned on. Groundwater levels remained elevated throughout the summer months and then slowly fell until about 2 weeks after the canal was turned on again in May 2013. The total water level change in the Murphy canal wells was about 5 ft (fig. 26).

Total canal leakage was estimated using the locations of active canals (MT-DNRC, 2007), aerial photographs (NAIP, 2011), and field observations. Leakage rates for unmonitored canals were estimated by classifying them as being similar to the Murphy canal (0.26 cfs/mi), the Carey canal (1.61 cfs/mi), or in between (0.94 cfs/mi). The duration of flow in each canal was assigned to an April–October (full season), April–September, or April–July period based on field observations, water level and discharge hydrographs, and land owner interviews (P. Carey, oral communication, 2013. The leakage rates, duration of canal flow, and canal length provided estimates of the timing, magnitude, and spatial distribution of canal leakage. The total average annual canal leakage was estimated to be about 16,570 acre-ft/yr.

Groundwater Inflow (GW_{in})

Groundwater inflow through the alluvium along the Boulder and Little Boulder Rivers was estimated by using the Darcy flux equation (Fetter, 1994).

$$Q=-KA\,(dh/dl),$$

where:

Q, flux (ft^3/d);

K, hydraulic conductivity (ft/d);

A, the saturated cross-sectional area of the alluvium (ft^2); and

(dh/dl), hydraulic gradient (ft/ft, unitless).

Based on aquifer test results for the Boulder Valley alluvium, hydraulic conductivities (K) of 30 and 70 ft/d were assigned to the alluvium. Cross-sectional areas (A) were estimated using geologic maps and well logs. Saturated thicknesses of 10 to 30 ft were evaluated. Where the Boulder River and Little Boulder Rivers enter the study area, alluvial sequences in the canyons are thin. Hydraulic gradients (dh/dl) were estimated to be 0.012 and 0.003 for the Boulder River and Little Boulder River, respectively. Total estimated groundwater inflow ranged from 44 to 310 acre-ft/yr; the best estimate was 150 acre-ft/yr.

Groundwater Outflow (GW_{out})

Groundwater outflow through the thin layer of alluvium over bedrock near Cardwell was estimated using the Darcy flux (Fetter, 1994). Saturated thicknesses of 10 to 30 ft were evaluated. Based on the potentiometric surface map, the groundwater gradient (dh/dl) was 0.0039. Hydraulic conductivities (K) from 30 and 70 ft/d were evaluated. Groundwater outflow estimates ranged from 45 to 316 acre-ft/yr, and the best estimate was 150 acre-ft/yr.

Riparian Vegetation Evapotranspiration (ET_r)

Riparian vegetation draws groundwater from the aquifer for transpiration. Riparian vegetation was divided into two types: large phreatophytes (e.g., cottonwood and willow; 3,791 acres) and grasses (3,603 acres). For large phreatophytes two studies conducted in southwest Montana and west-central Wyoming (Hackett and others, 1960; Lautz, 2008, respectively) reported groundwater consumptive use between 20 and 25 in per year. Lautz (2008) also reported ground-

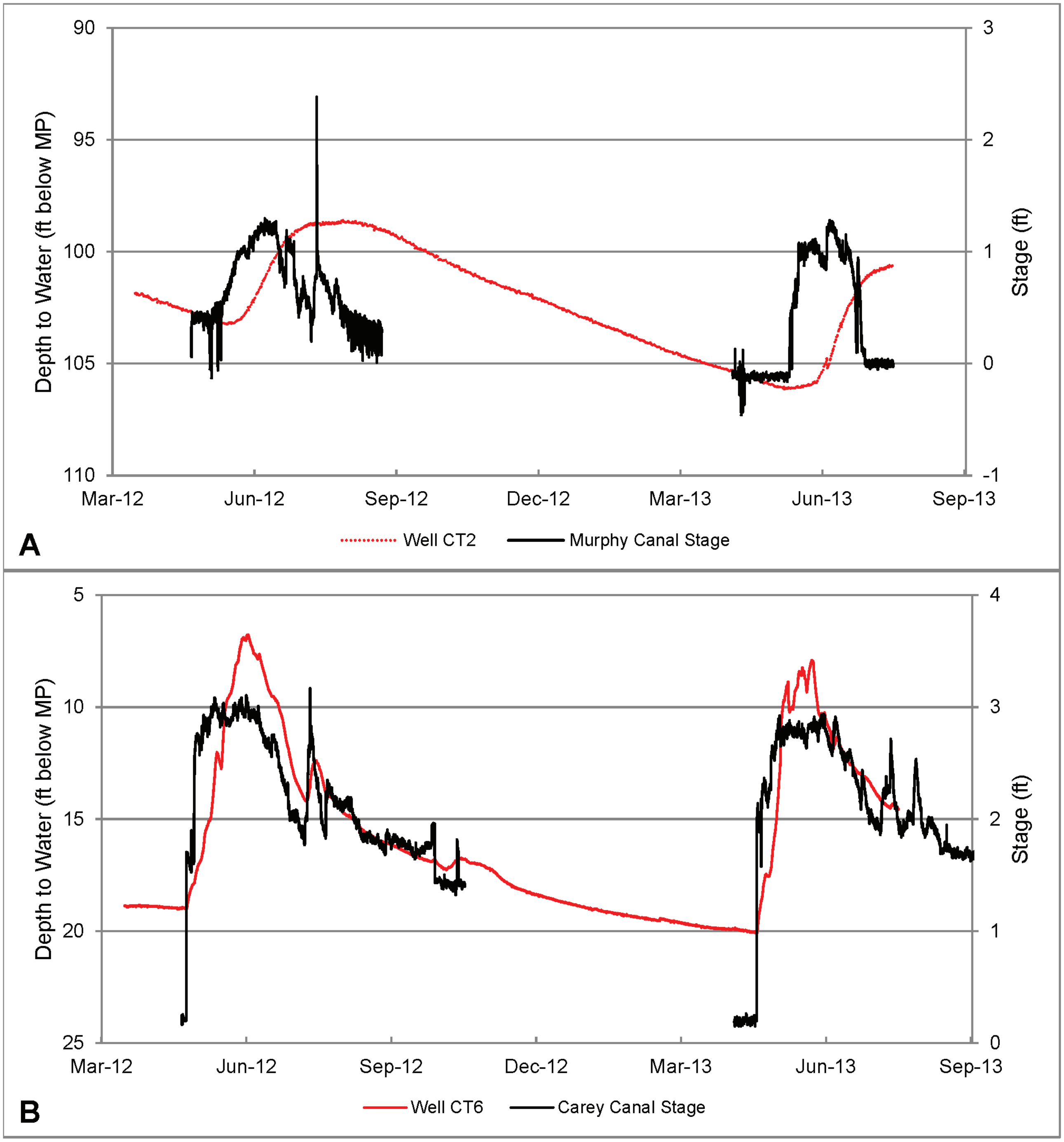

Figure 26. Leakage from the Murphy canal caused groundwater levels to rise and fall gradually (A). Groundwater levels near the Carey canal responded rapidly to changes in canal stage (B).

water consumptive use for meadow grasses at 3 in per year. Using an average of 22 in/yr for phreatophytes and 3 in/yr for grasses, the basin-wide ET_r value was 7,850 acre-ft/yr.

Groundwater Withdrawals from Wells (WL)

Pumping wells (WL) withdraw water from the aquifer, and the amount and timing of withdrawal depend on the well's use. The MBMG's GWIC database and the "Structures and Addresses" shapefile from the Montana Spatial Data Infrastructure dataset (Montana State Library, 2011) were used to identify potential well locations. Identified well uses included domestic, livestock, public water supply, and irrigation.

Domestic well net withdrawals (consumptive use) were calculated using the rates determined for the North Hills, near Helena, Montana (Bobst and others, 2014). The North Hills average annual consumptive use estimate was 435 gallons per day (gpd) per house; however, estimates from other sources ranged from about 300 to 500 gpd per house (Bobst and others, 2014). Two-hundred forty-nine homes were located outside the Boulder city water service areas. Using 435 gpd/home resulted in an annual total consumptive use of 112 acre-ft/yr.

Livestock water consumption from wells was calculated using the amount of grazing land and previous estimates of livestock water use. The study area contains about 33 percent of the grazing land in Jefferson County. County-wide livestock groundwater use is about 60,000 gpd (67 acre-ft/yr; Cannon and Johnson, 2004). For this study, all livestock water was considered consumptively used. Livestock use was about 23 acre-ft/yr.

Public water supply wells are used to supply water to the town of Boulder. Two of Boulder's four wells are typically in operation at any one time (D. Wortman, oral. com. 2012). Boulder's wells had limited pumping records, so more detailed records from Dillon, Montana (Abdo and others, 2013) were used to extrapolate consumptive use. From this it was calculated that approximately 690 acre-ft/yr of groundwater is pumped from the alluvial aquifer by the public supply wells, and consumptive use was set at 100% since the city's wastewater is discharged to the Boulder River.

Irrigation with groundwater was calculated based on water rights (MT-DNRC, 2013) and aerial photographs (NAIP, 2011). This analysis shows that groundwater irrigates about 1,080 acres. Irrigators use a combination of side-roll sprinklers and center pivots to apply this groundwater. The IWR method indicates that about 2,120 acre-ft/yr of groundwater is consumptively used for irrigation.

Groundwater Storage (ΔS)

Long-term monitoring wells show a very slight downward trend. This trend appears to be negligible for the purposes of the water-budget analysis. Over the long term, the system appears to be at equilibrium; therefore, the net change in storage is near zero.

River Gains (RG)

River gains are the amount of groundwater flowing to surface water, including Cold Spring. This was estimated using the difference in the groundwater budget (table 8 and fig. 27).

$$RG = [UR + IR + CL + GW_{in}] - [GW_{out} + ET_r + WL + \Delta S].$$

$$RG = [12{,}603 + 6{,}805 + 16{,}568 + 148] - [150 + 7{,}851 + 2{,}951 + 0] = 25{,}172.$$

This calculated difference equates to about 35 cfs. This compares well with measured increases in the Boulder River from I-15 to Cardwell at times when irrigation diversions were limited. In 2012 the increase was 36 cfs (26,080 acre-ft/yr), and in 2012 it was 43 cfs (31,150 acre-ft/yr). The steady-state model also compared well with this estimate, showing a net gain of 37 cfs.

Table 8. Average Annual Groundwater Budget (acre-ft/yr)

	Best Estimate	%	Estimated Range		Steady-State Model Budget
			Min	Max	
Upland Recharge	12,603	34.9%	11,343	13,863	12,603
Irrigation Recharge	6,805	18.8%	6,125	7,486	6,892
Canal Seepage	16,568	45.9%	14,520	17,747	16,511
Groundwater Inflow	148	0.4%	44	443	80
TOTAL INFLOW	36,124		32,032	39,539	36,086
Groundwater Outflow	150	0.4%	45	451	150
Riparian Evapotranspiration	7,851	21.7%	5,055	12,480	6,348
Well Withdrawals*	2,951	8.2%	2,656	3,246	2,951
River Gains	25,172	69.7%	22,655	27,689	26,636
Change in Storage	0		0	0	0
TOTAL OUTFLOW	36,124		30,411	43,866	36,086

*Well Withdrawals reflect the net consumptive use, not the pumping rate.

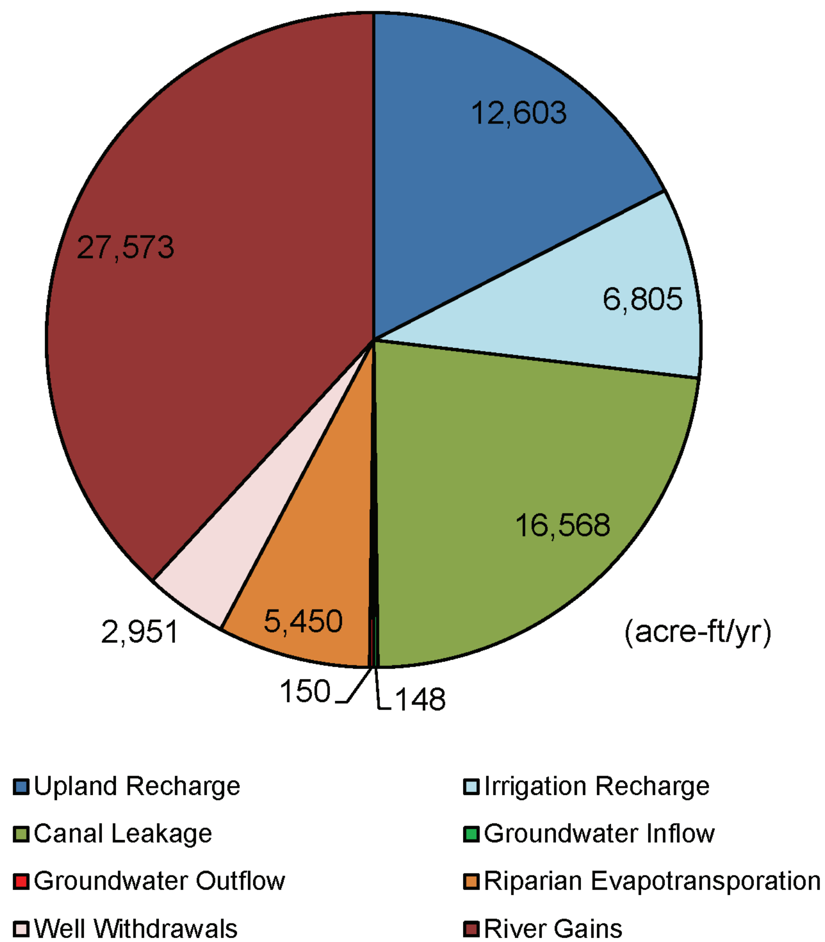

Figure 27. In the Boulder Valley, groundwater inputs are derived from canal seepage (46 percent), upland recharge (35 percent), irrigation recharge (19 percent) and groundwater inflow through the alluvium (<1 percent). Groundwater outputs go to surface water (76 percent), riparian vegetation (15 percent), well withdrawals (8 percent) and groundwater outflow through the alluvium (<1 percent).

Water Chemistry

For this report, the water chemistry types are based on the most abundant cation and anion in milliequivalents per liter (meq/L).

General Groundwater

Major Ions. The dominant groundwater type was calcium-bicarbonate (Ca-HCO_3; fig. 28; appendix B). This is consistent with the weathering of igneous rocks (granite and volcanic) and limestone (Hounslow, 1995), and is a common water type in western Montana (MBMG, 2016b). TDS concentrations were generally less than 200 mg/L in the northern portion of the study area, reflecting the relatively low solubility of the igneous rocks in the upper basin. TDS concentrations increased further south where carbonates and marine shales are present (fig. 2).

Other types were sodium–bicarbonate, calcium–sulfate, and sodium–sulfate-type waters, which reflect local conditions. Boulder Hot Springs has sodium–bicarbonate (Na-HCO_3) water with a TDS of about 420 mg/L (Sonderegger and others, 1981). Elevated sodium and TDS concentrations were found in samples from nearby wells (particularly in well 51692; fig. 28). Wells 49049 and 50002 (fig. 28) produced samples of calcium–sulfate (Ca-SO_4) water, which may represent dissolution of gypsum from Tertiary sediments.

Well 215992 (located at a Montana DOT facility) had a sodium–sulfate (Na-SO_4) water type and a TDS of 2,567 mg/L, which is about 3.7 times greater than any other sample (fig. 28). The water chemistry in well 215992 may be influenced by road salt and ion exchange. Wells 262259 and 170410 also had Na-SO_4 water types, but with much lower TDS values (608 and 428 mg/L, respectively; fig. 28).

Metals. Four wells (265187, 170410, 204849, and 265183; appendix B) had arsenic concentrations exceeding the 10 µg/L drinking water standard (MDEQ, 2010). Wells 265187 and 265183 are completed in the alluvium next to the Boulder River, and likely obtain the arsenic from the river water (see below). Well 204849 is completed in Tertiary sediments topographically below a known zone of natural hydrothermal alteration, as evidenced by abandoned lead mines in the bedrock (Metesh and others, 1998; MBMG, 2016). It is unclear why arsenic levels are high in well 170410.

Nutrients. Groundwater samples from wells 50007 and 215992 exceeded the drinking water standard for nitrate (10 mg/L). These wells had nitrate concentrations of 11.7 and 37.3 mg/L, respectively.

General Surface Water

Major Ions. Surface waters were calcium–bicarbonate type (fig. 29). TDS values were lowest (91 mg/L) at station 263601 at the upstream end of the study area, where granite and volcanic bedrock dominate. TDS increased to 208 mg/L at station 263602 at the downstream end of the study area.

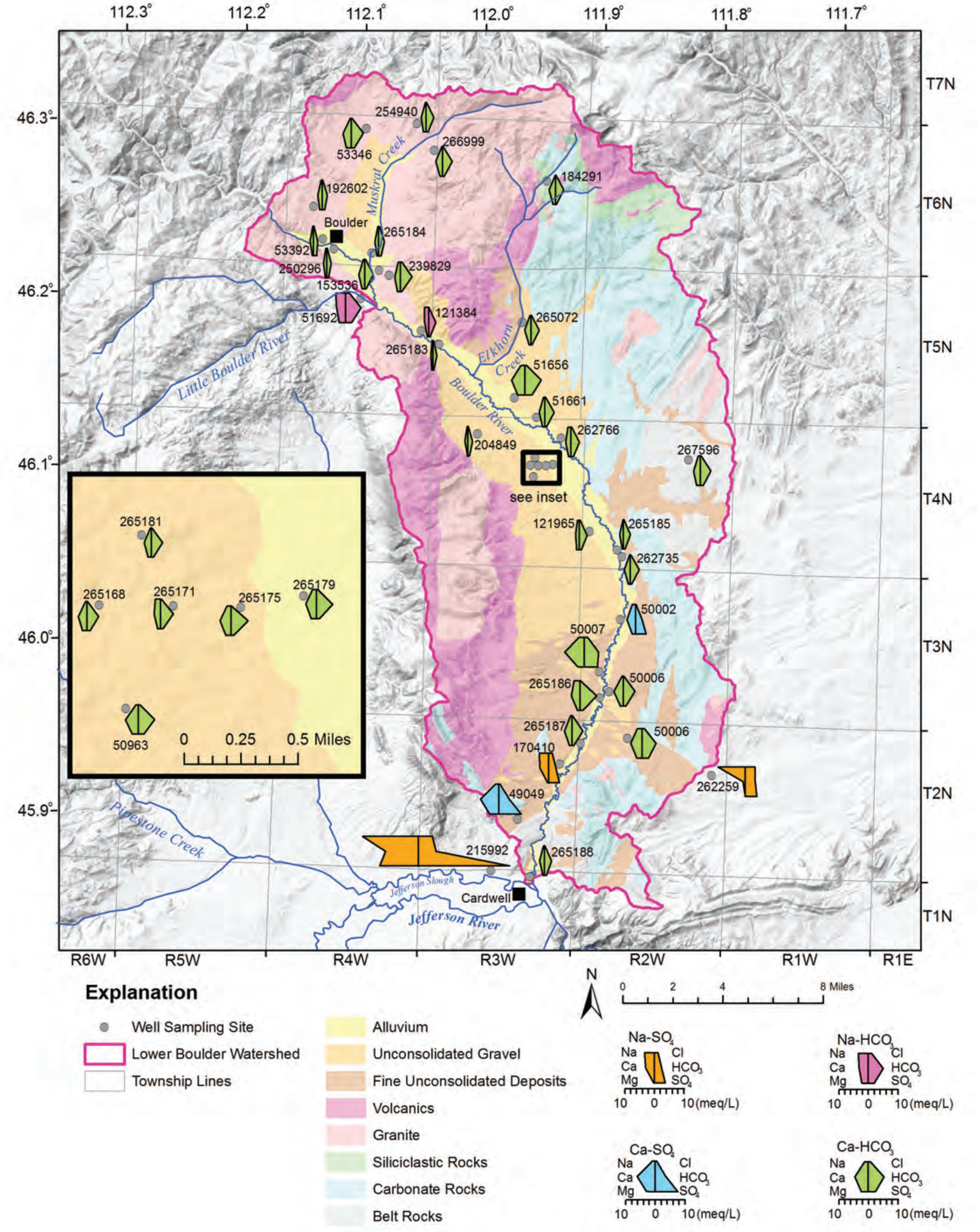

Figure 28. Calcium-bicarbonate groundwater is the most common type in the study area. Water types other than calcium-bicarbonate appear to result from local influences. In general TDS concentrations are lowest in the alluvium, and in bedrock wells completed in granite and volcanic rocks. TDS concentrations are generally higher in sedimentary bedrock wells.

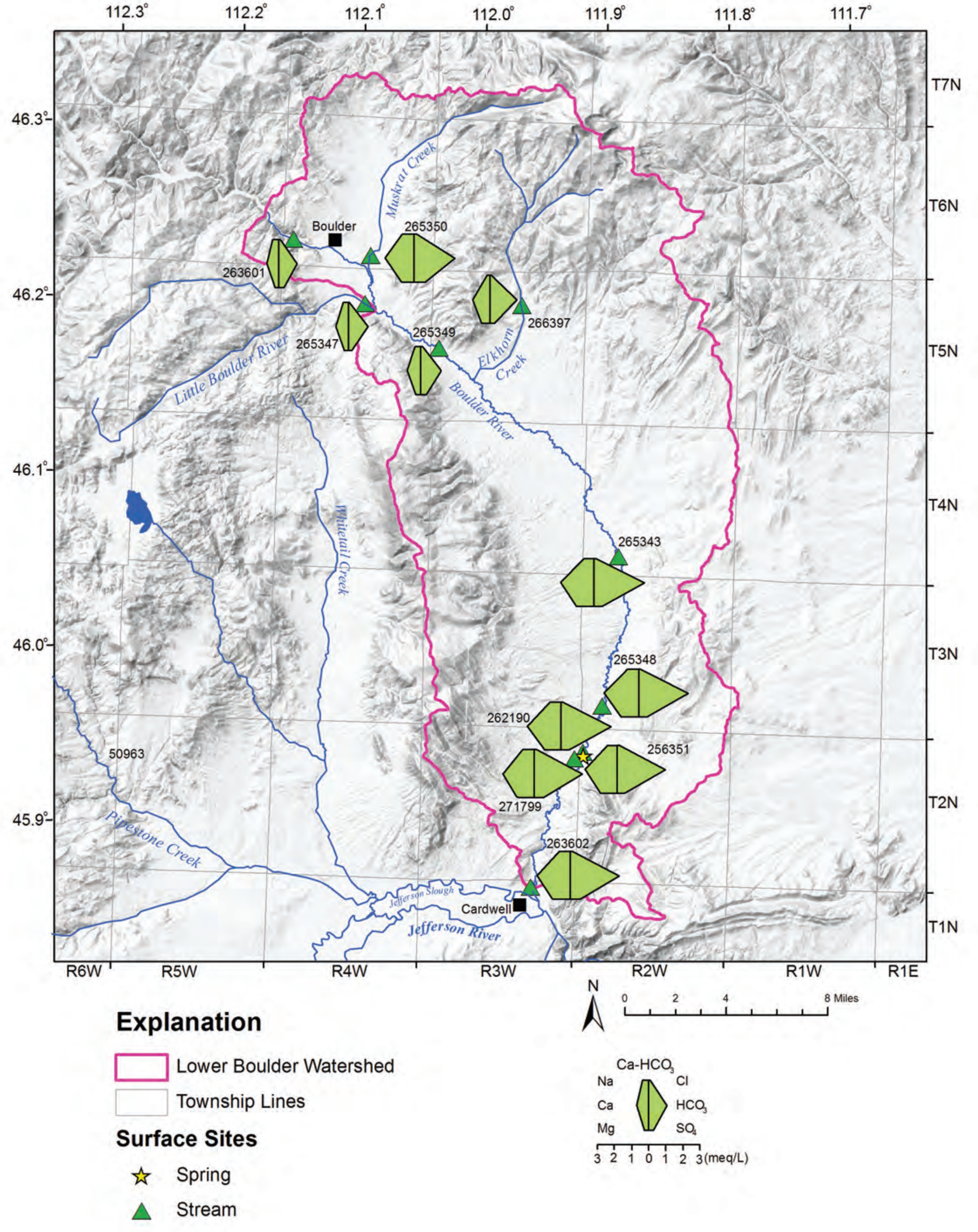

Figure 29. All surface-water samples were calcium-bicarbonate type. TDS is lowest on the upstream end of the study area, and increases downstream. Note that the stiff diagram scale for the surface-water sites is different than for the groundwater sites.

Metals. Four surface-water samples from the Boulder River exceeded the drinking water standard for arsenic (10 μg/L; stations 265349, 265343, 265348, and 262190). MDEQ (2012) has identified mining and milling as the probable sources of arsenic in the Boulder River. Natural sources of arsenic are also present within and upstream of the study area.

Nutrients. No surface-water sample exceeded the drinking water standards for nitrate or phosphorous.

Canal Leakage

Groundwater samples were taken in March (pre-irrigation), June (early irrigation), and August (late irrigation) 2012 from selected wells near the Murphy and Carey canals (fig. 30). The only sampled well that showed a clear response to canal leakage was CT6 (265175), adjacent to the Carey canal. Samples from CT6 show that most water-quality parameters decreased between the March and June sampling as low TDS canal water entered the aquifer; however, As increased because the Boulder River has a higher As concentration than does the groundwater. The concentrations of most parameters in CT6 rose between the June and August sampling events as groundwater levels declined and the amount of canal leakage diminished. CT6 As concentrations fell between the June and August sampling events.

Cold Spring

Nobel and others (1982) suggested that the water from Cold Spring comes from the Madison Formation. Kendy and Tresch (1996) observed that the Madison Formation is present beneath alluvium in the center of the valley.

Analytical results from samples collected in July 2012 showed that the spring water was dominated by calcium and bicarbonate ions ($Ca\text{-}HCO_3$), and that its TDS was 201 mg/L. Cold Spring water is similar to alluvial groundwater and Boulder River water; however, Cold Spring water had a lower As concentration (2.4 μg/L) than did water from the Boulder River (16.8 μg/L; 262190) or the nearby alluvial well (10.8 μg/L; 265187).

To better define the source of Cold Spring's water, additional samples were collected in April 2013 from Cold Spring in an upwelling area (256351), shallow alluvial groundwater (wells 265186 and 265187), groundwater from an upgradient well completed in Tertiary sediments (262242), and the Boulder River (sites 265348 and 271799). In addition to the standard suite of analytes, the samples were analyzed for stable isotopes of water (δD and $\delta^{18}O$), tritium (^{3}H), radon (Rn), dissolved inorganic carbon (DIC), stable carbon isotopes ($\delta^{13}C$), and strontium stable isotopes ($^{87}Sr/^{86}Sr$).

Stable isotopes of water (δD and δ^{18}O). Analysis of stable isotopes showed that Cold Spring water was most similar to Boulder River water (fig. 31). Groundwater from the Tertiary well (262242) was less enriched in the heavy isotopes (more negative) than was water from Cold Spring, perhaps reflecting water derived from higher elevations. The shallow alluvial water samples were more enriched in the heavy isotopes (more positive) than Cold Spring. All stable water isotope samples plotted slightly below the global meteoric water line (Rozanski and others, 1993), but close to the local meteoric water line (Gammons and others, 2006). The $\delta^{18}O$ values and silica concentrations are too low for hydrothermal sources (appendix B; Clark and Fritz, 1997). As such, the water appears to be meteoric.

Tritium (^{3}H). Tritium concentrations provide information on when water was last in contact with the atmosphere (Drever, 1997). Tritium results from the well completed in Tertiary sediments were non-detect [<3 tritium units (TU)], indicating that the groundwater was recharged prior to 1953. All other samples had tritium values between 6 and 8 TU, which indicates that recharge occurred after 1953 (i.e., post above ground nuclear testing; Plummer and others, 2003; appendix B), so the Cold Spring water is relatively young.

Radon (Rn). Radon is generated by the radioactive decay of uranium, and Rn itself has a half-life of 3.8 days (Drever, 1997). Because of its short half-life, radon concentrations in water decline rapidly when the water is removed from the source. Rn is also a gas, so it is outgassed from aerated water. The radon concentration of Cold Spring was similar to samples obtained from the Boulder River (appendix B), and 2 to 3 orders of magnitude lower than concentrations in the shallow alluvial and Tertiary groundwater samples. These results indicate that the water discharging at Cold Spring has either been in the ground for a short period of time, or the spring water's flow path near its discharge was low in radon. If the alluvial water was

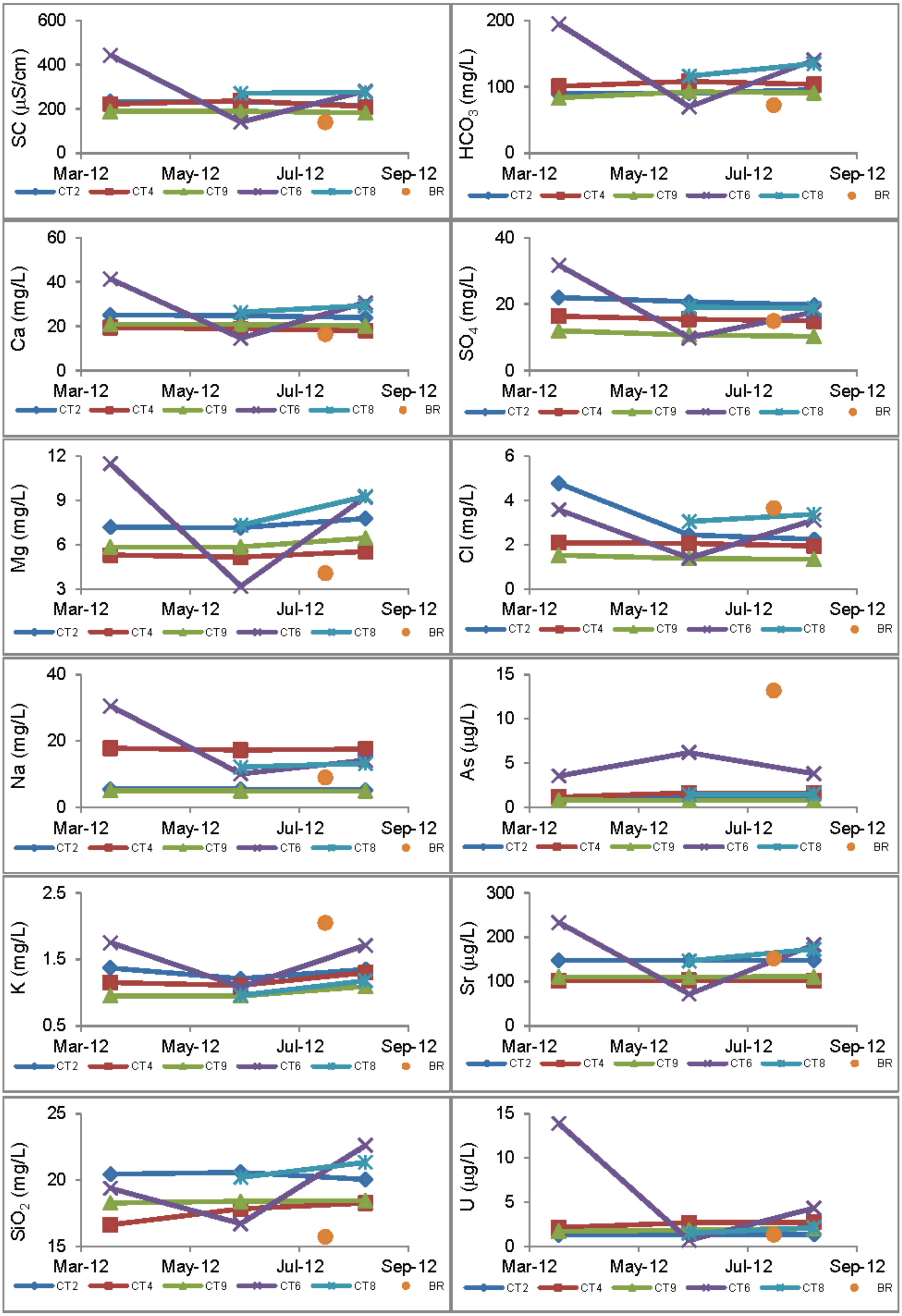

Figure 30. Canal leakage caused a noticeable change in the groundwater chemistry near the Carey canal (CT6; 265175). Other well locations (265168, 265171, 265181, and 265179) did not show clear changes. The sample marked as BR is for the Boulder River at White Bridge (265349) sampled on July 30, 2012.

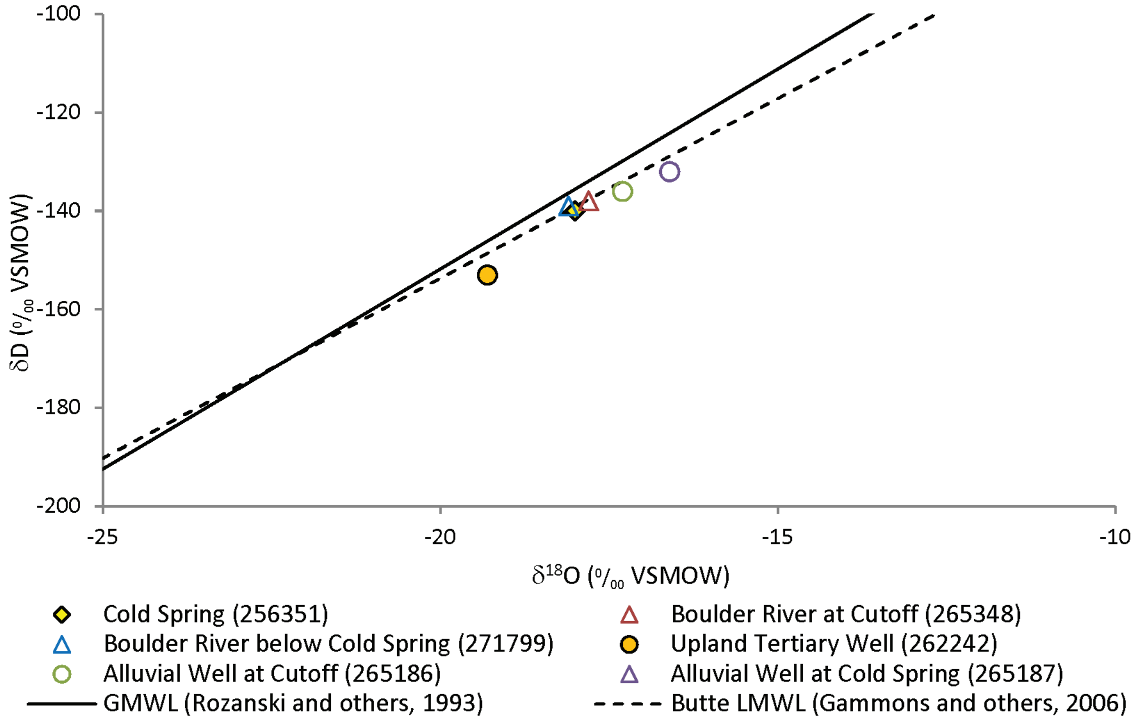

Figure 31. The stable isotopes of water indicate that discharge from Cold Spring is most similar to the Boulder River water. Alluvial water appears to be slightly evaporated river water.

isolated from all radon sources for about 16 days, it would have radon concentrations similar to those of spring water.

Stable carbon isotopes. Stable carbon isotopes can be used to identify the sources of carbon in water samples. Marine carbonates have $\delta^{13}C$ values that are near zero because the standard (PDB) is a marine carbonate. Atmospheric carbon $\delta^{13}C$ values are approximately -7‰, and native plants in this area (C_3-type plants) have $\delta^{13}C$ values between -23‰ and -34‰ (Faure, 1991). Cold Spring, the Boulder River, and the Tertiary well had $\delta^{13}C$ values between -8.2‰ and -6.4‰; and dissolved inorganic carbon (DIC) values between 7.9 mg/L and 18.6 mg/L. These values are consistent with carbon derived from atmospheric sources. Alluvial groundwater had more depleted $\delta^{13}C$ values (-14.0‰ and -12.5‰; fig. 32) and more DIC (39.2 mg/L and 44.8 mg/L; fig. 32), which is consistent with carbon from atmospheric sources and from plant remains. None of the carbon isotopes suggest a marine carbonate source.

Strontium isotope ratios ($^{87}Sr/^{86}Sr$). Strontium isotope ratios can be used to identify sources of Sr in water, and because Sr and Ca have similar behavior, Sr ratios can be used to infer the source of Ca (Drever, 1997). Mississippian carbonates (such as the Madison Formation) have $^{87}Sr/^{86}Sr$ ratios between 0.7078 and 0.7085 (Burke and others, 1982; Capo and others, 1998). Doe and others (1968) showed that a sample of granite from the upstream end of the study area had a $^{87}Sr/^{86}Sr$ ratio of 0.7151. $^{87}Sr/^{86}Sr$ results from all samples except for those from Cold Spring and the Boulder River below Cold Spring are consistent with weathering of Mississippian limestone (Ms). Water from Cold Spring had a $^{87}Sr/^{86}Sr$ ratio of 0.7095, the highest of the April 2013 samples (fig. 33). The $^{87}Sr/^{86}Sr$ ratio of the Boulder River below Cold Spring likely represents mixing between the Boulder River and Cold Spring.

Earlier work suggested that Cold Spring is derived from regional flow in the Madison Limestone (Nobel and others, 1982), but stable water isotopes (δD and $\delta^{18}O$) and tritium results indicate that the discharge is young meteoric water. Carbon and strontium isotope results indicate that this water has been in prolonged contact with granite (or alluvium containing granite clasts) and has had little contact with the Madison Limestone; however, radon results indicate that it could not have been in contact with granite for at least 16 days before being discharged. Thus it appears that Cold Spring's water is derived from the Quaternary alluvium, but that the water flowed through fractures and solution voids in the Madison Limestone near the end of its flow path. Flow through these secondary conduits also explains why the discharge is focused in

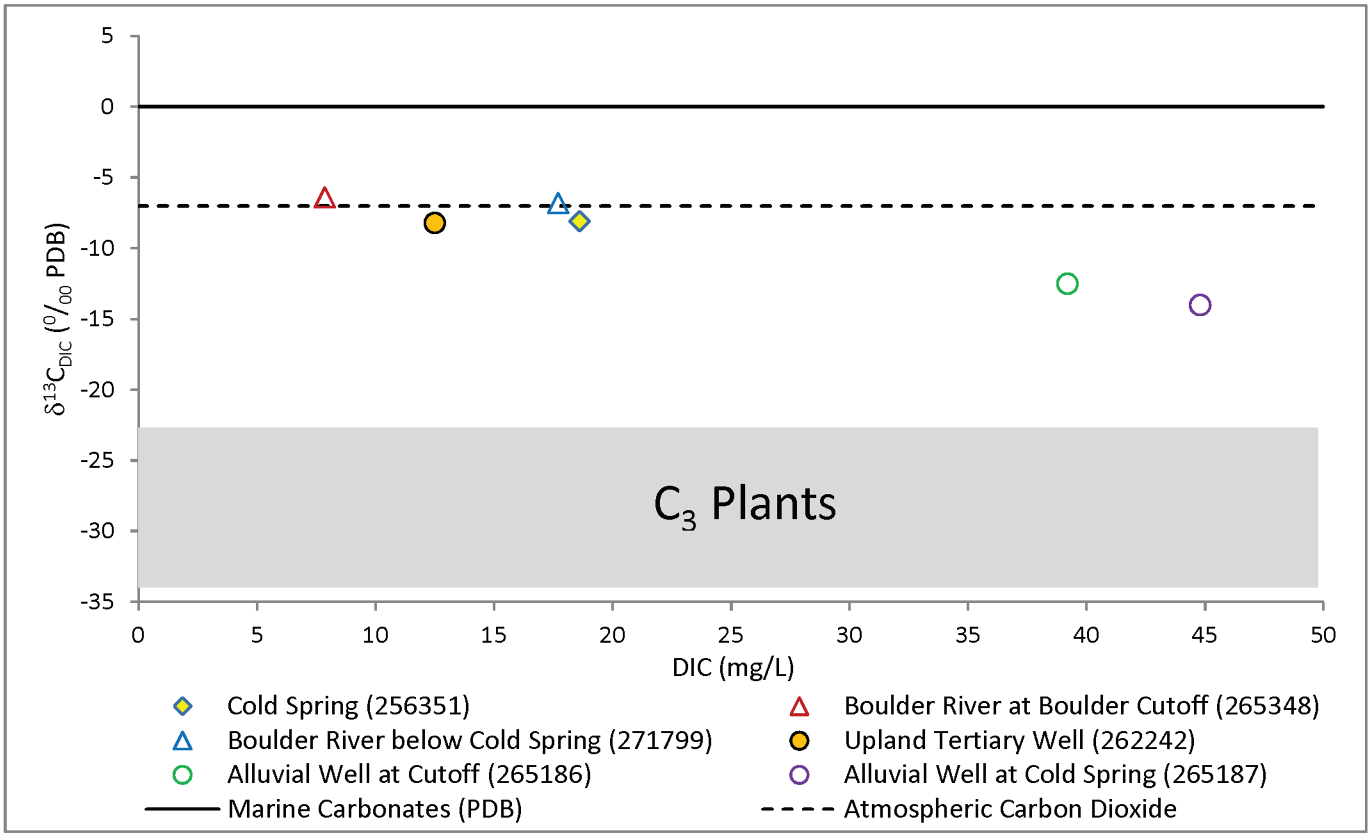

Figure 32. Alluvial groundwater had distinctly more DIC and lighter $\delta^{13}C$ values than the water from Cold Spring. Alluvial water composition is consistent with the mixing of water with atmospheric sources with decayed native plant remains. Other samples are consistent with carbon from atmospheric sources. Results from Cold Spring do not indicate marine carbonates.

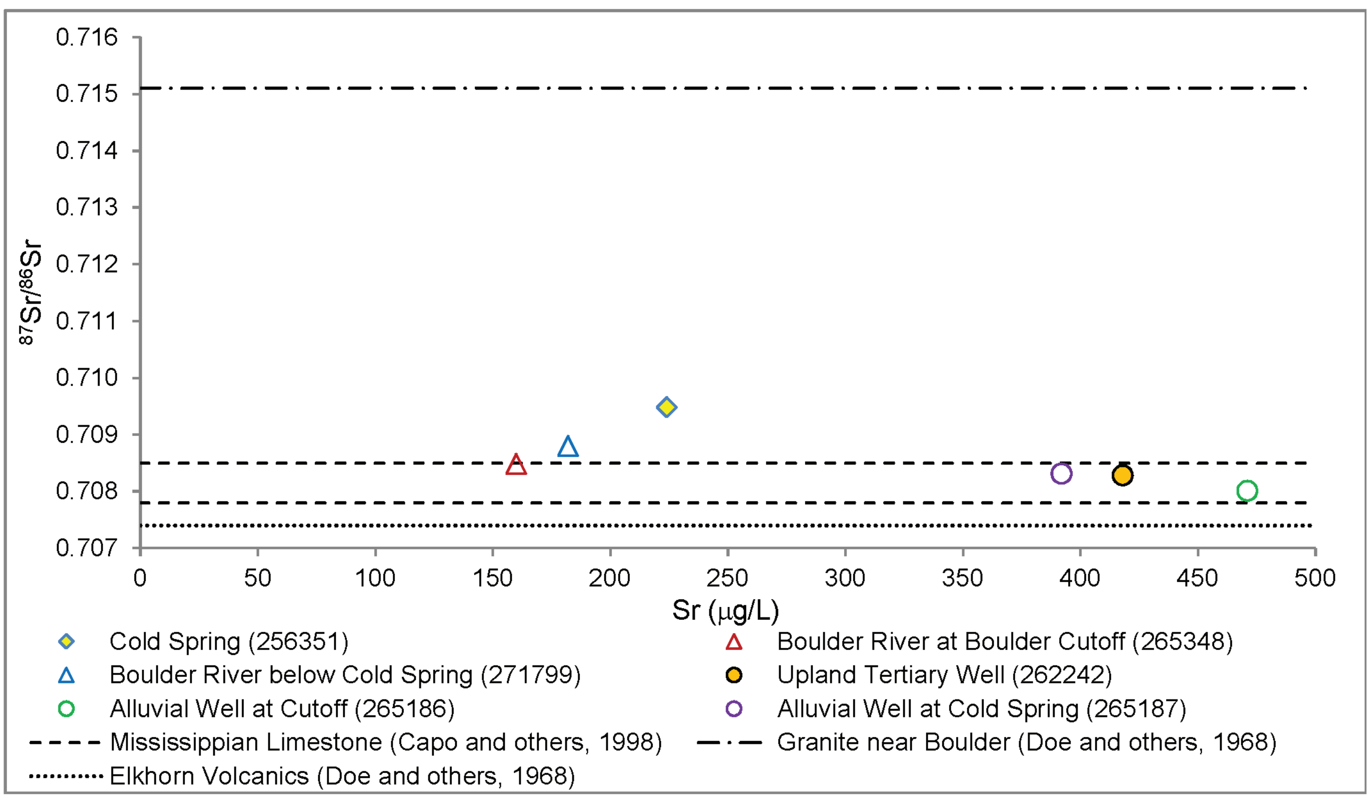

Figure 33. The elevated $^{87}Sr/^{86}Sr$ ratio for Cold Spring indicates potential interaction with granite ($^{87}Sr/^{86}Sr$ ratio ~0.7151; Doe and others, 1968), and the elevated value for the Boulder River below Cold Spring shows mixing between Cold Spring and the Boulder River. Other $^{87}Sr/^{86}Sr$ ratios are consistent with the weathering of Mississippian limestone.

a small area.

Numerical Modeling Scenarios

Area-Wide Model

The Area-Wide model's purpose was to quantify potential impacts from increased residential development using modeled changes in groundwater levels and stream flows. Groundwater-level declines were calculated using the maximum drawdown and the radius of the 1-ft drawdown contour beyond the edge of the well field. The results from each of the four scenarios (fig. 11) were compared to a 20-yr baseline model. The baseline model used average values for all stresses rather than historical or simulated future data and allowed changes to be clearly attributed to the new stress (i.e., new residential developments) rather than evaluating the new stress on top of natural variability.

Scenario 1: Full Development of an Existing Subdivision. Scenario 1 postulated that an existing 96-lot subdivision northeast of Boulder would be fully developed (fig. 11). Cadastral data from 2010 indicates that 58 of the 20-acre lots were vacant (Montana State Library, 2010). Full development was simulated by adding 58 wells to the model. Each new well was pumped on the same schedule as existing domestic wells, with the greatest net withdrawals occurring each summer.

Pumping from the new wells resulted in increased summertime drawdown, and an increased extent of the cone of depression. Maximum drawdown occurred in August of the last simulated year (year 20; fig. 34). The greatest drawdown of 14.1 ft occurred in the northwest part of the well field, which has the lowest permeabilities. The year-to-year change in drawdown decreased over time; it was 1.3 ft between years 1 and 2, but only 0.19 ft between years 19 and 20. The 1-ft drawdown contour extended a maximum of 1.2 mi north of the pumping center (fig. 34; table 9). This distance was approximate because the cone of depression reached its maximum extent to the north, where it intersected the no-flow boundary at the edge of the model grid.

Pumping the new wells also decreased the amount of groundwater that flowed to nearby streams, causing stream depletion (Theis, 1940). The greatest stream depletion of 0.04 cfs (18 gpm) occurred in the final year of the simulation (fig. 35), and the maximum cumulative stream depletion was 65.7 percent of the pumping rate (table 9). The remainder of the pumped water came from aquifer storage. Stream depletion increased over time, reflecting that aquifer storage becomes less of a source of water as drawdown stabilizes (Jenkins, 1968). Depletion was the greatest in the stream segments closest to the subdivision and occurred most in the reaches of Muskrat Creek within the subdivision. Near the subdivision, the only unaffected stream reaches were those that were dry in the baseline scenario.

Scenario 2: New Subdivision; 64 Residences on 20-acre Lots, NE of Boulder. Scenario 2 evaluated the potential development of a new 20-acre-lot subdivision along the eastern edge of the North Boulder Valley (fig. 11). The pumping scenario included 64 wells on 20-acre lots. The simulation resulted in a maximum drawdown of 11 ft, which occurred in August of the final year of pumping. The change in maximum drawdown was 1.4 ft between years 1 and 2, and 0.14 ft between years 19 and 20. The 1-ft drawdown contour extended a maximum of 1.9 mi north of the pumping center (fig. 36; table 9).

A maximum stream flow decrease of 0.03 cfs (13 gpm) occurred in the final year of the simulation (fig. 37). The maximum cumulative depletion was 36.3 percent of the pumping rate (table 9). The greatest depletion occurred in the lower reach of Muskrat Creek. Near the subdivision, the only unaffected stream reaches were those that were dry in the baseline scenario.

Scenario 3: New Subdivision; 128 Residences on 10-acre Lots, NE of Boulder. Scenario 3 featured wells in the same locations as in Scenario 2 (fig. 11). The only difference was that the pumping rates were double those in Scenario 2 in order to simulate 10-acre rather than 20-acre lots. The simulation results were proportional to the increased pumping rates. For instance, the maximum drawdown was 22 ft, or roughly double that of Scenario 2, and it occurred at the same time and location as in Scenario 2 (fig. 38). The change in maximum drawdown was 2.8 ft between years 1 and 2, and 0.29 ft between years 19 and 20. The 1-ft drawdown contour extended a maximum of 2.2 mi north of the pumping center (fig. 38; table 9).

A maximum decrease in stream flow of 0.06 cfs (26 gpm) occurred in the final year of the simulation

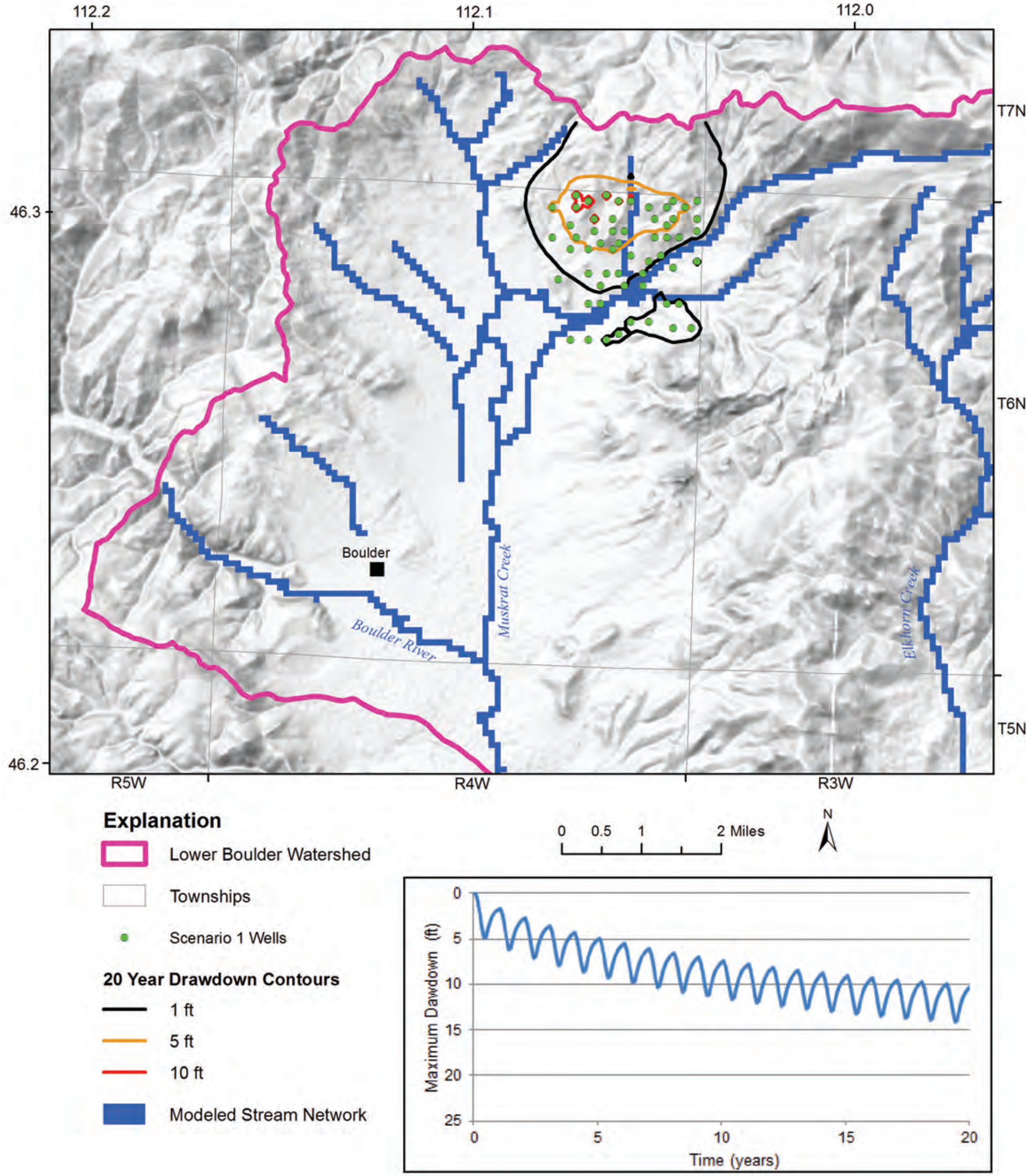

Figure 34. Scenario 1 showed that groundwater withdrawals from additional development in an existing subdivision would cause a maximum drawdown of about 14 ft, and the 1-ft drawdown contour would extend approximately 1.2 mi from the well field after 20 years.

Table 9. Area-Wide Model Predictive Scenario Results

Scenario	Number of New Domestic Wells Simulated	Maximum Radius of the 1-ft Drawdown Contour (mi)	Maximum Drawdown (ft)	Change in Drawdown in the First Year (ft)	Change in Drawdown in the Last Year (ft)	Maximum Stream Depletion as Decrease in Base Flow (cfs)	20-yr Cumulative Stream Depletion as Percent of Well Discharge
1	58	1.2*	14.1	1.3	0.19	0.041	65.7
2	64	1.9	11.1	1.4	0.14	0.03	36.3
3	128	2.2	22.3	2.8	0.29	0.06	36.2
4	64	1.4	8.2	0.9	0.07	0.041	65.6

*The maximum radius of the 1-ft drawdown contour was approximated in Scenario 1 due to the model boundary.

(fig. 39). The maximum cumulative depletion was 36.2 percent of the pumping rate. The greatest depletion occurred in the lower reach of Muskrat Creek. Near the subdivision, the only unaffected stream reaches were those that were dry in the baseline scenario (table 9).

Scenario 4: New Subdivision; 64 residences on 20-acre Lots, South of Jack Creek Subdivision. Scenario 4 was similar to Scenario 2 in that it featured a new subdivision with 20-acre lots and a total of 64 wells. The new development was located on the western benches of the central Boulder Valley, adjacent to the existing Jack Creek subdivision (fig. 11). The simulation resulted in a maximum drawdown of 8 ft, which occurred in August of the final year of pumping. The change in maximum drawdown was 0.85 ft between years 1 and 2, and 0.07 ft between years 19 and 20. The 1-ft drawdown contour extended a maximum of 1.4 mi north of the pumping center (fig. 40; table 9).

A maximum cumulative decrease in stream flow of 0.04 cfs (18 gpm) due to pumping occurred in the final year of the simulation (fig. 41). The maximum cumulative depletion was 65.6 percent of the pumping rate (table 9). Most of the depletion occurred in the Boulder River and Quinn Creek; however, Jack Creek also showed effects.

Area-Wide model scenario summary. Some model results were common to all four simulations. For instance, water levels continued to decline throughout each 20-yr scenario, although the annual rate of drawdown decreased by about an order of magnitude by the end of the simulation (table 9). Also, the location of maximum drawdown was in the least permeable area of each well field.

Results also showed differences between scenarios based on geology and the location of new stresses. The maximum drawdown was lowest in Scenario 4 because the underlying basin-fill materials are more permeable than the bedrock. A larger radius of influence was not associated with higher depletion percentages; rather, decreases in base flow were a function of the proximity to the streams and the duration of pumping.

Results also demonstrate that drawdown and depletion increased proportional to development density (withdrawal rate). In comparing Scenario 2 and Scenario 3, the maximum drawdown and depletion rate both doubled as the pumping rates doubled. Percent depletion did not increase with increased pumping rates. At the end of each simulation the depletion percentages were approximately equal. These results match conceptual and analytical models of stream depletion (Jenkins, 1968; Bredehoeft and others, 1982; Bredehoeft, 2002). The end-of-simulation depletion percentages for Scenarios 2 and 3 were also lower than those of Scenarios 1 and 4, as was their annual rate of decrease. These results indicate that the depletion percentage's magnitude and rate of decrease with time are both proportional to distance from the streams, because the Scenario 1 and 4 sites were closer to streams.

Although the magnitude of stream depletion may seem small [a maximum of 0.06 cfs (26 gpm) for Scenario 3], the results suggest that the depletion rates will continue to increase with time. While storage from the aquifer can buffer the effects of pumping, eventually all of the pumped water must be offset by increased aquifer recharge or decreased aquifer discharge (Thies, 1940).

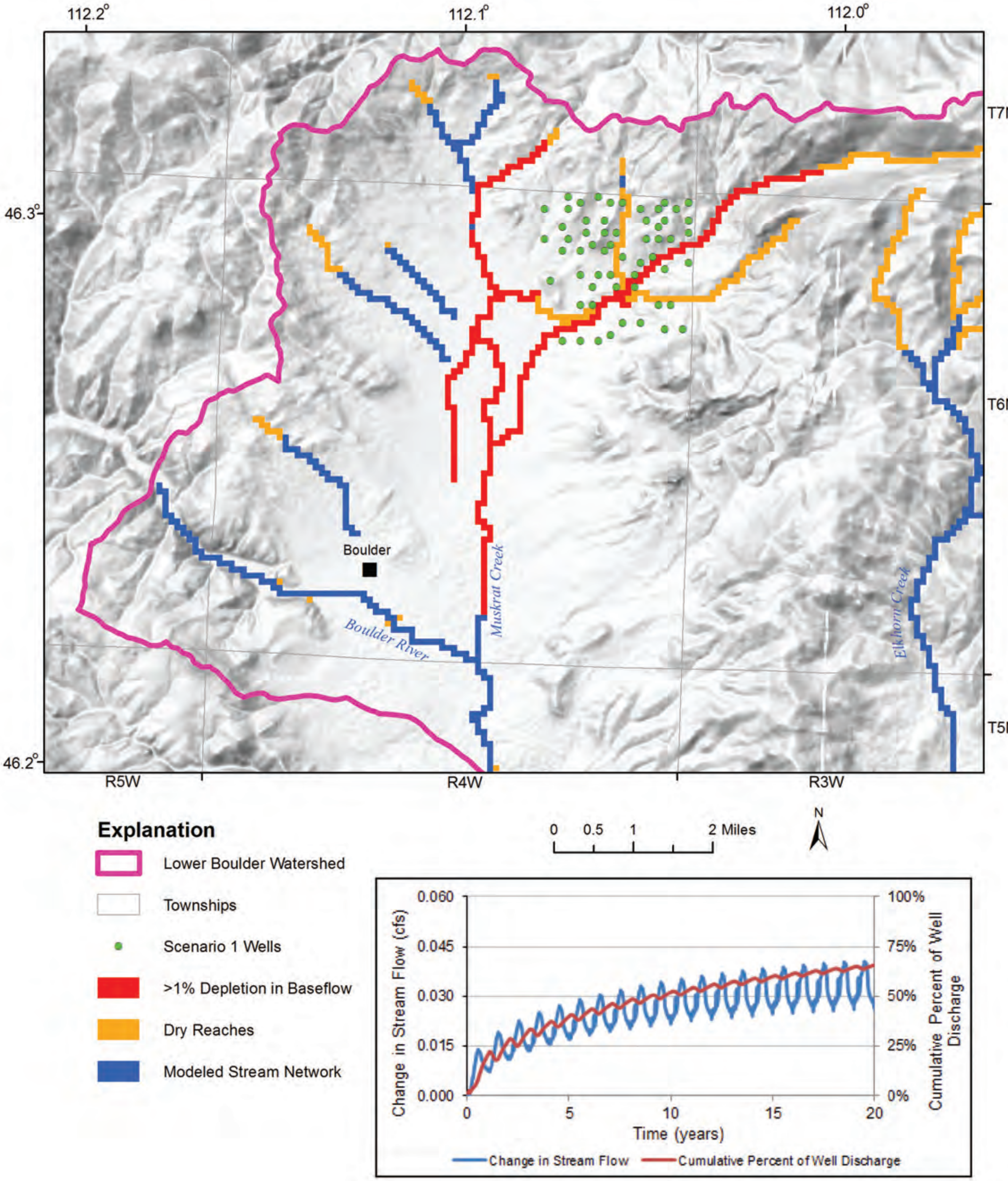

Figure 35. Development under Scenario 1 would cause a decrease in stream flow of about 0.04 cfs after 20 yr and over time a greater percentage of the water pumped from the wells would be obtained from stream depletion as aquifer storage is depleted. Most of the depletion would occur in Muskrat Creek, with less depletion in other streams.

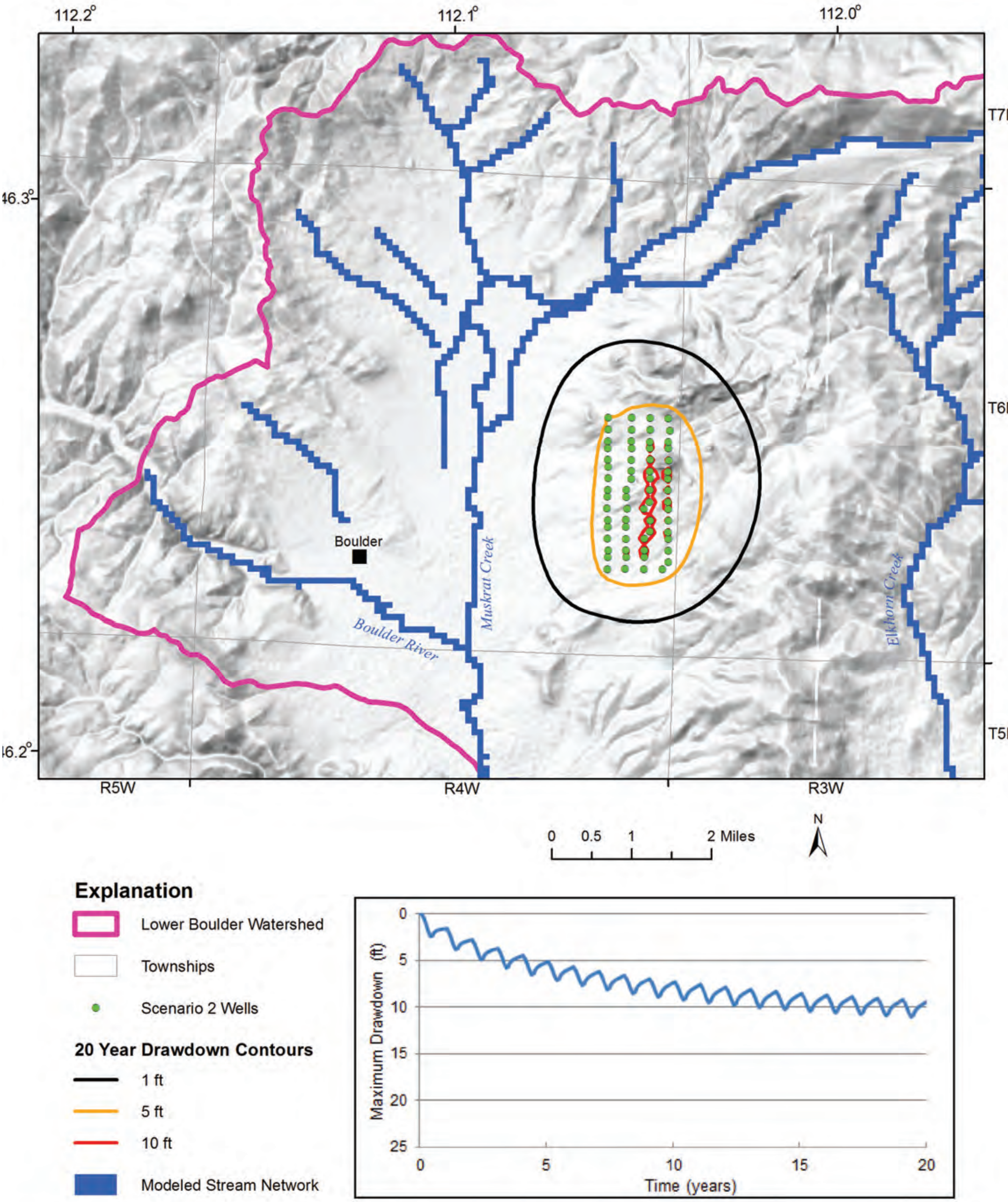

Figure 36. Scenario 2 results showed that 64 wells on 20-acre lots would result in a maximum drawdown of about 11 ft, and the 1-ft drawdown contour would extend approximately 1.9 mi from the well field after 20 yr.

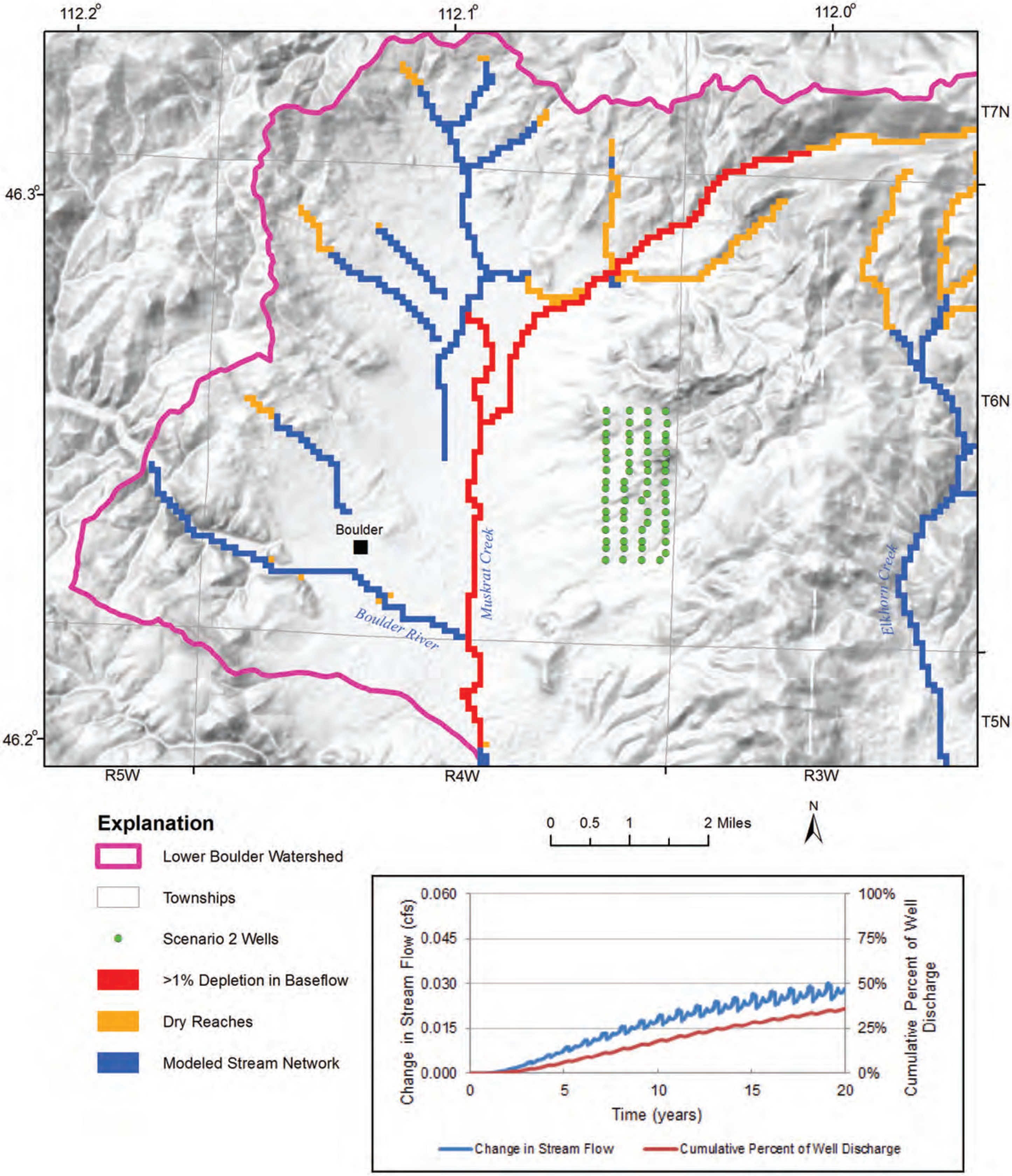

Figure 37. Development under Scenario 2 would cause a decrease in stream flow of about 0.03 cfs after 20 yr, and over time a greater percentage of the water pumped from the wells would be obtained from stream depletion as aquifer storage is depleted. Most of the depletion would occur in Muskrat Creek, with less depletion in other nearby streams.

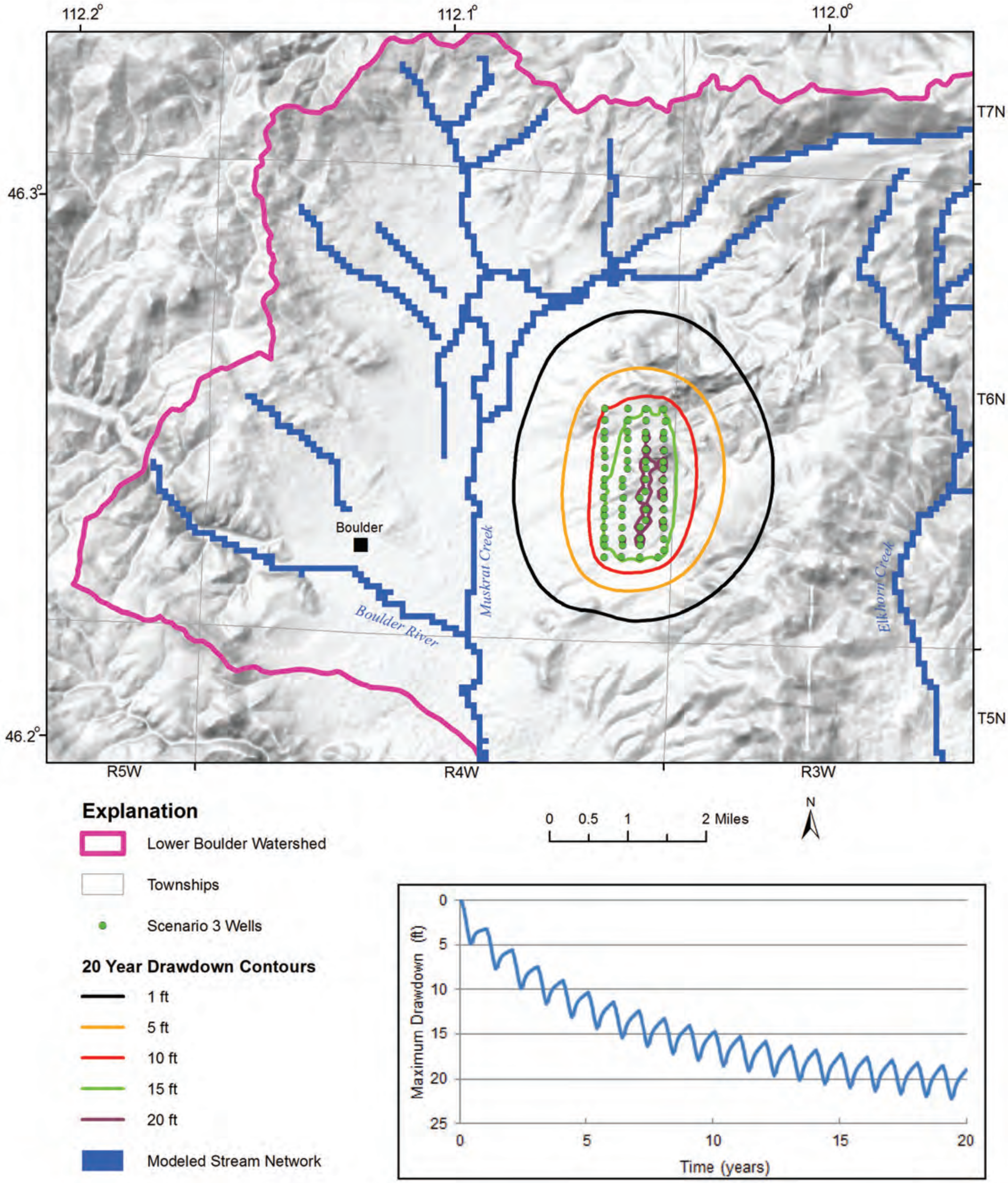

Figure 38. Scenario 3 results show that 128 wells on 10-acre lots would result in a maximum drawdown of about 22 ft, and the 1-ft drawdown contour would extend approximately 2.2 mi from the well field after 20 yr.

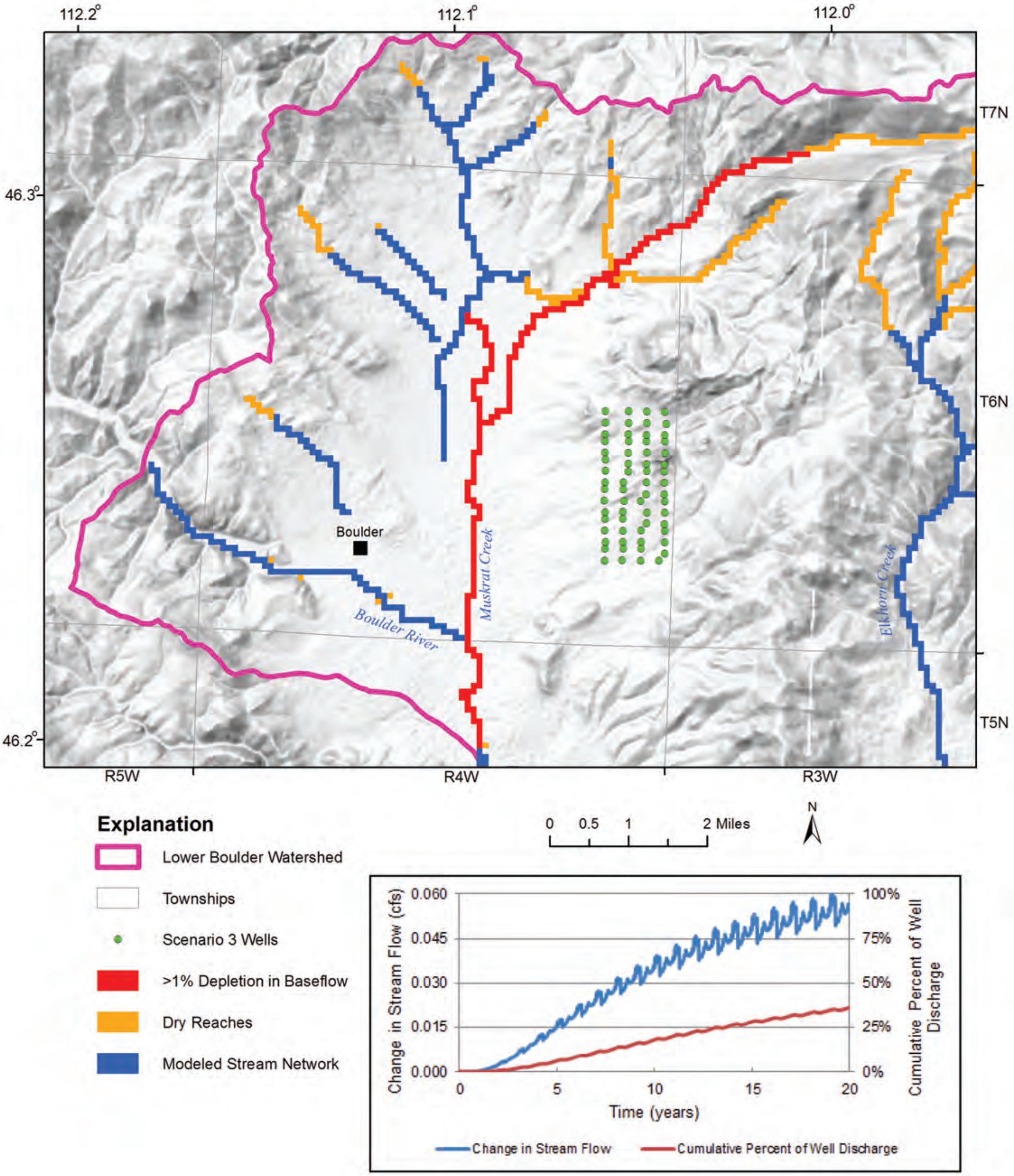

Figure 39. Development under Scenario 3 would cause a decrease in stream flow of about 0.06 cfs after 20 yr, and over time a greater percentage of the water pumped from the wells will be obtained from stream depletion as aquifer storage is depleted. Most depletion would occur in Muskrat Creek, with lesser amounts in other streams.

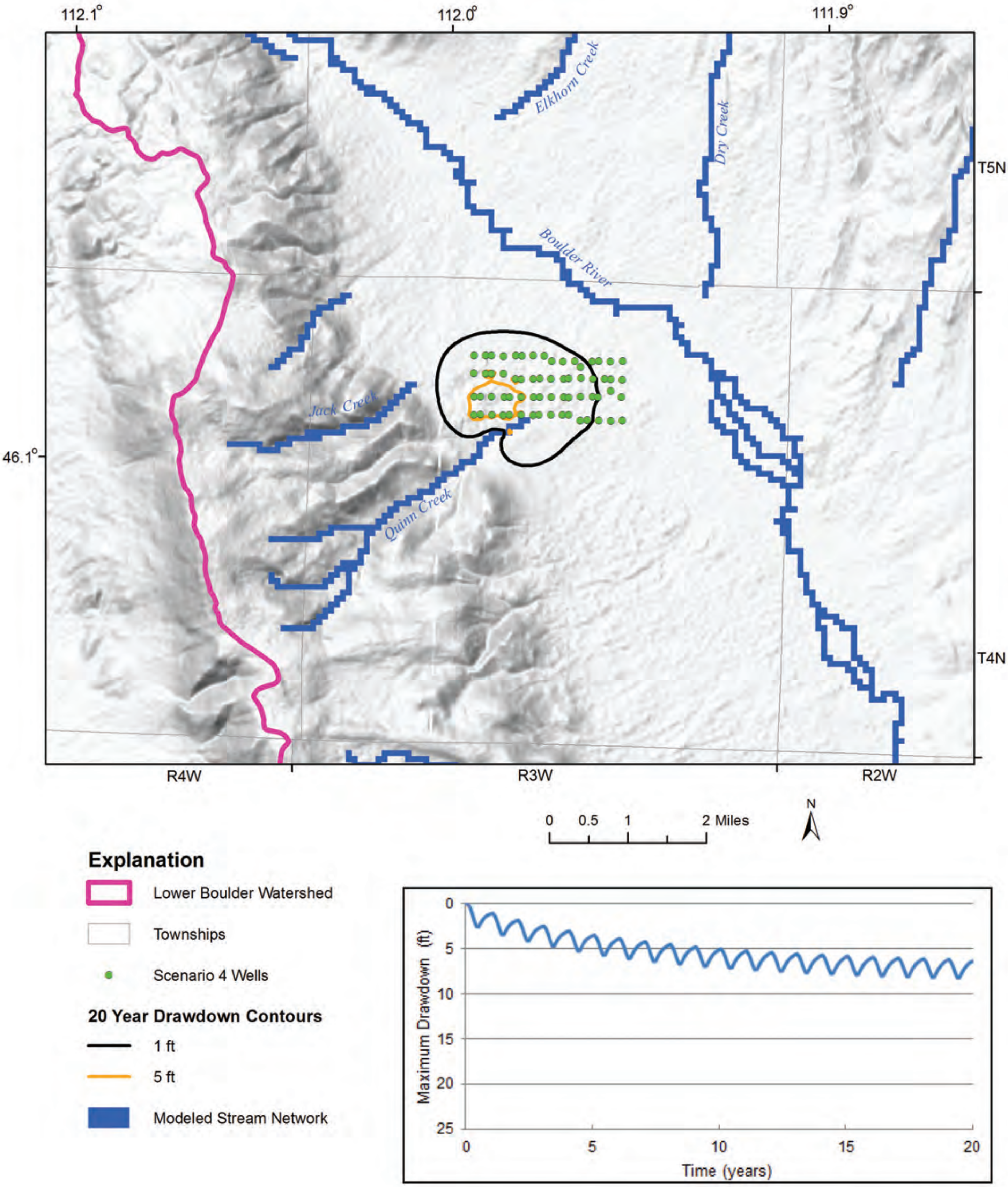

Figure 40. Scenario 4 results show that 64 wells on 20-acre lots near Jack Creek would result in a maximum drawdown of about 8 ft, and the 1-ft drawdown contour would extend approximately 1.4 mi from the well field after 20 yr.

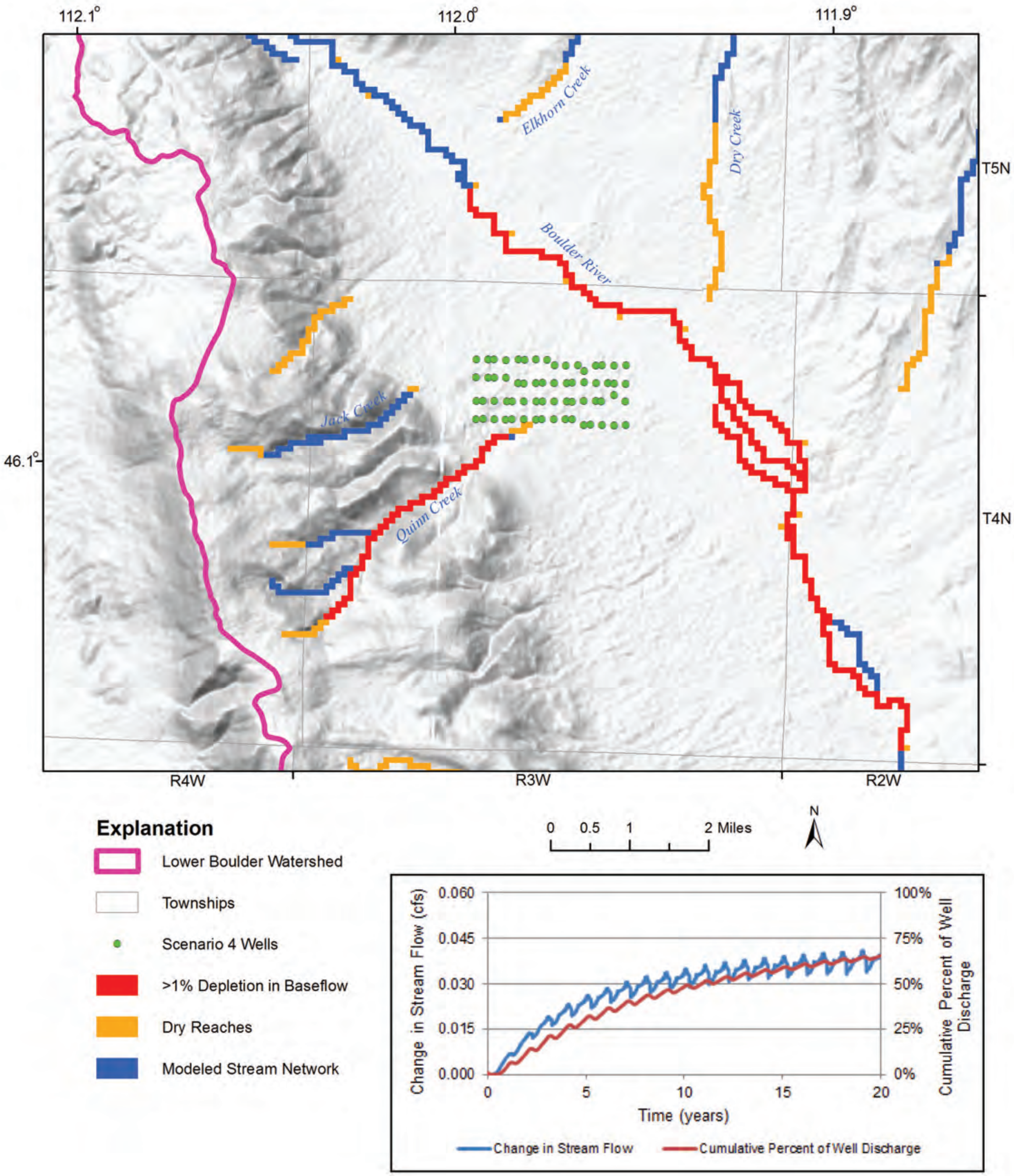

Figure 41. Development under Scenario 4 would decrease stream flow by about 0.04 cfs after 20 yr, and over time a greater percentage of the water pumped from the wells would be obtained from stream depletion as aquifer storage is depleted. Most depletion would occur in the Boulder River and Quinn Creek, with less depletion in other streams.

Managed-Recharge Model

The area simulated by the Managed-Recharge model is located within the area simulated by the Area-Wide model, but the models are independent. Within the modeled area the Boulder River shows a net loss, so the intent was to demonstrate the potential for managed recharge to reduce this loss and increase downstream river flow. Increased July to September stream flow could allow late season irrigation under existing water rights, for which water is currently not available. Managed recharge could also be a mitigation strategy to ensure that new groundwater developments would not negatively impact senior water rights.

A 20-yr baseline model was developed to simulate existing conditions. Baseline model results were compared to the results of each scenario to quantify changes resulting from each new stress. For each scenario, the model was run for 5 yr using existing stresses to ensure that it was stable. Stress changes were then applied for the remaining 15 yr. In all cases, the model was approaching a new equilibrium at the end of the model run.

Scenario 1: Irrigation Canal Leakage Terminated. The existing irrigation canals provide recharge to groundwater through canal leakage. While this recharge is not "managed," the physical process is analogous to using infiltration basins. Likewise, terminating canal leakage would be analogous to removing infiltration basins.

The model showed that eliminating canal leakage from the Carey canal would cause local groundwater elevations to decline approximately 12 ft and alluvial groundwater levels to decline approximately 3 ft (fig. 42A, B, and C). The average annual flow of the Boulder River would decrease by 5.3 cfs at the downstream end of the model (3,860 acre-ft/yr; table 10; fig. 43). Although the river would lose this water within the model domain, the water would remain in the alluvial aquifer and eventually return to the river as base flow. This return would likely occur south of the Boulder Cutoff Road (fig. 10).

Scenario 2: North Infiltration Basin (3.1 acres). In this scenario a 3.1-acre infiltration basin was simulated 3,000 ft south of the northern boundary of the model (fig. 11, location A). The basin was located immediately downgradient of the Murphy canal (the presumed source of water). The basin was simulated using specified flux cells. The specified flux was 86,400 ft^3/day from March 15 to May 9 (55 days; 109 acre-ft/yr). This was the most water that could be added without causing model cells to flood. In model year 20, Boulder River losses decreased by an average annual rate of 0.2 cfs (130 acre-ft/yr; table 10).

Scenario 3: Central Infiltration Basin (3.1 acres). This scenario is similar to scenario 2 but the infiltration basin was about 2 mi south of the northern model boundary (fig. 11, location B), and 345,600 ft^3/day of water could be added for 55 days without causing model cells to flood (436 acre-ft/yr). In model year 20, Boulder River losses decreased by an average annual rate of 0.7 cfs (500 acre-ft/yr; table 10).

Scenario 4: South Infiltration Basin (3.1 acres). Scenario 4 is similar to scenario 2 except the infiltration basin was about 3 mi south of the northern model boundary (fig. 11, location C), and 259,200 ft^3/day of water could be added for 55 days without causing flooding (327 acre-ft/yr). In model year 20, Boulder River losses decreased by an average annual rate of 0.6 cfs (450 acre-ft/yr; table 10).

Scenario 5: All Three Basins (9.3 acres). This scenario used all of the basins from scenarios 2–4, for a total flux of 691,200 ft^3/day for 55 days (873 acre-ft/yr). In model year 20, Boulder River losses decreased by an average annual rate of 1.2 cfs (860 acre-ft/yr; table 10). Some of the added water left the modeled area as groundwater outflow through the alluvium.

Scenario 6: Central Larger Basin (6.2 acres). This scenario placed an infiltration basin in the same location as scenario 3, but doubled its size (6.2 acres). This enlargement allowed it to accept the maximum capacity that the Murphy canal could supply. The flux was 648,000 ft^3/day (818 acre-ft/yr). In model year 20, the Boulder River losses decreased by an average annual rate of 1.2 cfs (860 acre-ft/yr; table 10).

Scenario 7: Central Long Narrow Basin (35 acres). This scenario was similar to scenario 6 except that the basin size was enlarged (35 acres) so that it would accept the volume of water diverted into the Murphy canal from the Boulder River. This assumes that the canal would be lined so leakage from the Murphy canal was also set to zero. The flux was 1,296,000 ft^3/day (1,636 acre-ft/yr). In model year 20 Boulder River losses decreased by an average annual rate of 1.9 cfs (1,400 acre-ft/yr; table 10; fig. 43). Again,

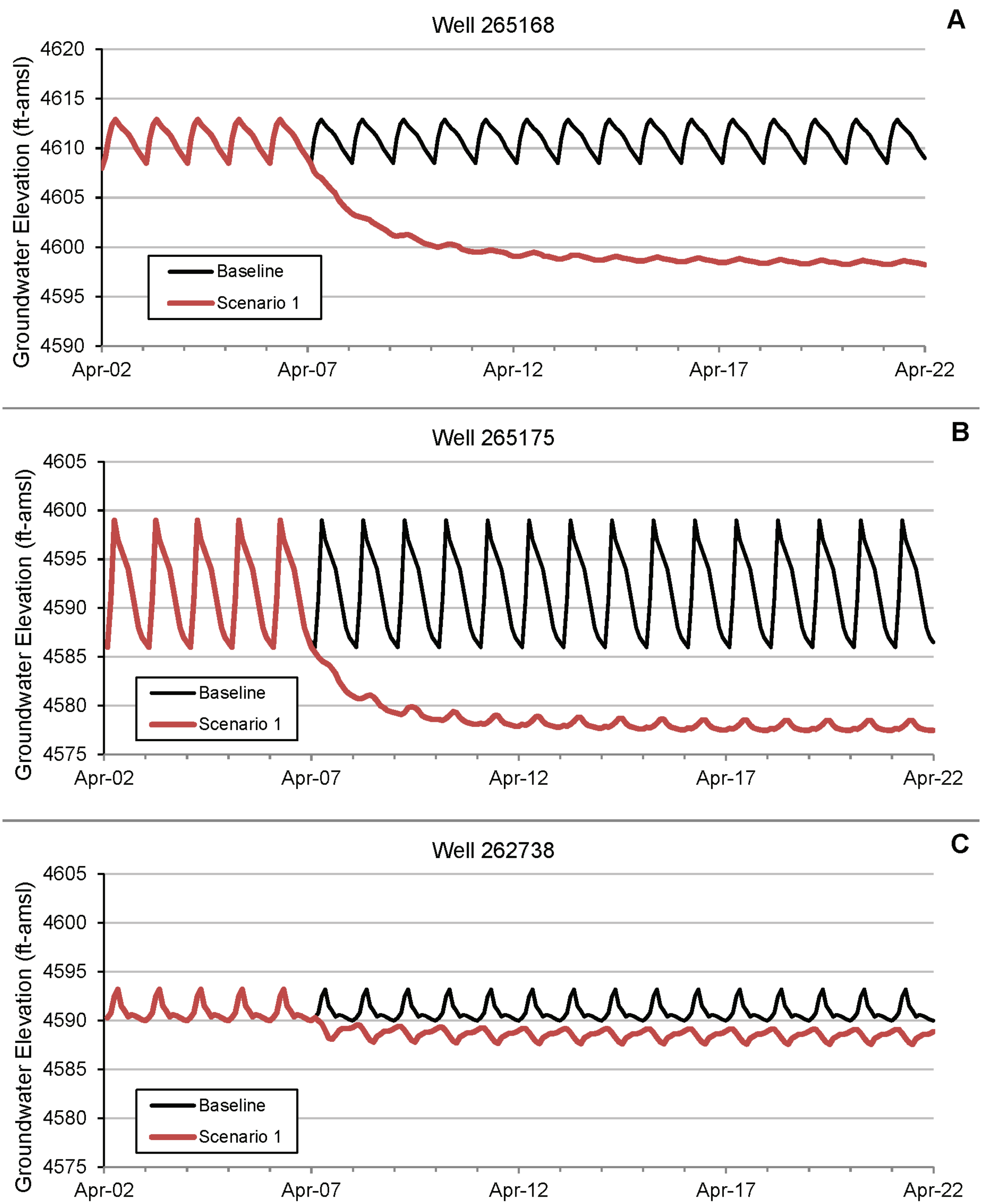

Figure 42. Scenario 1 of the Managed-Recharge model shows that canal leakage (which is physically analogous to infiltration basins) substantially raises the groundwater table near and downgradient of the canal.

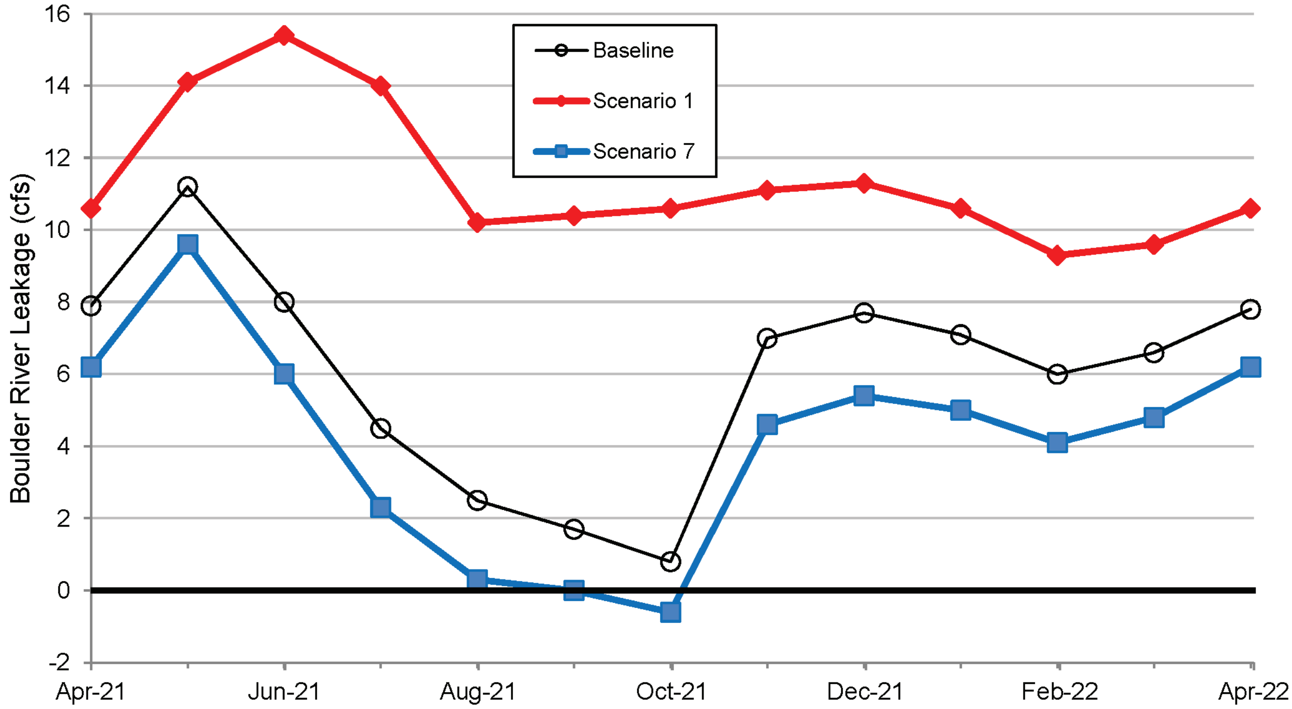

Figure 43. Comparison of scenarios from the Managed-Recharge model show that canal leakage termination would have the greatest effect on Boulder River leakage rates, increasing the average annual loss rate within the modeled area by about 5 cfs. The maximum infiltration scenario (7) showed that infiltrating the full diversion of the Murphy ditch would decrease the average annual loss by about 2 cfs within the modeled area.

Table 10. Managed-Recharge Model Predicted Average Annual Decrease in Boulder River Leakage to Groundwater

Scenario	Description	Decrease in Boulder River Leakage (cfs)	Decrease in Boulder River Leakage (acre-ft/yr)
1	Irrigation ditch leakage termination	-5.33	-3,861
2	North infiltration basin	0.18	130
3	Central infiltration basin	0.69	500
4	South infiltration basin	0.62	449
5	Combined infiltration basins	1.19	862
6	Maximum Murphy ditch capacity (unlined) delivered to the central basin location	1.19	862
7	Maximum Murphy ditch capacity (lined) across 2-mi portion of western pediment	1.93	1,398

some of the added water left as groundwater outflow through the alluvium.

Managed-Recharge scenario summary. For most of the infiltration basin scenarios, the volumes of Boulder River flow increases were slightly greater than the water volumes applied at the basins. Although gaining water may seem counterintuitive, it is caused by the Murphy canal leaking in the early spring when it would otherwise have been dry. Thus the additional recharge to the river was supplied by canal leakage. Canal leakage was not a factor in scenario 7 because the Murphy canal was assumed to be lined.

Overall the modeled scenarios show that a significant amount of groundwater recharge can occur by infiltrating water on the lower bench each spring (March 15 to May 9). The size and location of the infiltration basins would determine the amount of recharge, and the timing of effects on surface water. Infiltration basins on the lower portion of the bench appear to be physically suited to provide for late-summer stream flow enhancement. Because the infiltration basins were modeled as specified flux cells (i.e., injection wells), time lags associated with flow through the unsaturated zone and changes in infiltration rates over time were not assessed.

SUMMARY OF THE HYDROGEOLOGIC SYSTEM

The three general groups of geologic materials within the Boulder Valley study area are bedrock, Tertiary to Pleistocene sediments, and Quaternary alluvium (fig. 12). Bedrock has little primary permeability, and groundwater flows through fractures and solution voids. The older pre-Cambrian to Cretaceous bedrock, which has been fractured, tends to be somewhat more permeable than the younger, less fractured Cretaceous rocks of the Boulder Batholith and Elkhorn Volcanics. The Tertiary to Pleistocene sediments vary from mudstones to gravels and are weakly consolidated. These sediments have some intergranular primary permeability, so they are typically more productive than the bedrock aquifers. The Quaternary alluvium is unconsolidated and composed of gravel, sand, and silt. It has significant intergranular primary permeability, and is the most productive aquifer in the study area.

Bedrock is exposed in the mountainous areas and underlies the more permeable unconsolidated Tertiary and Quaternary units. The Tertiary to Pleistocene sediments extend across the valley from the mountain front faults on both sides, and underlie the Quaternary alluvium in its center. The combined thickness of the Tertiary and Quaternary units is more than 4,000 ft in the center of the valley. The Quaternary alluvium is typically less than 100 ft thick, and underlies the modern floodplain. Bedrock is exposed where the Boulder River enters the study area (Boulder Canyon), below the confluence of the Boulder and Little Boulder Rivers (northern bedrock notch), and at the southern end of the study area (southern bedrock notch). These bedrock constrictions split the basin-fill deposits into two basins, each of which is bounded by bedrock.

The groundwater budget provides an understanding of the major factors affecting groundwater availability. Sources of groundwater recharge are upland recharge in the mountains, canal leakage, irrigation recharge, and stream losses. Groundwater discharges to streams, is used by riparian plants, and is withdrawn by wells. Canal leakage accounts for 46% of groundwater recharge; 75% of groundwater discharges to surface waters in the southern (downstream) portion of the study area. Less than 1 percent of the groundwater enters or leaves the area in the subsurface because of bedrock constrictions at both ends of the study area.

The composite potentiometric surface (fig. 12) shows the groundwater flow generally mimics the local topography. In the north basin groundwater flow is towards the Quaternary alluvium along the Boulder River and Muskrat Creek. Within the Quaternary alluvium, flow is parallel to streams. Near the confluence of Muskrat Creek and the Boulder River, groundwater discharges to the Boulder River because the basin-fill materials thin at the northern bedrock notch (fig. 23). Below the northern bedrock notch, the Boulder River loses water to the Quaternary alluvium. In the southern basin groundwater flows towards the Quaternary alluvium from the surrounding bedrock and Tertiary to Pleistocene sediments. Groundwater flow in the Quaternary alluvium is parallel to the Boulder River. Because bedrock is at the surface in the southern portion of the study area, most of the water in the Quaternary alluvium must discharge to the Boulder River. Much of this water appears to be intercepted by fractures in the Madison Limestone, and is then routed through Cold Spring.

In the irrigated floodplain groundwater levels rise and fall as much as 20 ft in response to seasonal changes in recharge, including high stream losses in the spring, canal leakage, and irrigation recharge throughout the irrigation season. Although groundwater levels in alluvial wells show substantial seasonal variation, overall water-level trends appear flat during the study period. Wells completed in the Tertiary to Pleistocene sediments on the benches respond to spring snowmelt and infiltration, partly from ephemeral streams that lose water to basin-fill materials. Wells completed near irrigation canals or irrigated fields also respond to canal leakage and irrigation recharge. Seasonal water-level variations for these wells are typically less than 10 ft. The wells on the benches generally declined over the study period, reflecting the change from wet to dry conditions near the start of the study period. Bedrock wells also showed a decline over the study period due to a shift to drier conditions. Bedrock wells are not as consistent concerning the degree to which they respond to seasonal influences. Some bedrock wells show response to short-term influences (e.g., 160435) and others show very little short-term variation (e.g., 226319). This likely reflects differences in fracturing patterns at different sites, which causes some wells to be more directly influenced by changes at the surface.

Long-term groundwater level data (19–22 yr) are available for nine wells completed in the Tertiary to Pleistocene bench sediments and the Quaternary alluvium. These data show that most of these wells show a slight (0.01 to 0.07 ft/yr) downward trend over the period of record. The two wells with the most pronounced downward trends (0.37 ft/yr, 53392; and 0.44 ft/yr, 50963) were also evaluated for the 10-yr period from 2004 to 2013. Over this 10-yr period one well trended slightly down (0.07 ft/yr, 53392) and one well trended up (0.18 ft/yr, 50963). It appears that the overall decline in water levels is in response to the overall drier conditions experienced since 1997, and groundwater levels have been slightly rising due to somewhat higher precipitation since 2004.

Groundwater quality is also a reflection of hydrogeologic setting. The dominant groundwater type is calcium–bicarbonate, which is expected from the weathering of igneous rocks and limestone. Groundwater TDS concentrations are less than 200 mg/L in the northern portion of the study area, reflecting the low solubility of the igneous rocks in that area. TDS concentrations are somewhat higher in the southern portion of the study area where rocks containing more soluble salts (limestone and marine shales) are present. Near Boulder Hot Springs some groundwater samples show a sodium–bicarbonate type, consistent with influence from hydrothermal water. In the southern portion of the study area wells are generally of a mixed cation-sulfate type, reflecting the heterogeneous nature of these rocks, including their deformation and alteration history.

POTENTIAL IMPACTS FROM HOUSING DEVELOPMENTS

Domestic wells remove water from the groundwater system. Most in-house water use in rural homes returns to groundwater via septic systems. Water applied to lawns and gardens is mostly transpired by plants. Because of these factors, in this area about 98 percent of a typical home's consumptive water use is for the irrigation of lawns and gardens (Waren and others, 2012). Net groundwater withdrawals must be offset by an increase in groundwater recharge, or a decrease in groundwater discharge (Theis, 1940; Bredehoeft and others, 1982, Bredehoeft, 2002). An example of increased groundwater recharge is when a stream changes from gaining to losing in response to nearby pumping. Decreases in discharge occur when downgradient receptors such as surface-water features and wetlands receive less water than they would have otherwise. When pumping occurs near areas of groundwater recharge or discharge, high-magnitude, short-term effects to surface-water features occur. When pumping occurs more distant from surface water, effects are smaller but last longer. Often the highest magnitude effects occur after pumping has ceased because of the time needed for effects to propagate from the pumping well to the surface-water feature (Jenkins, 1968).

Area-Wide model scenarios show that the timing of stream depletion depends on the distance between the pumping center and the stream of interest, and aquifer properties. The magnitude of depletion is dependent on the net groundwater withdrawal rate. Over time stream depletion must offset net groundwater withdrawals.

In the 20-yr model scenarios the highest streamflow reduction was 0.06 cfs, which is 0.2 percent of the lowest mean monthly flow calculated at the USGS gauge at Red Bridge (27 cfs in January). By comparison, the Carey canal diverted at least 14 cfs during the irrigation season in 2012. Good stream flow measurements are considered to have an error of ±5 percent, so housing developments on 10- to 20-acre lots and of up to 128 homes would not measurably exacerbate the summertime water shortages that often occur in the lower Boulder Valley. It would take about 2,000 new homes to create a 5 percent change in the lowest mean monthly flow.

POTENTIAL FOR MANAGED RECHARGE

Using managed recharge to supplement late-summer flows appears to be physically feasible. The modeled infiltration basins increased average annual stream flow by up to 1.9 cfs. The timing of enhanced stream flow also matched the target timing, with the greatest increases occurring from July to September (Carlson, 2013). The simulated stream flow increases would not significantly increase irrigation supplies;

however, they could offset decreases caused by withdrawals for new housing developments.

Several issues need to be addressed before considering a managed recharge project:

• An understanding of water rights and the legal ramifications of "storing" water that would otherwise flow to the Missouri River reservoirs. Even though there may be local excess water during snowmelt, it is subject to downstream water rights.

• Arsenic concentrations are higher in the Boulder River than in the groundwater. Non-degradation criteria apply to arsenic, it is unlikely that a permit to degrade would be issued, and water treatment may be cost prohibitive.

• Unsaturated flow was not modeled. Analysis of the unsaturated flow component would require site-specific studies to determine the lag time for the infiltrated water to reach the aquifer. These analyses would likely include pilot tests. If the lag time was too great, the basins could be constructed closer to the river.

• Dissolution of salts was not modeled. Given the semi-arid setting, it is likely that soluble salts are present in the unsaturated zone. Managed recharge water infiltrating through the unsaturated zone can mobilize salt. Ion exchange reactions can result in the creation of highly saline waters (TDS > 100,000 mg/L; Healy and others, 2011), and water from the infiltration ponds could degrade the underlying groundwater, which has a TDS of 100 to 200 mg/L. While there would likely be an initial increase in groundwater salinity, the salts would flush out over time.

• Below freezing temperatures are common during the modeled infiltration period (mid-March to early May). Ice would make it difficult to use diversion structures, canals, and basins. These issues could be avoided by using injection wells; however, there would be additional permitting, cost, and maintenance issues.

RECOMMENDATIONS

New groundwater developments may impact groundwater levels and stream flows. These impacts should be considered at the planning stage. Efficient use of water (e.g., xeriscaping) would reduce the amount of water needed. If there are new developments, groundwater monitoring, impact thresholds (e.g., minimum groundwater levels), and defined management actions could be used to limit the severity of impacts.

Managed recharge could be used to offset stream flow impacts from new housing developments. Its effectiveness would depend on the local hydrogeology, surface-water/groundwater interactions, and development density. A detailed cost-benefit analysis is needed to determine if a managed recharge project is viable. Issues associated with water rights and water quality should also be thoroughly researched before conducting additional characterization of the physical system.

Reevaluating irrigation practices with the goal of increasing late-summer flow in the Boulder River would likely produce significant flow increases. Water lost from the ditches and that percolates through fields enters the alluvial aquifer and eventually reaches the Boulder River to become the most important source of late-summer flows. Therefore, it is not desirable to line canals, or curtail irrigation. Conversely, increased early season canal use and irrigation would provide additional recharge the groundwater system.

Coordinated actions between irrigators could also improve late-summer flow. The drought management plans used in the Upper Jefferson and Big Hole River watersheds could be good models. These plans rely on monitored river flow and temperature to trigger specific actions, including voluntary reductions in diversions. In the Upper Jefferson, Van Mullem (2006) showed that the most cost-effective water-saving measures included improving canal system management, canal operating structures, and measuring structures. A similar combination of approaches would likely also be the most cost effective in the Boulder Valley. During low-flow periods, such improvements would allow irrigators to better regulate the amount of water diverted. When excess water is diverted, the stream reach between the diversion and the return flow is needlessly dewatered.

Increased monitoring of surface waters, irrigation diversions, and return flows would greatly aid in understanding the surface-water flow system, and facilitate water-management decisions. These data could be used to develop surface-water models of the area to aid in efficiently managing this water-limited basin. Identifying the river reaches of most concern would help in developing a monitoring plan. For instance, the lowest flows in the Boulder River typically occur at either Quantance Lane or Dunn Lane, so stage measurements at one of those sites could provide a management trigger. In times of severe drought, such monitoring would be especially useful in selecting the most effective water-conservation measures.

ACKNOWLEDGMENTS

This study would not have been possible without the assistance of the many land owners and residents of the Boulder Valley who provided access to their property and wells. Bob Sims, Pat Carey, and Randy Kirk provided many introductions and insight into the hydrogeologic system. Jefferson County provided partial funding for this study, and the County Commissioners provided feedback on the study scope. Tom Harrington from MSU Extension offered much help based on his local knowledge.

Montana Tech students John Anderson, Mike Shirley, Nicole Brancheau, and Allison Brown provided assistance in both the field and the office. Editing by Susan Barth, MBMG.

REFERENCES

Abdo, G., Butler, J., Myse, T., Wheaton, J., Snyder, D., Metesh, J., and Shaw, G., 2013, Hydrogeologic investigation of the Beaverhead River study area, Beaverhead County, Montana: Montana Bureau of Mines and Geology Open-File Report 637, 132 p.

Alexander, T.G., 1955, Geology of the Whitehall area, Montana: Yellowstone–Bighorn Research Association, Inc., Yellowstone–Bighorn Research Project Contribution 195, 111 p.

Aquaveo, LLC, 2010, Groundwater Modeling System (GMS), version 8.3.

ASTM International, 2010, Determining subsurface hydraulic properties and groundwater modeling, 3rd ed.: ASTM International, West Conshohocken, PA, 358 p.

Becraft, G.E., and Pinckney, D.M., 1961, Preliminary map of the northwest quarter of the Boulder quadrangle, Montana: U.S. Geological Survey Mineral Investigations Field Studies Map MF-183, scale 1:24,000.

Becraft, G.E., Pinckney, D.M., and Rosenblum, S., 1963, Geology and mineral resources of the Jefferson City quadrangle, Jefferson and Lewis and Clark Counties, Montana: U.S. Geological Survey Professional Paper 428, 101 p.

Berry, G.W., 1943, Stratigraphy and structure at Three Forks, Montana: Geological Society of America Bulletin, v. 54, p. 1–30.

Billingsley, P., 1915, The Boulder Batholith of Montana: American Institute of Mining and Metallurgical Engineers Transactions, v. 51, p. 31–56.

Blaney, H.F., and Criddle, W.D., 1962, Determining consumptive use and irrigation water requirements: U.S. Department of Agriculture Technical Bulletin 1275, 59 p.

Bobst, A., Waren, K., Butler, J., Swierc, J., and Madison, J.D., 2013, Hydrologic investigation of the Scratchgravel Hills study area, Lewis and Clark County, Montana, interpretive report: Montana Bureau of Mines and Geology Open-File Report 636, 63 p.

Bobst, A., Waren, K., Swierc, J., and Madison, J.D., 2014, Hydrogeologic investigation of the North Hills study area, Lewis and Clark County, Montana, technical report: Montana Bureau of Mines and Geology Open-File Report 654, 376 p.

Botz, M.K., 1968, Groundwater study near Boulder: Montana Bureau of Mines and Geology unpublished manuscript.

Bredehoeft, J., Papadopulos, S., and Cooper, H., 1982, Groundwater: The water-budget myth, in Scientific basis of water-resource management, studies in geophysics: National Academy Press, Washington, D.C., p. 51–57.

Bredehoeft, J., 2002, The water budget myth revisited: Why hydrogeologists model: Ground Water, v. 40, n. 4, p. 340–345.

Briar, D.W., and Madison, J., 1992, Hydrogeology of the Helena valley-fill aquifer system, west-central Montana: U.S. Geological Survey Water Resources Investigations Report 92-4023, 92 p.

Briar, D.W., Lawlor, S.M., Stone, M.A.J., Parliman, D.J., Schaefer, J.L., and Kendy, E., 1996, Groundwater levels in intermontane basins of the Northern Rocky Mountains, Montana and Idaho: U.S. Geological Survey Hydrologic Investigations Atlas 738-B, 1 sheet, scale 1:750,000.

Brunner, P., Cook, P.G., and Simmons, C.T., 2009, Hydrogeologic controls on disconnection between surface water and groundwater: Water Resources Research, v. 45, W01422, 13 p.

Buck, F.E., and Bille, H.L., 1956, Water resources survey: Jefferson County, Montana: Montana State Engineer's Office, Helena, MT, 87 p.

Burke, W.H., Denison, R.E., Hetherington, E.A., Koepnick, R.B., Nelson, H.F. and Otto, J.B., 1982, Variation of seawater 87Sr/86Sr throughout Phanerozoic time: Geology, v. 10, no. 10, p. 516–519.

Butler, J., and Bobst, A., in preparation, Hydrogeologic investigation of the Boulder Valley study area, Jefferson County, Montana, modeling report: Montana Bureau of Mines and Geology Open-File Report.

Burfiend, W.J., 1967, A gravity investigation of the Tobacco Root Mountains, Jefferson basin, Boulder Batholith, and adjacent areas of southwestern Montana: Bloomington, Indiana University, Ph.D. dissertation, 90 p.

Byrne, J., and Hunter, F., 1901, Twelfth annual report of the Inspector of Mines of the State of Montana, Independent Publishing Company, Helena, MT.

Cannon, M., and Johnson, D., 2004, Estimated water use in Montana in 2000: U.S. Geological Survey Scientific Investigations Report 2004-5223, 61 p.

Caldwell, R.R., and Eddy-Miller, C.A., 2013, Groundwater and surface-water interaction within the upper Smith River watershed, Montana, 2006–2010: United States Geological Survey Scientific Investigations Report 2013-5051, 88 p.

Capo, R.C., Stewart, B.W., and Chadwick, O.A., 1998, Strontium isotopes as tracers of ecosystem processes: Theory and methods: Geoderma, v. 82, no. 1, p. 197–225.

Carlson, L., 2013, Managed recharge and base-flow enhancement in an unconsolidated aquifer in the Boulder River Valley, Montana: Montana Tech of the University of Montana, M.S. thesis, 164 p.

Chauvin, G.M., Flerchinger, G.N., Link, T.E., Marks, D., Winstral, A.H., and Seyfried, M.S., 2011, Long-term water balance and conceptual model of a semi-arid mountainous catchment: Journal of Hydrology, v. 400, p. 133–143.

Clark, D., and Dutton, D., 1996, Quality of ground water and surface water in intermontane basins of the northern Rocky Mountains, Montana and Idaho: USGS Hydrologic Atlas: 738-C.

Clark, I., and Fritz, P., 1997, Environmental isotopes in hydrogeology: Lewis Publishers, Boca Raton, FL, 352 p.

Constantz, J., 2008, Heat as a tracer to determine stream water exchanges: Water Resources Research, v. 44, W00D10, 20 p.

Constantz, J., and Stonestrom, D.A., 2003, Heat as a tracer of water movement near streams, p. 1–6, in Stonestrom, D.A., and Constantz, J., eds,, Heat as a tool for studying the movement of ground water near streams: USGS Circular 1260, 96 p.

Dalton, John C., 2003, Irrigation water requirements user manual, version 1.0, March 2003.

Darr, A., 1975, Boulder water job one step nearer: The Montana Standard, 2/9/1975: p. 17.

Dixon, R.M., and Wolfgram, D., 1998, Bedrock geology of the Elkhorn Mountains volcanics in the southern Bull Mountain area, Jefferson County, Montana: Montana Bureau of Mines and Geology Open-File Report 374, 13 p., 1 sheet, scale 1:24,000.

Doe, D.R., Tilling, R.I., Hedge, C.E., and Klepper, M.R., 1968, Lead and strontium isotope studies of the Boulder Batholith, southwestern Montana: Economic Geology, v. 63, p. 884–906.

Doherty, J.E., 2010, PEST model-independent parameter estimation user manual, 5th ed: Watermark Numerical Computing, 336. p. [Accessed from http://www.pesthomepage.org, 12/19/2013]

Doherty, J.E., 2013, Addendum to the PEST manual: Watermark Numerical Computing, 266 p. [Accessed from http://www.pesthomepage.org, 12/19/2013]

Drever, J.I., 1997, The geochemistry of natural waters: Surface and groundwater environments: Englewood Cliffs, N.J., Prentice Hall, 436 p.

Dutton, D.M., Lawlor, S.M., Briar, D.W., and Tresch, R.E., 1995, Hydrogeologic data for the northern Rocky Mountains intermontane basins, Montana: U.S. Geological Survey Open-File Report 95-143, 94 p.

Eddy-Miller, C.A., Wheeler, J.D., and Essaid, H.I., 2009, Characterization of interactions between surface water and near-stream groundwater along

Fish Creek, Teton County, Wyoming by using heat as a tracer: USGS SIR 2009-516, 53 p.

Environmental Simulations Incorporated, 2011, Guide to using Groundwater Vistas, version 6, 213 p.

Farnes, P.E., Huddleston, J., and Flynn, K., 2011, Montana electronic precipitation map: Proceedings of the Annual Western Snow Conference, 2011. [Accessed from http://nris.mt.gov/gis/, 10/16/14).

Faure, G., 1991, Principles and applications of inorganic geochemistry: Upper Saddle River, N.J., Prentice-Hall, Inc. 626 p.

Fetter, C.W., 1994, Applied hydrogeology, 3rd ed: New York, Macmillan, 691 p.

Freeze, R.A., and Cherry, J.A., 1979, Groundwater: Englewood Cliffs, N.J., Prentice-Hall, 604 p.

Gammons, C., Poulson, S., Pellicori, D., Reed, P., Rosesler, A., and Petrescu, E., 2006, The hydrogen and oxygen isotopic composition of precipitation, evaporated mine water, and river water in Montana, USA: Journal of Hydrology, v. 328, p. 319–330.

Hackett, O.M., Visher, F.N., McMurtrey, R.G., and Steinhilber, W.L., 1960, Geology and groundwater resources of the Gallatin Valley, Gallatin County, Montana: U.S. Geological Survey Water-Supply Paper 1482, 282 p.

Harbaugh A., Banta, E., Hill, M., and McDonald, M., 2000, MODFLOW-2000, The U.S. geological survey modular ground-water model—User guide to modularization concepts and the ground-water flow process: USGS Open-File Report: 2000-92, 121 p.

Healy, R.W., 2012, Estimating groundwater recharge (2nd ed): Cambridge, UK, Cambridge University Press, 245 p.

Healy, R.W., Bartos, T.T., Rice, C.A., McKinley, M.P., and Smith, B.D., 2011, Groundwater chemistry near an impoundment for produced water, Powder River Basin, Wyoming, USA: Journal of Hydrology, v. 403, p. 37–48.

Hill, M., 2003, Preconditioned conjugate-gradient 2 (PCG2), a computer program for solving groundwater flow equations: USGS Water-Resources Investigations Report 90-4048, 31 p.

Hounslow, A., 1995, Water quality data, analysis and interpretation: Boca Raton, Fla., CRC Press–Lewis Publishers, 397 p.

Jenkins, C.T., 1968, Computation of rate and volume of stream depletion by wells: U.S. Geological Survey Techniques of Water-Resources Investigations, book 4, chap. D1, 17 p.

Johns, E. (ed.), 1989, Water use by naturally occurring vegetation, including an annotated bibliography: American Society of Civil Engineers, New York, 216 p.

Johnson, R.W., Henderson, J.R., and Tyson, N.S., 1965, Aeromagnetic map of the Boulder Batholith area, southwestern Montana: U.S. Geological Survey Geophysical Investigations Map GP-538, scale 1:250,000.

Jolly, W.A., 1982, Project Development and Maintenance—Boulder River Watershed: unpublished manuscript.

Kendy, E., and Tresch, R.E., 1996, Geographic, geologic and hydrologic summaries of intermontane basins of the Northern Rocky Mountains, Montana: U.S. Geological Survey Water-Resources Investigations Report 96-4025, 233 p.

Kinoshita, W.T., Davis, W.E., and Robinson, G.D., 1965, Aeromagnetic, Bouguer gravity, and generalized geologic map of Toston and Radersburg quadrangles and part of the Devils Fence quadrangle, Gallatin, Broadwater and Jefferson Counties, Montana: U.S. Geological Survey Geophysical Investigations Map GP-496, 2 sheets, scale 1:62,500.

Klepper, M.R., Weeks, R.A., and Ruppel, E.T., 1957, Geology of the southern Elkhorn Mountains, Jefferson and Broadwater Counties, Montana: U.S. Geological Survey Professional Paper 292, 82 p.

Knopf, A., 1913, Ore deposits of the Helena mining region, Montana: U.S. Geological Survey Bulletin 527, 143 p.

Kuenzi, W.D., and Fields, R.W., 1971, Tertiary stratigraphy, structure, and geologic history, Jefferson Basin, Montana: Geological Society of America Bulletin, v. 82, p. 3373–3394.

Lautz, L.K., 2008. Estimating groundwater evapotranspiration rates using diurnal water-table fluctuations in a semi-arid riparian zone: Hydrogeology Journal, v. 16, p. 483–497.

Leenhouts, J.M., Stromber, J.C., and Scott, R.L., eds., 2006, Hydrologic requirements of and consumptive ground-water use by riparian vegetation along the San Pedro River, Arizona: U.S. Geological Survey Scientific Investigations Report 2005-5163, 154 p.

Lewis, R.S. (compiler), 1998, Geologic map of the Butte 1o x 2o quadrangle, south-western Montana: Montana Bureau of Mines and Geology Open-File Report 363, 16 p., 1 sheet, scale 1:250,000.

Lofgren, D.L., 1985, Tertiary vertebrate paleontology, stratigraphy, and structure, north Boulder River basin, Jefferson County, Montana: University of Montana MS thesis, 113 p.

Marvin, R.K., Metesh, J.J., Hargrave, P.A., Lonn, J.D., Watson, J.E., Bowler, T.P., and Madison, J.P., 1997, Abandoned/inactive mines of Montana, U.S. Bureau of Land Management: Montana Bureau of Mines and Geology Open-File Report 348, 544 p.

Marvin, R.K., Hargrave, P.A., Lonn, J.D., Abdo, G.N., Metesh, J.J., 1998, Abandoned-inactive mines of the southern Beaverhead Deerlodge National Forest: Montana Bureau of Mines and Geology Open-File Report 379, 345 p.

MesoWest, 2014, Current and archived weather observations [Accessed from http://mesowest.utah.edu, 6/3/14]

Metesh, J.J., Duaime, T., Lonn, J., Madison, J.P., Marvin, R.K., and Wintergerst, R., 1998, Abandoned-inactive mines program, Deerlodge National Forest, volume V: Boulder/Jefferson River drainages: Montana Bureau of Mines and Geology Open-File Report 347, 179 p., 2 sheets.

Montana Bureau of Mines and Geology (MBMG), 2016a, Montana abandoned and inactive mines database. [Accessed from http://nris.mt.gov/nsdi/nris/shape/abdmine.zip, 5/21/13]

Montana Bureau of Mines and Geology (MBMG), 2016b, Montana Groundwater Information Center Water Well Data. [Accessed from http://nris.mt.gov/gis/, 8/30/2016]

Montana Bureau of Mines and Geology–Groundwater Assessment Program (MBMG-GWAP), 2016, Groundwater assessment. [Accessed from http://www.mbmg.mtech.edu/gwap/grw-assessment.asp, 2/19/16]

Montana Department of Environmental Quality (MDEQ), 2008, Golden Dream Mine Project–EA cover letter. [Accessed from http://deq.mt.gov/ea/hardrock.mcpx, 3/5/13]

Montana Department of Environmental Quality (MDEQ), 2010, Montana numeric water quality standards: Circular DEQ-7, 61 p.

Montana Department of Environmental Quality (MDEQ), 2012, Boulder-Elkhorn metals TMDLs and framework water quality improvement plan: MDEQ document number M04-TMDL-01aF.

Montana Department of Environmental Quality (MDEQ), 2013, Historic narrative of the Elkhorn mining district. [Accessed from http://www.deq.mt.gov/abandonedmines/linkdocs/79tech.mcpx, 3/5/13]

Montana Department of Revenue (MT-DOR), 2012, Revenue final land unit (FLU) classification. [Accessed from http://nris.mt.gov/nsdi/nris/mdb/revenue_flu.zip, 5/16/13]

Montana Department of Natural Resources and Conservation (MT-DNRC), 2007, Digitized ditch reference data from Montana's Water Resources Survey (http://www.dnrc.mt.gov/wrd/water_rts/survey_books/default.asp), based on the State Engineer's Office WRS publication for Jefferson County, June 1956. [Accessed 2/2/09]

Montana Department of Natural Resources and Conservation (MT-DNRC), 2013, DNRC Water Right Query System. [Accessed from http://nris.mt.gov/dnrc/waterrights/default.aspx, April 2013]

Montana Fish Wildlife and Parks (FWP), 2012, Montana Statewide Fisheries Management Plan—2013–2018: Montana Fish Wildlife and Parks, Helena, Mont., 478 p.

Montana State Library, 2010, Cadastral (http://nris.mt.gov/gis/) version updated on 11/10/10.

Montana State Library, 2011, Structures Framework (http://nris.mt.gov/gis/) version updated on 9/1/11.

Montana Water Resources Board, 1968, Boulder River Project #62.

National Agricultural Imagery Program (NAIP), 2011, Natural-Color Aerial Photos of Montana, 2011. [Accessed from http://nris.mt.gov/gis/, 9/4/13]

National Oceanic and Atmospheric Administration (NOAA), 2011, NOAA's 1981–2010 Climate Normals. [Accessed from http://www.ncdc.noaa.gov/oa/climate/normals/usnormals.html, 3/4/13]

Natural Resources Conservation Service (NRCS), 1993, Soil survey manual: U.S. Department of Agriculture Handbook 18, 437 p.

Natural Resources Conservation Service (NRCS), 2012, IWR Program [Accessed from http://www.nrcs.usda.gov/wps/portal/nrcs/detailfull/national/water/manage/irrigation/?&cid=stelprdb1044890), October 2012]

Natural Resources Conservation Service (NRCS), 2014, Snow telemetry (SNOWTEL) and snow course data and products. [Accessed from http://www.wcc.nrcs.usda.gov/snow/index.html, November 2014]

Nelson, W.L., 1962, A seismic study of North Boulder Valley and other selected areas, Jefferson and Madison Counties, Montana: Bloomington, Ind., Indiana University, M.A. thesis, 33 p.

Nimick, D.A., Church, S.E., and Finger, S.E., 2004, Integrated investigations of environmental effects of historical mining in the Basin and Boulder mining districts, Boulder River watershed, Jefferson County, Montana: U.S. Geological Survey Professional Paper 1652, 523 p.

Niswonger, R.G., Panday, S., and Ibaraki, M., 2011, MODFLOW-NWT, A Newton formulation for MODFLOW-2005: USGS Techniques and Methods 6-A37, 44 p.

Nobel, R.A., Bergantino, R.N., Patton, T.W., Sholes, B.C., Daniel, F., and Schofield, J., 1982, Occurrence and characteristics of ground water in Montana, volume 2, the Rocky Mountain region: Montana Bureau of Mines and Geology Open-File Report 99, 132 p.

Pardee, J.T., and Schrader, F.C., 1933, Metalliferous deposits of the greater Helena mining region, Montana: U.S. Geological Survey Bulletin 842, 318 p.

Parker, J.S., 1961, A preliminary seismic investigation of Tertiary basin fill in the Jefferson Island quadrangle, Montana: Bloomington, Ind., Indiana University, M.A. thesis, 35 p.

Peale, A.C., 1896, Three Forks, Montana: U.S. Geological Survey Folio 24.

Persson, G., 1995, Willow stand evapotranspiration simulated for Swedish soils: Agricultural Water Management, v. 28, p. 271–293.

Petersen, M.R., and Hill, R.W., 1985, Evapotranspiration of small conifers: Journal of Irrigation and Drainage Engineering, v. 111, no. 4, p. 341–351.

Plummer, L.N., Bohkle, J.K., and Busenberg, E., 2003, Approaches for groundwater dating, in Lindsey, B.D., Phillisp, S.W., Donnelly, C.A., Speiran, G.K., Plummer, L.N., Bohlke, J.K., Focazio, M.J., Burton, W.C., and Busenberg, E., Residence times and nitrate transport in ground water discharging to streams in the Chesapeake Bay watershed: U.S. Geological Survey Water-Resources Investigations Report 03-4035, p. 12–24.

PRISM Climate Group, Oregon State University, 2012, United States Average Monthly or Annual Precipitation, 1981–2010. [Accessed from http://prism.oregonstate.edu, 5/16/13]

Reynolds, M.W., and Brandt, T.R., 2006, Preliminary geologic map of the Townsend 30' x 60' quadrangle, Montana: U.S. Geological Survey Open-File Report 2006-1138, scale 1:100,000.

Richard, B.H., 1966, Geologic history of the intermontane basins of the Jefferson Island quadrangle, Montana: Bloomington, Ind., Indiana University, Ph.D. dissertation, 121 p.

Roby, R.N., Ackerman, W.C., Fulkerson, F.B., and Crowley, F.A., 1960, Mines and mineral deposits (except fuels), Jefferson County: Montana Bureau of Mines and Geology Bulletin 16, 120 p.

Rosenberry, D.O., and Winter, T.C., 1997, Dynamics of water-table fluctuations in an upland between two prairie-pothole wetlands in North Dakota: Journal of Hydrology, v. 191, p. 266–289.

Rozanski, K., Araguas-Arguas, L., and Gonfiantini, R., 1993, Isotope pattern in modern global precipitation, in Swart, P., Lohwan, K., Mekenzie, J., and Savin, S. (eds.), Climate change in continental isotopic records: AGU Monograph 78, p. 1–37.

Sanford, W. E., and Selnick, D. L., 2012, Estimation of evapotranspiration across the conterminous United States using a regression with climate and land-cover data: Journal of the American Water Resources Association, v. 9, no. 1, p. 217–230.

Scott, R.L., Edwards, E.A., Shuttleworth, W.J., Huxman, T.E., Watts, E., and Goodrich, D.C., 2004, Interannual and seasonal variations in fluxes of water and carbon dioxide from a riparian woodland ecosystem: Agricultural and Forest Meteorology, v. 122, p. 65–84.

Soil Conservation Service (SCS), 1975, Draft plan and draft environmental impacts statement Boulder River watershed, Jefferson County, Montana.

Sonderegger, J.L., Bergantino, R.N., and Kovacich, S., 1981, Geothermal resources map of Montana: Montana Bureau of Mines and Geology Hydrogeologic Map 4, 1 sheet, 9 p., scale 1:1,000,000.

Stone, R.W., 1911, Geologic relations of ore deposits in the Elkhorn Mountains, Montana: U.S. Geological Survey Bulletin 470, p. 75–98.

Theis, C.V., 1940, The source of water derived from wells: Essential factors controlling the response of an aquifer to development: Civil Engineering, v. 10, p. 277–280.

Tucker, C.S., 2008, The Elkhorn Mine, Jefferson County, Montana: Rocks and Minerals, v. 83, no. 1, p. 20–33.

U.S. Bureau of Land Management (BLM), 1975, Environmental Analysis Report—Boulder Hot Springs Geothermal Development: BLM document, 135 p.

U.S. Geological Survey (USGS), 1999, National elevation dataset (NED). [Accessed from http://ned.usgs.gov/, 5/16/13]

U.S. Geological Survey (USGS), 2010a, LANDFIRE Existing Vegetation Type (LANDFIRE.US_110EVT). [Accessed from http://www.landfire.gov/NationalProductDescriptions21.php, 3/8/13]

U.S. Geological Survey (USGS), 2010b, National Land Cover GAP Analysis Project. [Accessed from http://gapanalysis.usgs.gov/gaplandcover/data/download/, 4/2/13]

U.S. Geological Survey (USGS), 2011, 2006 National Land Cover Data. [Accessed from http://www.mrlc.gov/nlcd06_data.php, 4/2/13]

Van Mullem, J., 2006, Upper Jefferson River irrigation delivery improvement project: Prepared for the Jefferson River Watershed Council and Trout Unlimited.

Vuke, S.M., Coppinger, W.W., Cox, B.E., 2004, Geologic map of Cenozoic deposits in the Upper Jefferson Valley, southwestern Montana: Montana Bureau of Mines and Geology Open-File Report 505, 35 p., 1 sheet, scale 1:50,000.

Vuke, S.M., Lonn, J.D., Berg, R.B., and Kellogg, K.S., 2014, Geologic map of the Bozeman 30’ x 60’ quadrangle, southwestern Montana: Montana Bureau of Mines and Geology, Open-File Report 648, 44 p., 1 sheet, scale 1:100,000.

Waren, K., Bobst, A., Swierc, J., and Madison, J.D., 2012, Hydrogeologic investigation of the North Hills study area, Lewis and Clark County, Montana: Montana Bureau of Mines and Geology Open-File Report 610, 99 p.

Wallace, C.A., Schmidt, R.G., Lidke, D.J., Waters, M.R., Elliott, J.E., French, A.B., Whipple, J.W., Zarske, S.E., Blaskowski, M.J., Heise, B.A., Yeoman, R.A., O’Neill, J.M., Lopez, D.A., Robinson, G.D., and Klepper, M.R., 1986, Preliminary map of the Butte 1o x 2o quadrangle, western Montana: U.S. Geological Survey Open-File Report 86-292, scale 1:250,000.

Weed, W.H., 1901, Geology and ore deposits of the Elkhorn mining district, Jefferson County, Montana: U.S. Geological Survey Annual Report 22, Part 2, p. 399–510.

Weed, W.H., 1912, Geology and ore deposits of the Butte district, Montana: U.S. Geological Survey Professional Paper 74, 262 p.

Weeks, R.A., 1974, Geologic map of the Bull Mountain area, Jefferson County, Montana: U.S. Geological Survey Open-File Report 74-354, scale 1:48:000.

Wilson, D.A., 1962, A seismic and gravity investigation of the North Boulder River and Jefferson River Valleys, Madison and Jefferson Counties, Montana: Bloomington, Indiana University, M.A. thesis, 43 p.

Winter, T.C., Harvey, J.W., Franke, O.L., and Alley, W.M., 1999, Ground water and surface water: A single resource: United States Geological Survey Circular 1139, 79 p.

Woodhouse, B., 2008, Approaches to ET measurement: Southwest Hydrology, v. 7, no. 1, p. 20–21.

APPENDIX A

Appendix A: Boulder River Groundwater Investigation Monitored Site List

GWIC ID	Type	Latitude	Longitude	Geomethod	Township	Range	Section	Ground-Surface Altitude (ft-amsl)	Total Depth (ft)	Static Water Level (ft)	Aquifer
262097	WELL	45.872288	-111.944130	SUR-GPS	01N	03W	2	4284.78	NR	7	110ALVM
265188	WELL	45.871085	-111.943065	SUR-GPS	01N	03W	2	4278.30	16	3	110ALVM
215992	WELL	45.874090	-111.974955	SUR-GPS	01N	03W	4	4344.47	98	65	120SNGR
262259	WELL	45.932832	-111.794939	SUR-GPS	02N	01W	12	5060.37	326	108	221MRSN
262242	WELL	45.952733	-111.865681	SUR-GPS	02N	02W	4	4654.90	53	14	120SDMS
265187	WELL	45.949076	-111.904069	SUR-GPS	02N	02W	6	4374.48	15	5	110ALVM
49040	WELL	45.956118	-111.924558	SUR-GPS	02N	03W	1	4517.55	279	20	120SDMS
170410	WELL	45.936889	-111.920813	NAV-GPS	02N	03W	12	4400	133	48	120SDMS
49049	WELL	45.904119	-111.954410	SUR-GPS	02N	03W	22	4518.50	74	8	120SDMS
192299	WELL	45.881892	-111.942565	SUR-GPS	02N	03W	35	4326.83	283	60	400LHOD
50002	WELL	46.021052	-111.874165	SUR-GPS	03N	02W	8	4466.73	45	17	111SNGR
50006	WELL	45.979576	-111.881899	SUR-GPS	03N	02W	29	4454.30	80	65	120SDMS
50007	WELL	45.990937	-111.890364	SUR-GPS	03N	02W	30	4434.92	31	17	110ALVM
50008	WELL	45.985926	-111.893683	SUR-GPS	03N	02W	30	4439.36	NR	120	120SDMS
265186	WELL	45.975721	-111.889440	SUR-GPS	03N	02W	31	4403.16	15	3	110ALVM
50010	WELL	45.972090	-111.865170	SUR-GPS	03N	02W	33	4512.08	158	105	120SDMS
249318	WELL	46.129389	-111.851823	SUR-GPS	04N	02W	4	4999.31	330	80	400SPKN
267567	WELL	46.114685	-111.821489	SURVEY	04N	02W	11	5342.37	460	350	400GRSN
267569	WELL	46.114621	-111.821501	SURVEY	04N	02W	11	5343.20	460	350	400GRSN
121965	WELL	46.071487	-111.902182	SUR-GPS	04N	02W	30	4532.37	225	28	120SDMS
262735	WELL	46.057481	-111.874567	SUR-GPS	04N	02W	32	4501.77	87	23	337MSNC
265185	WELL	46.061255	-111.878995	SUR-GPS	04N	02W	32	4491.82	16	5	110ALVM
262766	WELL	46.124868	-111.928131	SUR-GPS	04N	03W	1	4592.39	87	28	110ALVM
50949	WELL	46.132928	-111.929961	SUR-GPS	04N	03W	2	4636.38	98	12	120SDMS
228786	WELL	46.130717	-111.987546	SUR-GPS	04N	03W	4	4783.58	180	120	120SNGR
204849	WELL	46.125868	-111.997825	SUR-GPS	04N	03W	5	4959.90	326	253	120SNGR
265167	WELL	46.108620	-111.953295	SUR-GPS	04N	03W	10	4709.65	119	101	110ALVF
265168	WELL	46.108623	-111.952969	SUR-GPS	04N	03W	10	4707.14	118	99	110ALVF
265170	WELL	46.108625	-111.952727	SUR-GPS	04N	03W	10	4704.44	113	98	110ALVF
262738	WELL	46.120121	-111.942174	SUR-GPS	04N	03W	11	4595.42	45	4	110ALVM

GWIC ID	Type	Latitude	Longitude	Geomethod	Township	Range	Section	Ground-Surface Altitude (ft-amsl)	Total Depth (ft)	Static Water Level (ft)	Aquifer
265171	WELL	46.108699	-111.946198	SUR-GPS	04N	03W	11	4647.62	55	50	110ALVF
265179	WELL	46.109608	-111.934292	SUR-GPS	04N	03W	11	4580.82	14	7	110ALVM
265181	WELL	46.113162	-111.949308	SUR-GPS	04N	03W	11	4663.37	75	58	110ALVF
50963	WELL	46.102105	-111.950238	SUR-GPS	04N	03W	14	4704.34	201	50	120SDMS
265172	WELL	46.108749	-111.940332	SUR-GPS	04N	03W	14	4610.79	25	18	110ALVF
265175	WELL	46.108755	-111.940021	SUR-GPS	04N	03W	14	4608.96	22	19	110ALVF
265176	WELL	46.108790	-111.939815	SUR-GPS	04N	03W	14	4607.16	24	15	110ALVF
158371	WELL	46.104906	-112.009819	SUR-GPS	04N	03W	17	5737.74	140	39	211BDBT
258713	WELL	46.106431	-112.000084	SUR-GPS	04N	03W	17	5487.18	240	145	211BDBT
262734	WELL	46.093935	-111.920653	SUR-GPS	04N	03W	24	4561.39	32	7	110ALVM
265073	WELL	46.201390	-111.964757	SUR-GPS	05N	03W	10	5099.39	NR	20	120SNGR
265072	WELL	46.191152	-111.963263	SUR-GPS	05N	03W	15	4972.99	NR	22	110ALVM
265183	WELL	46.176967	-112.031885	SUR-GPS	05N	03W	19	4723.07	19	6	110ALVM
198172	WELL	46.172208	-112.000402	SUR-GPS	05N	03W	20	4731.48	200	50	211ELKM
51656	WELL	46.147479	-111.968066	SUR-GPS	05N	03W	34	4681.53	77	12	120SDMS
50951	WELL	46.136287	-111.948602	SUR-GPS	05N	03W	35	4626.51	36	26	120SDMS
51661	WELL	46.136458	-111.949104	SUR-GPS	05N	03W	35	4631.44	38	22	120SDMS
170893	WELL	46.217537	-112.076723	SUR-GPS	05N	04W	2	4968.53	312	150	211BDBT
239829	WELL	46.215907	-112.075668	SUR-GPS	05N	04W	2	5001.79	547	240	211BDBT
153536	WELL	46.218488	-112.084075	SUR-GPS	05N	04W	3	4847.31	160	10	211BDBT
147850	WELL	46.213723	-112.135335	SUR-GPS	05N	04W	5	5131.02	426	117	211BDBT
51692	WELL	46.201867	-112.098584	SUR-GPS	05N	04W	10	4846.36	240	60	211BDBT
121384	WELL	46.184503	-112.047177	SUR-GPS	05N	04W	13	4760.59	100	18	110ALVM
184291	WELL	46.273300	-111.946592	SUR-GPS	06N	03W	14	6401.17	188	50	374PARK
264613	WELL	46.277393	-111.942936	SUR-GPS	06N	03W	14	6593.26	NR	144	341JFRS
254940	WELL	46.304146	-112.056289	SUR-GPS	06N	04W	1	5257.77	220	13	211BDBT
264212	WELL	46.303785	-112.055905	SUR-GPS	06N	04W	1	5282.55	301	29	211BDBT
53346	WELL	46.300125	-112.098523	SUR-GPS	06N	04W	3	5060.65	70	4	211PLNC
226319	WELL	46.283577	-112.056988	SUR-GPS	06N	04W	12	5222.66	407	185	211BDBT
266999	WELL	46.288957	-112.041231	SURVEY	06N	04W	12	5284.70	100	42	211BDBT
267568	WELL	46.289013	-112.041296	SURVEY	06N	04W	12	5287.18	100	46	211BDBT

GWIC ID	Type	Latitude	Longitude	Geomethod	Township	Range	Section	Ground-Surface Altitude (ft-amsl)	Total Depth (ft)	Static Water Level (ft)	Aquifer
267570	WELL	46.288952	-112.041346	SURVEY	06N	04W	12	5280.00	100	35	211BDBT
162617	WELL	46.252594	-112.134549	SUR-GPS	06N	04W	20	5222.26	165	25	211BDBT
192602	WELL	46.254346	-112.140224	SUR-GPS	06N	04W	20	5384.39	398	25	211BDBT
264284	WELL	46.261798	-112.081067	SUR-GPS	06N	04W	22	4897.88	NR	22	110ALVM
53361	WELL	46.241163	-112.075992	SUR-GPS	06N	04W	26	4915.48	38	30	211BDBT
262737	WELL	46.241192	-112.076123	NAV-GPS	06N	04W	26	4920	300	55	211BDBT
129843	WELL	46.248060	-112.143104	SUR-GPS	06N	04W	30	5275.77	145	30	211BDBT
53392	WELL	46.235728	-112.131634	NAV-GPS	06N	04W	32	4930	49	31	110ALVM
227316	WELL	46.227107	-112.121522	SUR-GPS	06N	04W	32	4900.98	100	40	110ALVM
250296	WELL	46.230140	-112.122186	SUR-GPS	06N	04W	32	4905.86	59	28	110ALVM
262736	WELL	46.234278	-112.083651	SUR-GPS	06N	04W	34	4856.67	143	3	110ALVM
265184	WELL	46.228392	-112.090461	SUR-GPS	06N	04W	34	4846.58	12	2	110ALVM
55803	WELL	46.312260	-112.107655	SUR-GPS	07N	04W	33	5391.38	167	20	211BDBT
160435	WELL	46.312597	-112.073886	SUR-GPS	07N	04W	36	5568.36	197	92	211BDBT
256351	SPRING	45.946698	-111.903199	SUR-GPS	02N	02W	7	4368.32	NA	NA	110ALVM
262899	CANAL	46.132083	-111.969908	SUR-GPS	04N	03W	3	4621.04	NA	NA	NA
265345	CANAL	46.108793	-111.953129	SUR-GPS	04N	03W	10	4705.79	NA	NA	NA
265346	CANAL	46.108747	-111.940125	SUR-GPS	04N	03W	14	4607.21	NA	NA	NA
267934	CANAL	46.14974	-112.00638	MAP	05N	03W	32	4715	NA	NA	NA
263602	STREAM	45.870832	-111.943014	SUR-GPS	01N	03W	2	4272.89	NA	NA	NA
262190	STREAM	45.948918	-111.903645	SUR-GPS	02N	02W	6	4367.45	NA	NA	NA
271799	STREAM	45.945303	-111.910308	NAV-GPS	02N	03W	12	4357	NA	NA	NA
265348	STREAM	45.975586	-111.888819	SUR-GPS	03N	02W	31	4398.51	NA	NA	NA
265343	STREAM	46.061128	-111.879173	SUR-GPS	04N	02W	32	4486.78	NA	NA	NA
265344	STREAM	46.113501	-111.919306	SUR-GPS	04N	03W	12	4567.40	NA	NA	NA
266397	STREAM	46.202905	-111.964919	SUR-GPS	05N	03W	10	5095.13	NA	NA	NA
265349	STREAM	46.177031	-112.032051	SUR-GPS	05N	03W	19	4718.77	NA	NA	NA
265943	STREAM	46.21111	-112.09083	MAP	05N	04W	3	4810	NA	NA	NA
265347	STREAM	46.200955	-112.094158	SUR-GPS	05N	04W	10	4805.22	NA	NA	NA
263601	STREAM	46.236470	-112.154499	SUR-GPS	06N	04W	30	4969.31	NA	NA	NA
265350	STREAM	46.228695	-112.090525	SUR-GPS	06N	04W	34	4843.73	NA	NA	NA

APPENDIX B

Table B1. Analytical parameters for water-quality samples collected in the Boulder Valley study area.

Major Ions (mg/L)	
Calcium*	Ca
Magnesium*	Mg
Sodium*	Na
Potassium*	K
Iron	Fe
Manganese	Mn
Silica*	SiO_2
Bicarbonate*	HCO_3
Carbonate	CO_3
Chlorine*	Cl
Sulfate*	SO_4
Nitrate*	as N
Fluoride	F
Orthophosphate	as P

Field Parameters		
Field Conductivity	Field SC	mmhos
Field pH	Field pH	---
Water Temperature*	Temp	°C

Other Parameters		
Total Dissolved Solids*	TDS	mg/L
Sum of Dissolved Constituents	---	mg/L
Lab Conductivity*	Lab SC	mmhos
Lab pH*	Lab pH	---
Nitrate + Nitrite	as N	mg/L
Total Nitrogen	as N	mg/L
Hardness	as $CaCO_3$	mg/L
Alkalinity	as $CaCO_3$	mg/L
Ryznar Stability Index	---	---
Sodium Adsorption Ratio	SAR	---
Langlier Saturation Index	---	---
Phosphate (TD)	as P	mg/l
Deuterium Fraction of Water*	dD	0/00 SMOW
^{18}O Fraction of Water*	$d^{18}O$	0/00 SMOW

Trace Elements (mg/L)	
Aluminum	Al
Antimony	Sb
Arsenic*	As
Barium	Ba
Beryllium	Be
Boron	B
Bromide	Br
Cadmium	Cd
Cerium	Ce
Cesium	Cs
Chromium	Cr
Cobalt	Co
Copper	Cu
Gallium	Ga
Lanthanum	La
Lead	Pb
Lithium	Li
Molybdenum	Mo
Nickel	Ni
Niobium	Nb
Neodymium	Nd
Palladium	Pd
Praseodymium	Pr
Radon*	Rn
Rubidium	Rb
Silver	Ag
Selenium	Se
Strontium*	Sr
Thallium	Tl
Thorium	Th
Tin	Sn
Titanium	Ti
Tungsten	W
Uranium	U
Vanadium	V
Zinc	Zn
Zirconium	Zr

mmhos, micromhos per centimeter at 25°C.

*Parameters included in Table B2. Other parameters are available from the GWIC database.

Table B2. Supplemental sampling for evaluation of Cold Springs—April, 2013.

GWIC ID	Description	Site Type	Sample Date	Tritium Units	DIC (mg/L)	$\delta^{13}C$	$^{87}Sr/^{86}Sr$
256351	Cold Spring	SPRING	4/11/2013 11:45	8	18.6	-8.1	0.709481
271799	Boulder below Cold Springs	STREAM	4/11/2013 14:05	8	17.7	-6.8	0.708803
265348	Boulder at Cutoff	STREAM	4/11/2013 15:25	6	7.9	-6.4	0.708486
265186	Alluvium at Cutoff	WELL	4/11/2013 17:20	6	39.2	-12.5	0.708012
265187	Alluvium at Cold Springs	WELL	4/12/2013 11:57	7	44.8	-14.0	0.708314
262242	Tertiary Sediments Well	WELL	4/12/2013 14:45	ND (3)	12.5	-8.2	0.708288

ND(#), this parameter was not detected above the detection limit in parentheses.

Table B3. Water chemistry results for selected parameters.

GWIC ID	Sample Date	Temp °C	Lab pH	Lab SC (mmhos)	TDS (mg/L)	Ca (mg/L)	Mg (mg/L)	Na (mg/L)	K (mg/L)	SiO_2 (mg/L)	HCO_3 (mg/L)	Cl (mg/L)	SO_4 (mg/L)	NO_3 (mg/L as N)
263602	7/31/12	18.9	8.08	320	208	39.5	12.5	16.3	2.9	18.7	175.4	27.2	5.1	0.1
263602	8/21/14	18.0	8.33	340	218	43.1	11.4	13.7	2.1	18.9	177.5	32.0	5.8	0.1
265188	8/1/12	9.7	7.56	280	169	35.3	7.3	11.1	1.6	18.0	137.8	23.0	4.2	0.1
215992	8/9/12	11.8	7.38	3864	2567	209.7	150.0	408.8	21.5	47.6	328.9	1379.0	149.8	37.3
262259	8/9/12	10.7	8.09	925	608	16.1	2.3	207.1	1.0	7.3	195.6	172.1	104.9	0.5
262242	7/26/12	10.8	7.64	585	416	75.2	22.4	38.9	3.0	20.1	271.3	95.4	27.6	0.1
262242	4/12/13	10.1	7.42	794	431	77.7	20.6	36.6	2.8	21.1	274.6	105.9	30.3	0.1
262190	7/31/12	23.0	7.98	310	206	39.7	11.4	15.7	3.5	21.4	179.5	21.0	4.6	ND (0.01)
265187	7/26/12	17.7	6.88	323	239	49.7	10.6	13.3	2.9	29.7	214.8	20.2	3.8	ND (0.01)
265187	4/12/13	10.6	6.82	507	279	59.7	11.9	15.0	2.6	26.2	232.8	39.6	6.1	ND (0.01)
256351	7/31/12	15.0	7.92	313	201	37.9	12.7	15.8	2.4	18.6	171.5	24.4	5.0	0.4
256351	4/11/13	12.1	7.37	402	208	40.8	10.9	13.7	1.7	19.7	175.3	27.9	5.8	0.5
271799	4/11/13	9.9	7.41	254	144	27.1	6.6	10.1	1.8	18.3	105.5	24.1	4.4	0.2
170410	8/9/12	12.7	7.82	612	428	58.6	4.1	75.4	3.7	25.1	134.9	160.3	35.0	ND (0.01)
50002	8/9/12	11.8	7.66	492	366	58.1	14.5	27.5	5.8	36.8	121.3	159.3	5.3	0.4
50007	8/9/12	11.1	7.31	946	635	130.1	27.2	45.7	5.4	33.6	278.6	201.7	40.6	11.7
265186	7/26/12	10.6	7.41	500	362	59.0	11.9	47.5	5.2	37.8	318.0	37.0	6.0	1.0
265186	4/11/13	8.1	7.13	784	429	73.3	14.0	52.5	5.4	40.0	335.1	66.9	10.4	2.1
265348	7/31/12	25.8	8.54	314	213	41.5	12.8	16.3	3.2	20.9	176.2	21.5	4.8	0.1
265348	4/11/13	8.5	7.36	204	116	20.6	4.6	8.1	1.7	17.3	75.3	22.5	3.6	0.1
267569	10/5/12	NR	7.64	429	250	47.3	15.6	19.8	1.6	15.2	204.9	38.3	9.9	0.7
121965	7/24/12	14.2	7.73	274	182	27.5	13.0	17.2	2.0	15.8	145.9	27.6	5.7	0.3
262735	7/24/12	11.0	7.33	268	190	41.5	8.4	10.5	2.4	21.9	174.9	14.6	3.7	0.1
265343	7/31/12	25.0	7.85	311	204	39.7	12.6	14.6	2.7	21.3	178.9	19.3	5.0	0.1
265185	7/26/12	17.7	6.85	201	148	27.2	6.4	9.1	2.7	23.0	124.4	14.0	3.4	ND (0.01)
262766	8/8/12	14.1	7.81	360	233	38.8	10.8	25.8	2.7	19.4	174.0	37.8	10.0	0.5
204849	8/8/12	15.3	7.79	174	137	23.1	3.0	12.0	1.6	28.7	89.2	21.2	2.8	0.2
265168	3/30/12	NR	7.22	235	130	25.2	7.2	5.6	1.4	20.4	89.4	22.0	4.8	0.1
265168	6/12/12	13.3	7.21	234	126	24.8	7.1	5.5	1.2	20.6	90.3	20.7	2.4	0.1
265168	8/22/12	11.0	7.14	214	126	23.9	7.8	5.2	1.4	20.0	95.5	19.7	2.2	0.1
265181	3/30/12	10.3	7.34	188	106	21.0	5.9	5.1	1.0	18.3	83.2	12.0	1.5	0.1

Note. Yellow indicates exceedance of a standard. See table B1 for parameter abbreviations.
ND(#), Not detected at the method detection limit in parentheses; P, preserved sample; NR, no reading; J, detected above the method detection limit, but below the method reporting limit.

Table B3—*Continued*.

GWIC ID	Sample Date	Temp °C	Lab pH	Lab SC (mmhos)	TDS (mg/L)	Ca (mg/L)	Mg (mg/L)	Na (mg/L)	K (mg/L)	SiO_2 (mg/L)	HCO_3 (mg/L)	Cl (mg/L)	SO_4 (mg/L)	NO_3 (mg/L as N)
265181	6/12/12	10.7	7.24	189	108	20.7	5.9	5.0	1.0	18.4	92.5	10.7	1.4	0.1
265181	8/22/12	11.2	7.22	182	106	20.2	6.4	5.0	1.1	18.4	90.6	10.3	1.3	0.1
265171	3/30/12	11.3	7.65	222	129	19.5	5.3	17.8	1.2	16.6	100.8	16.4	2.1	0.2
265171	6/12/12	10.6	7.51	237	130	18.8	5.2	17.3	1.1	17.8	107.9	15.5	2.1	0.2
265171	8/22/12	11.2	7.48	210	129	18.0	5.5	17.6	1.3	18.3	103.6	14.9	1.9	0.2
265179	6/12/12	10.2	6.96	271	146	26.4	7.3	12.2	1.0	20.2	116.2	19.0	3.1	0.4
265179	8/22/12	12.6	6.96	275	162	29.3	9.3	13.2	1.2	21.3	134.7	18.8	3.4	0.3
265175	3/30/12	10.3	7.40	443	239	41.3	11.5	30.5	1.8	19.4	194.7	31.7	3.6	2.2
265175	6/12/12	9.3	7.22	141	91	14.6	3.2	10.1	1.1	16.7	69.8	9.9	1.4	0.1
265175	8/22/12	13.6	7.22	281	170	30.7	9.2	14.2	1.7	22.6	140.1	17.6	3.1	0.8
50963	9/5/13	12.4	7.25	261	174	33.5	10.5	9.9	1.3	19.4	137.0	27.7	4.5	0.3
266397	7/31/12	20.0	7.88	153	108	21.2	6.5	5.2	1.4	17.4	94.2	10.0	1.1	ND (0.01)
265072	8/1/12	11.5	6.95	314	191	43.5	7.0	11.5	0.8	25.5	164.7	16.8	5.4	0.1
265349	7/30/12	20.9	7.58	140	102	16.5	4.1	9.0	2.1	15.7	72.5	14.9	3.7	ND (0.01)
265183	7/25/12	19.4	6.71	135	106	17.2	4.3	8.1	2.8	18.3	76.5	13.5	3.4	ND (0.01)
51656	8/6/13	9.4	7.37	667	430	78.6	27.4	32.3	0.5	20.4	334.0	91.7	13.5	0.5
51661	8/8/12	NR	7.66	309	206	40.5	10.7	14.6	2.2	21.2	181.3	22.6	5.1	0.2
239829	8/2/12	15.1	7.44	413	257	42.1	15.8	22.0	4.5	30.1	232.3	16.1	10.8	ND (0.01)
153536	7/23/12	10.6	6.76	307	210	41.2	11.1	14.3	3.4	25.1	178.7	16.5	8.2	1.4
51692	8/7/12	13.5	7.53	755	496	59.4	26.5	76.8	7.6	27.0	312.2	96.3	46.1	1.3
265347	7/30/12	20.9	7.41	112	91	15.1	3.5	7.6	1.9	18.2	70.0	8.9	1.1	ND (0.01)
121384	8/7/12	11.9	6.92	286	200	25.2	5.5	33.3	1.9	27.7	146.1	25.6	5.6	0.3
184291	8/1/12	7.1	7.40	317	176	45.2	10.5	3.8	0.7	12.8	173.5	14.4	1.7	1.3
254940	8/2/12	9.4	6.96	270	177	34.6	11.4	7.3	1.9	18.8	149.8	26.9	2.0	0.3
53346	8/7/12	11.3	7.28	462	290	56.3	20.8	15.0	2.7	20.0	243.0	46.5	7.1	2.1
266999	7/23/12	11.3	7.47	315	212	48.1	11.8	8.3	2.0	14.2	197.5	28.9	2.3	0.2
192602	8/7/12	11.3	6.85	286	179	30.3	11.2	10.0	3.4	22.0	105.9	42.6	5.8	0.7
263601	7/30/12	20.7	8.15	109	91	14.6	3.2	9.1	1.9	14.7	63.3	12.6	2.9	ND (0.01)
250296	8/2/12	11.7	6.76	207	137	23.6	6.4	9.7	2.0	17.9	86.8	25.8	7.0	0.6
265350	7/30/12	15.7	7.16	284	188	34.9	9.4	16.7	2.5	17.7	144.8	28.1	5.6	0.4
265184	7/25/12	9.6	6.58	235	162	27.5	8.5	11.3	2.5	20.0	107.0	29.3	7.7	1.0

Table B3—*Continued*.

GWIC ID	Sample Date	As (mg/L)	Sr (mg/L)	$\delta^{18}O$ 0/00 SMOW	δD 0/00 SMOW	Rn (pCi/L)	Tritium Units	DIC (mg/L)	$\delta^{13}C$ 0/00 PDB	$^{87}Sr/^{86}Sr$
263602	7/31/12	9.1	280	NR	NR	NR	NR	NR	NR	NR
263602	8/21/14	6.1	244	-17.4	-136	NR	NR	NR	NR	NR
265188	8/1/12	5.4	199	NR	NR	NR	NR	NR	NR	NR
215992	8/9/12	3.9 J	4339	NR	NR	NR	NR	NR	NR	NR
262259	8/9/12	0.9 J	420	NR	NR	NR	NR	NR	NR	NR
262242	7/26/12	1.5	423	NR	NR	NR	NR	NR	NR	NR
262242	4/12/13	1.7	405	-19.3	-153	3003.0	ND (3)	12.5	-8.2	0.708288
262190	7/31/12	16.8	314	NR	NR	NR	NR	NR	NR	NR
265187	7/26/12	10.8	326	NR	NR	NR	NR	NR	NR	NR
265187	4/12/13	7.9	378	-16.6	-132	630.4	7	44.8	-14.0	0.708314
256351	7/31/12	2.4	236	NR	NR	NR	NR	NR	NR	NR
256351	4/11/13	2.1	216	-18.0	-140	34.3	8	18.6	-8.1	0.709481
271799	4/11/13	6.2	179	-18.1	-139	24.0 J	8	17.7	-6.8	0.708803
170410	8/9/12	22.0	898	NR	NR	NR	NR	NR	NR	NR
50002	8/9/12	6.7	666	NR	NR	NR	NR	NR	NR	NR
50007	8/9/12	2.0	840	NR	NR	NR	NR	NR	NR	NR
265186	7/26/12	3.4	385	NR	NR	NR	NR	NR	NR	NR
265186	4/11/13	2.9	464	-17.3	-136	724.4	6	39.2	-12.5	0.708012
265348	7/31/12	17.9	331	NR	NR	NR	NR	NR	NR	NR
265348	4/11/13	7.2	158	-17.8	-138	31.4	6	7.9	-6.4	0.708486
267569	10/5/12	1.7	535	NR	NR	NR	NR	NR	NR	NR
121965	7/24/12	3.0	244	NR	NR	NR	NR	NR	NR	NR
262735	7/24/12	9.4	256	NR	NR	NR	NR	NR	NR	NR
265343	7/31/12	12.8	348	NR	NR	NR	NR	NR	NR	NR
265185	7/26/12	8.4	218	NR	NR	NR	NR	NR	NR	NR
262766	8/8/12	3.7	211	NR	NR	NR	NR	NR	NR	NR
204849	8/8/12	72.2	221	NR	NR	NR	NR	NR	NR	NR
265168	3/30/12	0.9	148	NR	NR	NR	NR	NR	NR	NR
265168	6/12/12	1.1	147	NR	NR	NR	NR	NR	NR	NR
265168	8/22/12	1.0	147	NR	NR	NR	NR	NR	NR	NR
265181	3/30/12	0.8	111	NR	NR	NR	NR	NR	NR	NR

Table B2—*Continued*.

GWIC ID	Sample Date	As (mg/L)	Sr (mg/L)	$\delta^{18}O$ 0/00 SMOW	δD 0/00 SMOW	Rn (pCi/L)	Tritium Units	DIC (mg/L)	$\delta^{13}C$ 0/00 PDB	$^{87}Sr/^{86}Sr$
265181	6/12/12	0.8	110	NR	NR	NR	NR	NR	NR	NR
265181	8/22/12	0.8	111	NR	NR	NR	NR	NR	NR	NR
265171	3/30/12	1.2	102	NR	NR	NR	NR	NR	NR	NR
265171	6/12/12	1.7	103	NR	NR	NR	NR	NR	NR	NR
265171	8/22/12	1.7	103	NR	NR	NR	NR	NR	NR	NR
265179	6/12/12	1.5	147	NR	NR	NR	NR	NR	NR	NR
265179	8/22/12	1.5	173	NR	NR	NR	NR	NR	NR	NR
265175	3/30/12	3.6	233	NR	NR	NR	NR	NR	NR	NR
265175	6/12/12	6.2	72	NR	NR	NR	NR	NR	NR	NR
265175	8/22/12	3.8	183	NR	NR	NR	NR	NR	NR	NR
50963	9/5/13	2.5	227	-18.2	-139	NR	NR	NR	NR	NR
266397	7/31/12	5.9	116	NR	NR	NR	NR	NR	NR	NR
265072	8/1/12	1.0	166	NR	NR	NR	NR	NR	NR	NR
265349	7/30/12	13.2	152	NR	NR	NR	NR	NR	NR	NR
265183	7/25/12	16.3	150	NR	NR	NR	NR	NR	NR	NR
51656	8/6/13	4.2	549	-17.5	-136	NR	NR	NR	NR	NR
51661	8/8/12	3.8	295	NR	NR	NR	NR	NR	NR	NR
239829	8/2/12	1.8	446	NR	NR	NR	NR	NR	NR	NR
153536	7/23/12	0.2 J	216	NR	NR	NR	NR	NR	NR	NR
51692	8/7/12	0.6	1022	NR	NR	NR	NR	NR	NR	NR
265347	7/30/12	2.3	124	NR	NR	NR	NR	NR	NR	NR
121384	8/7/12	7.4	213	NR	NR	NR	NR	NR	NR	NR
184291	8/1/12	6.1	82	NR	NR	NR	NR	NR	NR	NR
254940	8/2/12	0.1 J	265	NR	NR	NR	NR	NR	NR	NR
53346	8/7/12	1.0	465	NR	NR	NR	NR	NR	NR	NR
266999	7/23/12	0.2 J	225	NR	NR	NR	NR	NR	NR	NR
192602	8/7/12	0.1 J	292	NR	NR	NR	NR	NR	NR	NR
263601	7/30/12	8.84	134	NR	NR	NR	NR	NR	NR	NR
250296	8/2/12	0.55	204	NR	NR	NR	NR	NR	NR	NR
265350	7/30/12	1.3	279	NR	NR	NR	NR	NR	NR	NR
265184	7/25/12	0.5 J	271	NR	NR	NR	NR	NR	NR	NR